Structure and proteolytic digestion of the intrinsically disordered C-terminal tail of cardiac troponin I

by

Somaya Zahran

A thesis submitted in partial fulfillment of the requirements for the degree of

Doctor of Philosophy

Department of Medicine
University of Alberta

Abstract

Intrinsically disordered regions (IDRs) are protein sequences that do not acquire a fixed 3-D configuration under physiologic conditions. Their solvent-exposed nature makes them susceptible to post-translational modifications like proteolysis, which makes them vital for cellular regulation. However, this can also make the production of these protein sequences in the lab challenging. One method of overcoming this difficulty is to direct their expression into inclusion bodies by attaching IDRs to fusion partners. We used a membrane protein, PagP, as a novel fusion partner to produce large IDRs, like the ones found in the cardiac troponin complex (cTn), from *E. coli* bacteria.

cTn is part of the cardiac thin filament. It is comprised of three subunits: cTnI, the inhibitory subunit; cTnT, the tropomyosin binding subunit; and cTnC, the Ca^{2+} binding subunit. cTnI contains a well-structured core that is tightly bound to the other cTn subunits and two extended IDRs corresponding to its N- and C-terminal tails. The cTnI C-terminal tail plays a vital role in shutting off myocardial contraction by anchoring troponin-tropomyosin to a position on actin that blocks actin-myosin cross-bridging, but the structural details have not yet been fully elucidated. We were able to produce pure amounts of the cTnI C-terminal tail and study its structure alone and also when bound to actin. Our NMR structural studies revealed that while the tail is predominantly disordered, it does contain regions with helical propensity that become more ordered in the presence of actin.

cTn leaks into the bloodstream in myocardial injury, along with other cardiac proteins. Clinical assays measuring cTnI and cTnT have shown superior sensitivity and specificity for cardiac

tissue, establishing them as the current gold standard biomarkers for diagnosing myocardial infarction, that is, irreversible heart muscle death due to prolonged ischemia. The traditional view is that cTn release requires irreversible cardiac myocyte death. However, studies have documented cTn elevations in healthy volunteers after strenuous activity or with reversible cardiac injuries without detectable infarcts by radiologic imaging. In addition, cTn levels were found to poorly correlate with infarct size as measured by cardiac MRI. Thus, we and many others postulate that cTn can in fact be released by sub-lethal injuries. Moreover, since cell death leads to extensive activation of proteases, we further proposed that focal necrosis in myocardial infarction would lead to extensively proteolyzed cTnI, while less severe reversible cardiac injuries would release cTnI in a more intact form. We conducted a pilot study on 29 patients with a wide variety of underlying cardiac injuries and found this assertion to be true. cTnI was proteolyzed most consistently at its C-terminal tail with increasing severity of injury/infarct. Our results suggest that accounting for the extent of cTnI proteolysis could improve the correlation between serum cTnI concentrations and the severity of the underlying cardiac injury.

Our studies on characterising the structure and function of the disordered C terminal tail of cTnI reveal a greater role for structural biology in overcoming current limitations of the cTn assay and enhancing its clinical utility.

Preface

Chapter 1 of this thesis will be submitted for publication as Somaya Zahran, Zabed Mahmud, Richard Schulz, Peter M. Hwang, “Implications of The Proteolytic Digestion of Cardiac Troponin”, Basic Research in Cardiology.

Chapter 2 of this thesis has been published as Somaya Zahran, Jonathan S.Pan, Philip B. Liu, Peter M. Hwang, “Combining a PagP Fusion Protein System With Nickel Ion-Catalyzed Cleavage To Produce Intrinsically Disordered Proteins In E. Coli”, Protein Expression and Purification, 2015 Dec;116:133-8. doi: 10.1016/j.pep.

Chapter 3 of this thesis has been published as Somaya Zahran, Vivian P. Figueiredo, Michelle M. Graham, Richard Schulz, Peter M. Hwang, “Proteolytic Digestion of Serum Cardiac Troponin I as Marker of Ischemic Severity” Journal of Applied Laboratory Medicine, 2017.025254. This research project received research ethics approval from the University of Alberta Research Ethics Board, Project Name “Distinguishing cardiac troponin fragment sizes in type 1 vs. type 2 myocardial infarction patients”, No. Pro00054543, Nov 13th 2015.

Chapter 4 of this thesis has been submitted for publication as Zabed Mahmud§, Somaya Zahran§, Philip B. Liu, Bela Reiz, Brandon Y.H Chan, Andrej Roczkowsky, Christian-Scott E. McCartney, Peter L. Davies, Liang Li, Richard Schulz, Peter M. Hwang, “Structure and proteolytic susceptibility of the inhibitory C-terminal tail of cardiac troponin I,” Biochimica et Biophysica Acta. The first two authors are equal contributors. The authors contributed as follows: Somaya Zahran: Conceptualization; Data curation; Formal analysis; Investigation;

Methodology; Writing-original draft; Equal contribution. Zabed Mahmud: Conceptualization; Data curation; Formal analysis; Methodology; Writing-original draft.

Dedication

In the name of Allah, the most merciful and gracious: (And say, "Do [as you will], for Allah will see your deeds, and [so, will] His Messenger and the believers. And you will be returned to the Knower of the unseen and the witnessed, and He will inform you of what you used to do.") Quran 9:105

My first gratitude goes to Allah Almighty, who enabled me to pursue this PhD and blessed me with amazing companions throughout my life.

To the memory of my first teacher and first hero, my father, whom I still miss every day and whose example is my greatest source of inspiration.

To my mother, whose unconditional love and everlasting support shaped the individual who I am today.

To Asem and Yomna, my siblings, whose passionate encouragement and prayers supported me every day.

To Mostafa, my one and only sweetheart, whose sacrificial care for me and our children made it possible for me to achieve this work.

To Omar, Sarah, and Maryam, my young blossoms, for spreading joy to my life.

To my extended family and to my friends, for their ongoing care and support.

Acknowledgments

I would like to thank my supervisor, Dr Peter Hwang for being always there for me, in all aspects of my career. For providing guidance, support, and, above all, empathy.

I would like to thank my committee members: Dr Raj Padwal for being always available and supportive, and Dr Richard Schulz, for adopting me in his lab and sharing his expertise to guide my professional development.

I would like to thank the members of Hwang lab and Schulz lab for their ongoing care and support.

Contents

Abstract ..... **ii**
Preface ..... **iv**
Dedication ..... **vi**
Acknowledgments ..... **vii**
List of Tables ..... **xi**
List of Figures ..... **xii**
List of Abbreviations ..... **xvi**
Chapter 1. Introduction **1**
1.1 Introduction 1
1.2 Structure of the Troponin Complex 1
1.3 Truncation Studies and Mutational Data of cTnI and cTnT Clarifying the Function of Their Different Regions 7
1.3.1 The N-terminal tail of cTnI 7
1.3.2 The C-terminal tail of cTnI 9
1.3.3 N-terminal region of cTnT 11
1.4 Studies of Proteolytic Degradation 11
1.4.1 Myocardial ischemia and ischemia reperfusion injury [mainly cTnI C-terminal degradation and cTnT N-terminal degradation] 13
1.4.2 Microgravity [Mainly cTnI N-terminal degradation] 16
1.4.3 Miscellaneous conditions 17
1.5 Role of Troponins as a Biomarker of Cardiac Injury 18
1.6 Objectives and Hypotheses: 24
1.6.1 Combining a PagP fusion protein system with nickel ion-catalyzed cleavage to produce intrinsically disordered proteins in E. coli 25
1.6.2 Degradation of serum cTnI C-terminal tail as a more specific marker for the severity of myocardial infarction 26
1.6.3 Determining the structure of cTnI C-terminal tail (135-209) alone and in the presence of actin using NMR spectroscopy 26
Chapter 2. **Combining a PagP fusion protein system with nickel ion-catalyzed cleavage to produce intrinsically disordered proteins in *E. coli*** **28**
2.1 Abstract 28

2.2 Introduction....29
2.3 Materials and Methods....32
2.3.1 Design of PagP fusion partner plasmid....32
2.3.2 Protein expression and purification....34
2.3.3 Nickel cleavage and final purification....35
2.4 Results....36
2.4.1 Protein expression and purification....36
2.4.2 Nickel ion-catalyzed cleavage....37
2.4.3 Isolation and characterization of final product....39
2.5 Discussion....40
Chapter 3. Proteolytic digestion of serum cardiac troponin I as a marker of ischemic severity....44
3.1 Abstract....44
3.2 Introduction....45
3.3 Methods....47
3.3.1 Design of troponin I degradation assay....47
3.3.2 Patient sample collection....50
3.4 Results....51
3.4.1 Patients....51
3.4.2 cTnI is extensively degraded in STEMI patients....52
3.4.3 Degradation of cTnI is variable in Type 2 MI patients....57
3.5 Discussion....58
Chapter 4. Structure and proteolytic susceptibility of the inhibitory C-terminal tail of cardiac troponin I....59
4.1 Abstract....59
4.2 Introduction....60
4.3 Materials and methods....64
4.3.1 Protein expression and purification....64
4.3.2 NMR Spectroscopy....64
4.3.3 SDS-PAGE analysis of *in vitro* proteolysis....65
4.3.4 Mass spectrometric analysis of *in vitro* proteolysis....66
4.4 Results....68
4.4.1 Structure of free $cTnI_{135-209}$ by NMR spectroscopy....68
4.4.2 Rigidification of $cTnI_{135-209}$ in the presence of monomeric actin-DNase I....71
4.4.3 *In vitro* proteolysis of cTnI by MMP-2 and calpain-2....74
4.4.4 Mass spectrometric identification of MMP-2 cleavage sites of cTnI....75
4.4.5 Mass spectrometric identification of calpain-2 cleavage sites of cTnI....77

4.4.6 *In vitro* proteolysis of $cTnI_{1-77}$ in the presence of cTnC....79
4.4.7 *In vitro* proteolysis of $cTnI_{135-209}$ in the presence of cTnC....81
4.4.8 *In vitro* proteolysis of $cTnI_{135-209}$ in the presence of actin....82
4.5 Discussion....84
Chapter 5. Conclusions....88
Bibliography....97
Appendix A....121
Appendix B....125
Appendix C....129

List of Tables

Table 3-1 Clinical presentation and characteristics of study patients classified as having type 2 MI. (Abbrevations: Hgb, hemoglobin; pCO2, partial pressure carbon dioxide; COPD, chronic obstructive pulmonary disease).....51

List of Figures

Figure 1-1 Calcium-saturated cardiac troponin complex. Cardiac troponin C (cTnC) consists of an N-terminal domain (cNTnC) and a C-terminal domain (cCTnC) shown in green. Troponin I (cTnI) is shown in red. The intrinsically disordered tails of cTnI (1-37) and (135-209) are drawn manually as scribbles. Figure prepared using PyMOL and structure 4Y99 (PDB code). Calcium ions are shown in both N and C domain of cTnC as yellow spheres. During systole, cNTnC binds calcium and adopts an open conformation that binds the cTnI switch region (146-158) releasing the cTnI (135-209) inhibitory tail from actin and allowing muscle contraction to proceed.....3

Figure 1-2 The structural and functional regions of cTnI (A) and cTnT (288 a.a isoform) (B) highlighting binding sites to tropomyosin, actin, and troponin subunits above and structural elements below.....5

Figure 2-1 (A) The cTnI[135-209]-SRHW-PagP-His_6 fusion protein. The SRHW sequence allows for nickel-catalyzed peptide bond cleavage N-terminal to the serine residue, allowing separation of the cTnI[135-209] target protein from SRHW-PagP-His_6. (B) Amino acid sequence of cTnI[135-209]-SRHW-PagP-His_6. The nickel-sensitive SRHW sequence, His_6 tag, and former methionine residues in PagP mutated to other residues are highlighted in red.....33

Figure 2-2 A map of the cTnI[135-209]-SRHW-PagP-His_6 expression plasmid. The graphic was produced using the website: http://www.premierbiosoft.com/plasmid_maps/index.html, using the SimVector application.....34

Figure 2-3 SDS-PAGE gel stained with Coomassie Brilliant Blue, showing production and purification of cTnI[135-209]-PagP-His6 protein. Lane 1: whole cells prior to induction. Lane 2: whole cells 6 hours post-induction with IPTG. Lane 3: cell lysate, soluble fraction. Lane 4: cell lysate, insoluble fraction. Lane 5: insoluble fraction dissolved in 6 M Gdn-HCl and purified on a Ni-NTA column under denaturing conditions.....37

Figure 2-4 Nickel cleavage time course. Lane 1: Purified fusion protein before cleavage. Lane 2: After 30 minutes. Lane 3: 60 minutes. Lane 4: 90 minutes. Lane 5: 2 hours. Lane 6: 3 hours. Lane 7: 4 hours.....38

Figure 2-5 Different conditions for Nickel cleavage of cTnI[135-209]-PagP-His_6, all taken after 4 hours. Lane 1: Purified protein before cleavage. Lane 2: pH 7.0 at 45°C. Lane3: pH 7.5

at 45°C. Lane 3: pH 8.0 at 45°C. Lane 4: pH 8.5, at 45°C. Lane 5: pH 9.0, at 45°C. Lane 6: pH 9.0 at 37°C. Lane 7: pH 9.0 at 30°C. Lane 8: pH 9.0 at 25°C.....38

Figure 2-6 Matrix-assisted laser desorption/ionization time-of-flight (MALDI-TOF) mass spectrometry of final purified cTnI[135-209] product.....40

Figure 3-1 Ribbon diagram of the human cardiac troponin complex (PDB code 1J1E). The unstructured ends of troponin I have been drawn in as squiggles and are highlighted in cyan. These are solvent-exposed and susceptible to proteolytic degradation. Antibodies used in this study and their epitopes in cardiac troponin I are shown below. In the current study, antibody 19C7 is used as the capture antibody, while antibodies M18, 560, and MF4 detect the N-terminal, core, and C-terminal regions, respectively. The Beckman Access system uses antibodies that bind epitopes that correspond to 19C7 for capture and 3C7 for detection.....48

Figure 3-2 Schematic showing the impact of increasing severity of focal atherosclerotic lesions (along x-axis) and generalized cardiac strain (along y-axis) on infarct size in the heart (shown as circles on an oval-shaped heart). Both the quantity of troponin released, and its degree of proteolytic degradation increase with increasing ischemic severity. The boxed area with dashed border highlights situations in which the decision of whether or not to proceed with angiography is debatable.....49

Figure 3-3 Plasma/serum troponin I levels in patients with type 1 MI (plus one patient, 37, with myocarditis. Troponin levels measured using two different detection antibodies: 560 (core region) versus MF4 (C-terminal region). Error bars represent the average standard deviation between duplicate measurements.....53

Figure 3-4 Plasma/serum troponin I levels in patients with type 1 MI (plus one patient, 37, with myocarditis). Troponin levels measured using two different detection antibodies: 560 detects the core region of troponin I, while M18 detects the N-terminal region.. 54

Figure 3-5 **(A):** Patients ordered according to total troponin level (measured by the Beckman Access system). **(B)** Patients ordered according to the proportion of troponin I degraded, determined by the ratio of troponin level determined using MF4 detection antibody (corresponding to intact troponin) to that determined using 560 detection antibody (corresponding to total troponin). The ratios were normalized to patient 27, assuming that the patient that showed the least amount of degradation had no degradation…56

Figure 3-6 Patients with potential type 2 MI. Comparison between troponin levels detected by antibody 560 (core region) and MF4 (C-terminal region).....57

Figure 4-1 Calcium-saturated cardiac troponin complex. Cardiac troponin C (cTnC) is shown in blue and consists of an N-terminal domain (cNTnC) and a C-terminal domain (cCTnC). Troponin I (cTnI) is shown in magenta and red, with the red regions corresponding to the two constructs used in this study: $cTnI_{1-77}$ and $cTnI_{135-209}$. The inset highlights the N- and C-terminal tails of cTnI, with intrinsically disordered drawn manually as squiggles. Figure prepared using PyMOL and structure 4Y99 (PDB code). At resting calcium concentrations, cNTnC releases calcium (yellow sphere), adopts a closed conformation, and $cTnI_{135-209}$ binds to actin.....61

Figure 4-2 **(A)** Residue-specific secondary structure of $cTnI_{135-209}$ calculated by the program δ2D using backbone NMR chemical shifts. The functional regions shown highlight the results of limited binding studies in the past, rather than exact boundaries determined from structure. **(B)** Summary of medium-range NOE connectivities $d_{\alpha\beta\ (i,\ i+3)}$ that are specific for alpha helix. **(C)** Representative strip plots showing helical medium-range NOEs from 3D ^{15}N- edited NOESY-HSQC and 3D ^{13}C edited NOESY-HSQC.....70

Figure 4-3 2D [^{1}H, ^{15}N]-HSQC NMR spectra of $cTnI_{135-209}$. **(A)** $cTnI_{135-209}$ alone (left) or with actin (right). The insets show the ^{15}N-upfield region of the spectrum containing, Gly, Ser, and Thr residues. Addition of a small amount of monomeric actin-DNase I complex into $cTnI_{135-209}$ causes differential signal broadening (right). **(B)** The observed reduction in signal intensities in the 2D [^{1}H, ^{15}N]-HSQC signals of $cTnI_{135-209}$ when actin-DNase I complex is added. Overlapped signals or signals with weak intensity were excluded.72

Figure 4-4 Representative Coomassie Blue-stained 16% Tris-Tricine gels illustrating in vitro proteolysis of $cTnI_{1-77}$ or $cTnI_{135-209}$ by proteases MMP-2 or calpain-2 (N=3). Molar protease-to-substrate are shown above each gel. 2 µg of cTnI was loaded in every reaction lane. Incubations were 2 h at 37 °C. Inhibition of MMP-2 and calpain-2 activities by ARP-100 and MDL-28710, respectively, is also shown.....75

Figure 4-5 Summary of mass spectrometric analysis identifying MMP-2 and calpain-2 cleavage sites within $cTnI_{1-77}$ and $cTnI_{135-209}$. Note that our numbering of cTnI excludes the N-terminal methionine, which is removed and replaced by an acetyl group in post-translational processing.....76

Figure 4-6 Comparison of in vitro proteolysis of $cTnI_{1-77}$ and $cTnI_{135-209}$ in the presence or absence of cTnC by MMP-2 **(A, B)** and calpain-2 (**C, D**) in representative Coomassie Blue-stained SDS–PAGE gel (N=3). Cardiac troponin C is not susceptible to either MMP-2 or calpain-2 proteolysis and appears intact as a single band at ~21 KDa**.** 2 µg of cTnI was loaded in every reaction lane. Molar cTnI-to-cTnC ratio was 1 to 1. The incubation period was 2 h at 37 °C.....81

Figure 4-7 Representative Coomassie Blue-stained SDS–PAGE gels showing in vitro proteolysis of $cTnI_{135-209}$ in the presence of **A)** MMP-2 (N=3) or **B)** calpain-2 (N=3). Molar actin:cTnI ratios are indicated above the gel. Incubation duration was 2 h at 37°C. 2 µg of cTnI was loaded in every reaction lane. MMP-2-to-cTnI ratio was 1:500, and calpain-2-to-cTnI ratio was 1:250.....84

List of Abbreviations

CAD:	Coronary Artery Disease
cTn:	cardiac Troponin
DCM:	Dilated Cardiomyopathy
ELISA:	Enzyme-linked immunosorbent assay
HCM:	Hypertrophic Cardiomyopathy
IDR:	Intrinsically Disordered Regions
IR:	Ischemia Reperfusion
MI:	Myocardial infarction
MMP-2:	Matrix MetalloProteinase -2
MRI:	Magnetic Resonance Imaging
NSTEMI:	Non-ST-elevation myocardial infarction
PBS:	Phosphate Buffered Saline
PCI:	Percutaneous Coronary Intervention
PKA:	PhosphoKinase A
RCM:	Restrictive Cardiomyopathy
STEMI:	ST-elevation myocardial infarction
SVT:	SupraVentricular Tachycardia

Chapter 1. Introduction

1.1 Introduction

The troponin [Tn] protein complex was discovered in 1965 as the critical protein factor in the thin filament linking muscle contraction to intracellular calcium[1]. That was followed by the discovery in 1972 of the distinct subunits of the Tn complex, using a skeletal muscle preparation[2]. The Tn complex consists of three subunits, C, I, and T, whose names are closely related to their functions. TnC is the calcium binding subunit. TnI is the inhibitory subunit that blocks acto-myosin ATPase activity to shut down muscle contraction. Finally, TnT is the tropomyosin binding subunit that interlocks together all the subunits of the troponin-tropomyosin (Tn-Tm) complex.

There are three different isoforms of each Tn subunit: cardiac, slow skeletal and fast skeletal. For TnT and TnI, each of the isoforms is expressed by a separate gene[3]. However, cardiac and slow skeletal muscle forms of TnC share the same isoform, which is distinct from the fast skeletal isoform.

1.2 Structure of the Troponin Complex

Human cardiac TnI is initially expressed as a 210-amino acid protein, but the first methionine residue is subsequently removed and the following alanine is acetylated[4], leaving the complex with 209 amino acid residues and a total MW of 24 kDa. Because of this post-translational modification, there are two alternative numbering systems used for the amino acid sequence of cTnI. I will refer to the N-terminal acetylated alanine as residue 1 in this thesis.

In 2003, the X-ray crystal structure of the human cTn complex was solved[5] (Figure 1 -1). The structure, for the first time, revealed the core of the troponin complex, where subunits C, I, and T come together to form the rigid "IT arm". $cTnI_{39-60}$ forms an alpha helix that binds with high affinity to a large hydrophobic patch on the C-terminal domain of cTnC. $cTnI_{90-135}$ forms a helical coiled coil with $cTnT_{226-271}$, with the $cTnT_{226-271}$ helix interacting with the other side of the cTnC C-terminal domain. This structured IT-arm remains the same throughout the cardiac cycle and is not believed to interact with actin or tropomyosin on the thin filament. While the X-ray crystal structure was a major landmark in the structural biology of the thin filament, it provides no information on the regions of the troponin complex that interact with tropomyosin and actin and is missing more than half of cTnI and cTnT. These missing regions contain almost all of the known cardiomyopathy-associated regions and are suspected to have a large proportion of intrinsically disordered regions that are susceptible to post-translational modifications like phosphorylation and proteolysis[6,7].

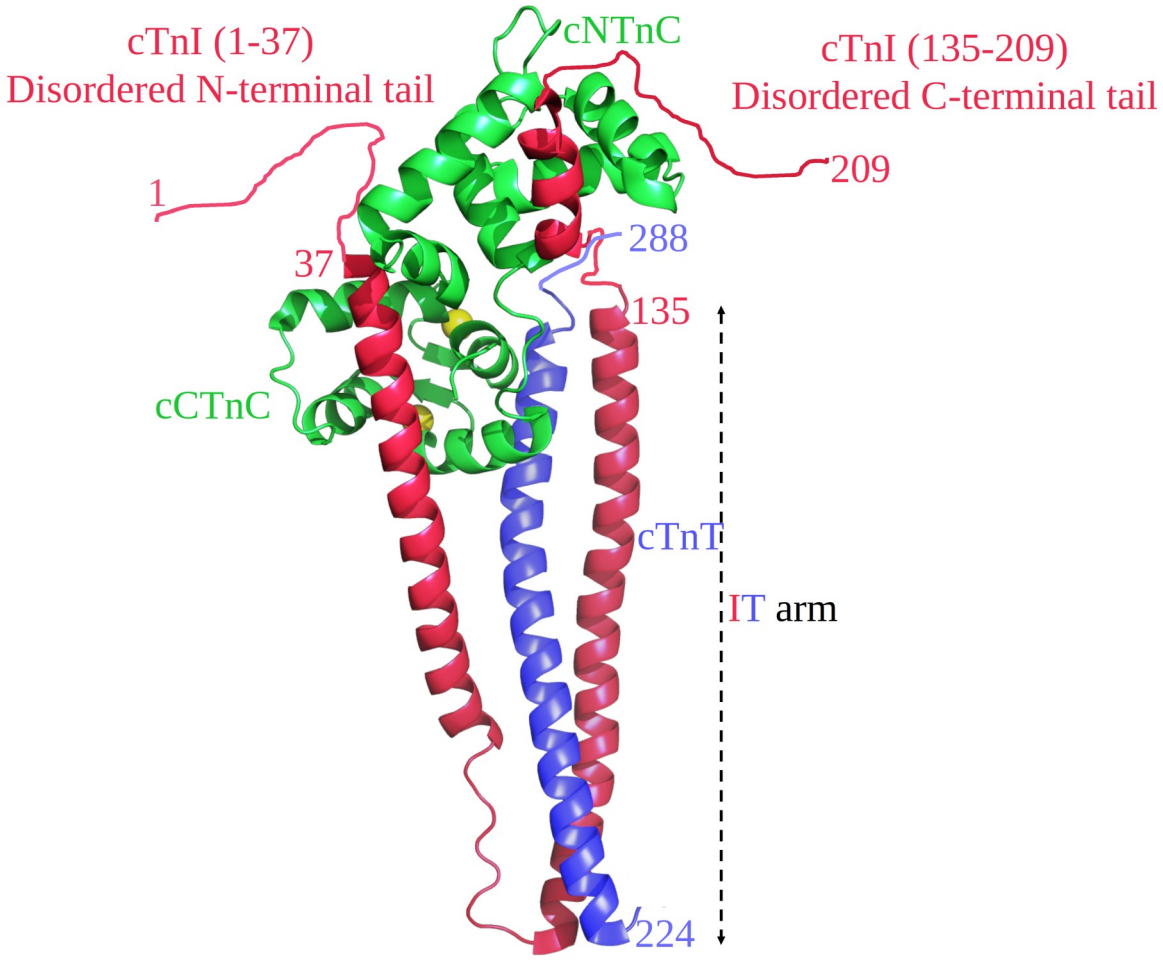

Figure 1-1 Calcium-saturated cardiac troponin complex. Cardiac troponin C (cTnC) consists of an N-terminal domain (cNTnC) and a C-terminal domain (cCTnC) shown in green. Troponin I (cTnI) is shown in red. The intrinsically disordered tails of cTnI (1-37) and (135-209) are drawn manually as scribbles. Figure prepared using PyMOL and structure 4Y99 (PDB code). Calcium ions are shown in both N and C domain of cTnC as yellow spheres. During systole, cNTnC binds calcium and adopts an open conformation that binds the cTnI switch region (146-158) releasing the cTnI (135-209) inhibitory tail from actin and allowing muscle contraction to proceed.

During diastole, the troponin complex anchors tropomyosin into a “blocked” position that obstructs actin-myosin cross-bridging, preventing muscle contraction and promoting relaxation[8]. This anchoring depends on the large N-terminal region of $cTnT_{72-223}$ holding the troponin complex to tropomyosin, while the C-terminal tail of cTnI, residues 135-209, binds to actin to anchor the entire troponin-tropomyosin complex to the blocked position (Figure 1 -2). During

systole, the cytoplasmic calcium concentration increases, and calcium binds to the regulatory N-terminal domain of cTnC, which then binds to the switch region, residues146-158, of cTnI. This releases $cTnI_{135-209}$ from actin, and the troponin-tropomyosin complex falls into a "closed" position on the thin filament that allows actin-myosin cross-bridging and cardiac muscle contraction to proceed[9]. This continues until diastole, when calcium is pumped out of the cell (as well as into the sarcoplasmic reticulum), cTnC releases the switch region, and $cTnI_{135-209}$ binds again to actin to bring troponin-tropomyosin back into the blocked position[9]. Very little is known about the structural details of the interaction between $cTnT_{72-223}$ and tropomyosin and between $cTnI_{135-209}$ and actin. On their own, these regions do not fold into soluble globular domains like the two domains of cTnC. Instead, they are intrinsically disordered, but likely acquire some structure upon binding to tropomyosin and actin, respectively. The small peptide comprised of the cTnI inhibitory region 136 – 147 alone is sufficient to inhibit acto-myosin ATPase activity[10], whereas residues 146 – 158 comprise the key switch region that binds the cTnC N-domain under high calcium concentration as detailed above. cTnI residues 159 – 209 appear to further potentiate the action of the inhibitory region[11].

The first N-terminal 32 amino acids of cTnI are unique to the cardiac isoform and are intrinsically disordered[12]. This tail interacts with the regulatory N-terminal domain of cTnC to modulate its calcium binding affinity. Our lab found that amino acid residues 19-37 are highly positively charged, and these interact electrostatically with the highly negatively charged cTnC N-terminal domain[12]. We proposed that this interaction fixes the N-terminal domain into an orientation that is ideally positioned to bind to the cTnI switch region, and this enhances activation of the thin filament and the calcium sensitivity of the thin filament[11–17].

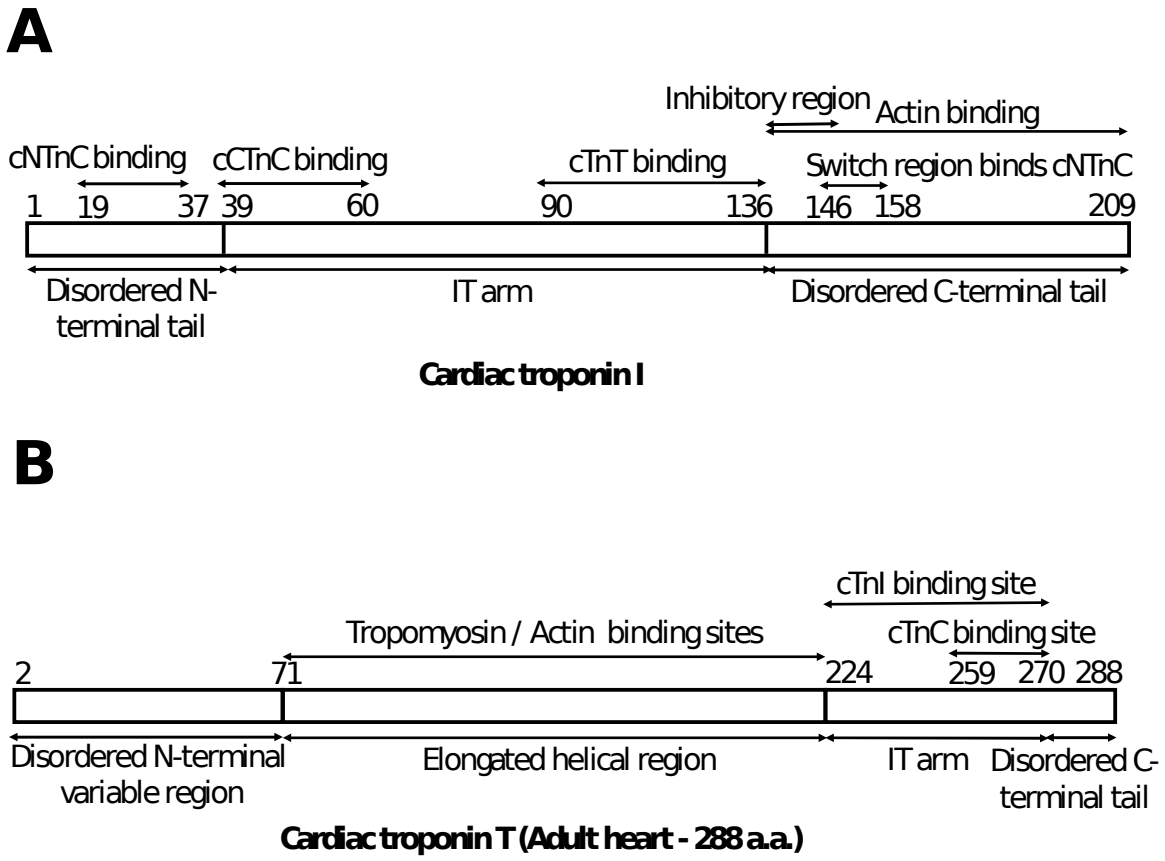

Figure 1-2 The structural and functional regions of cTnI (A) and cTnT (288 a.a isoform) (B) highlighting binding sites to tropomyosin, actin, and troponin subunits above and structural elements below.

cTnT, the tropomyosin-binding subunit of the troponin complex, is a 34–35 kDa protein and its gene contains 15-17 exons[18]. Alternative splicing of exons 4 and 5, located in the N-terminal variable region, generates four different cTnT isoforms: cTnT1 (298 a.a) contains both exons and is the most dominant isoform expressed in the embryonic heart. Exon 4 is spliced out in cTnT2 (293 a.a), which is also expressed in the embryonic heart, but to a lesser degree. In cTnT3 (288 amino acids), exon 5 is spliced out, and over prenatal development, it becomes the most dominant form of cTnT and remains so in the adult heart[13].

The N-terminal hypervariable region (1-71 a.a) of cTnT is not present in the slow or fast skeletal muscle isoforms[19]. The region is very acidic, comprised of mostly aspartate and glutamate residues, so it is expected to be intrinsically disordered. It does not have any known binding sites for either tropomyosin or actin[20]. The middle conserved region of cTnT, comprised of residues 72-223, is also intrinsically disordered, but likely acquires a substantial amount of helical structure upon binding to tropomyosin. The "first tropomyosin binding site" has been localized to cTnT residues 88-127 and binds to the head-to-tail junction of tropomyosin[21]. (Human cardiac tropomyosin is 284 amino acids long and forms a continuous helical coiled coil dimer that lies across 7 actin monomers along the thin filament.). The precise structural understanding of this interaction is controversial, though there is an X-ray crystal structure of a short cTnT-derived peptide (PDB: 2Z5H) bound to the head-to-tail junction of tropomyosin[22]. A second tropomyosin binding site was mapped between cTnT residues 206 to 230[21] and is thought to be near Cys190 of tropoymosin[23]. Apart from its multiple binding sites for tropomyosin, the middle $cTnT_{72-223}$ segment is also believed to contain binding sites for actin that promote activation of actin-myosin ATPase activity[24].

The high resolution crystal structure of the cardiac troponin complex demonstrated the precise binding sites of cTnT with cTnC and cTnI within the "IT arm"[5]. $cTnT_{224-271}$ interacts with $cTnI_{89-135}$ to form a long coiled-coil. A small segment of cTnT, $cTnT_{259-271}$, also interacts with the C-terminal domain of cTnC[5] (Figure 1 -2). The arrangement places the C-terminal tail of cTnT, $cTnT_{275-288}$, directly adjacent to the key $cTnI_{135-147}$ inhibitory region that is essential for shutting down cardiac muscle contraction by binding to actin. The exact role of the intrinsically disordered C-terminal tail of cTnT, $cTnT_{275-288}$ is still unknown, but it is also important in promoting relaxation[25].

1.3 Truncation Studies and Mutational Data of cTnI and cTnT Clarifying the Function of Their Different Regions

1.3.1 The N-terminal tail of cTnI

As the N-terminal 31 amino acids are unique to the cardiac isoform of TnI, this region has been extensively studied to understand its role in cardiac contraction. Truncation mutants of this region have revealed disruption to the capacity of cardiac muscle to compensate for different pathological and physiological stressors.

The first 10 amino acids of cTnI are intrinsically disordered[12] and not known to interact with any other component of the thin filament. An A1V mutation affecting the N-terminal alanine residue was linked to dilated cardiomyopathy (DCM)[26], but this particular mutation was only identified in a single family with remote consanguinity, and the DCM phenotype was manifested only in homozygous individuals, indicating recessive disease. It is possible that this mutation is incidental, rather than causative. Notably, transgenic mice bearing a deletion of the first N-terminal 10 amino acid residues of cTnI showed no evidence of DCM and had anatomically normal hearts, though the authors noted a decrease in maximal force generation[27].

Truncation mutations involving more of the cTnI N-terminal tail would be expected to have a greater effect on cTn function. Knock-in mice lacking the first 28 amino acid residues of the cTnI N-terminal tail had significantly faster rates of relaxation, with rates similar to wildtype mouse hearts under β-adrenergic stimulation[28]. In a related study, replacing cTnI with slow skeletal TnI, which altogether lacks the cardiac N-terminal 31 a.a residues, in transgenic mice, resulted in cardiomyocytes that showed no contractile response to PKA phosphorylation [29].

The cTnI N-terminal tail is the main phosphorylation site in humans[28]. The first studies that revealed the effect of phosphorylation on the heart also uncovered the importance of the cTnI N-terminus to cardiac function[30,31]. It mainly functions to enhance calcium affinity of the regulatory N-terminal domain of cTnC, and phosphorylation at Ser 22/23 attenuates this effect. Phosphorylation at this site is known to result from sympathetic stimulation of the heart through adrenergic β receptors[30]. It is well known that β-adrenergic stimulation of the heart is a crucial regulator of cardiac performance[32]. It enhances contractile force (positive inotropy) and accelerates heart rate (positive chronotropy) and relaxation rate (positive lusitropy)[33]. β stimulation causes cAMP-mediated phosphorylation of many key targets via protein kinase A (PKA)[34]. Phosphorylating myofilament proteins like cTnI and myosin binding protein C decreases calcium sensitivity and enhances cross bridge cycling, respectively, with both effects contributing to the positive lusitropic effect. Phosphorylating sarcoplasmic proteins like phospholamban and ryanodine receptors also mediates positive lusi- and inotropic effects through higher rates of calcium uptake and release kinetics, respectively[35]. Finally, phosphorylating plasma membrane proteins like L type calcium channels further contributes to positive inotropy due to increased calcium influx during action potential[35].

R20C is a mutation in cTnI associated with hypertrophic cardiomyopathy (HCM) in humans[36]. The mutation would be expected to interfere with PKA phosphorylation of Ser22/Ser23. Consistent with these expectations, skinned cardiac muscle fibers with mutant R20C-cTnI exchanged in showed a blunted response to PKA phosphorylation, and increased susceptibility to cleavage by M-calpain compared to wild type was also observed[36]. However, the net inhibitory activity of cTnI was not altered. Both homozygous and heterozygous knock-in mice with the R20C mutation developed HCM[37].

A biophysical study of progressive cTnI N-terminal truncation mutants was performed, analyzing the impact on the calcium sensitivity of actomyosin ATPase activity or calcium release rates from the cardiac troponin complex [38]. Removing up to the first 15 a.a residues did not significantly impact calcium sensitivity or calcium release rates (the new N-terminal sequence was ^{16}APIRRRSS^{23}). More extensive removal significantly decreased calcium sensitivity and abolished PKA phosphorylation effects[38].

1.3.2 The C-terminal tail of cTnI

The C-terminal tail of cTnI, comprising residues 135-209, is one of the most important intrinsically disordered regions for the functioning of the heart. The inhibitory region (residues 136-147) binds actin to shut off cardiac contraction, while the switch region (classically, residues 147-163, but we are redefining it to 146-158 based on the X-ray crystal structure) is bound by cTnC in a calcium-dependent manner to activate cardiac contraction[5,11]. Residues 159-209 are less critical for function, but this region does bind to actin[11,14] and appears to play an important role in promoting cardiac muscle relaxation.

One study examined three different cTnI C-terminal truncation mutants: 1-199, 1-188 and 1-151 versus the wild type in cardiac myofibrils[39]. Native cardiac troponin complexes were exchanged out for excess cTnT, and then the mutant cTnI constructs were diffused in. The authors demonstrated that the wild type and the 1-199 mutant have similar capability to maximally inhibit actomyosin ATPase in a concentration-dependant manner, while the other shorter mutants only partially inhibited it.

One group has made a transgenic mouse expressing a truncated cTnI missing the 17 C-terminal residues[40]. Although expression levels of the mutant transgene only made up < 20% total cTnI

expression, the authors found that the mice had dilated ventricles with depressed systolic function, though no histologic features of dilated cardiomyopathy and no biomarker evidence of heart failure. Further biophysical studies on this mutant using reconstituted cardiac thin filaments revealed that the calcium-bound closed state of tropomyosin-troponin was shifted more towards an activated state compared to the wildtype[41]. The same truncation mutant was found to enhance calcium sensitivity in myofibrils without impacting maximal tension generation compared to the wild type[42].

Perhaps the best indication of the role of the cTnI C-terminal tail is the large numbers of human mutations found in this region associated with HCM[43]. The most common of these mutations are located mainly in the inhibitory region [R140Q - R144G - R144W - R144Q] and the C-terminal actin binding tail [R161Q - R161W - S165F -ΔK182 – R185Q – S198N - ΔG202] as well as a mutation in the switch region [A156V][44–46]. There are also about a dozen mutations in the C-terminal tail associated with restrictive cardiomyopathy[44]. Numerous biophysical studies have shown increased calcium sensitivity and force generation associated with all these mutations when compared to wild type[47]. Additionally, greater enhancement of calcium sensitivity was repeatedly reported in mutations that were associated with restrictive cardiomyopathy (RCM)[48–50]. C-terminal truncations of cTnI were associated with HCM when 8 amino acids were deleted[51], or RCM with the deletion of 42[52] or 15 C-terminal amino acid residues[49].

In conclusion, the cTnI flexible C-terminal tail plays a critical role in promoting cardiac relaxation, which is disrupted upon truncation.

1.3.3 N-terminal region of cTnT

An increased level of N-terminally truncated cTnT was observed in primary cultures of adult cardiomyocytes upon calcium overload[53]. Given that μ-calpain is a calcium-activated protease, selective proteolysis of cTnT could be due to μ-calpain.

Expression of the N-terminally truncated cTnT in transgenic mice hearts preserved overall cardiac function. However, this truncation mutant exhibited moderately reduced velocity of ventricular contraction, which significantly prolonged left ventricular rapid ejection phase and increased stroke volume at high afterload[54].

1.4 Studies of Proteolytic Degradation

Proteolytic digestion of cTnI and cTnT was shown to negatively affect cardiac function beyond the direct tissue damage caused by the original insult, as in ischemia reperfusion (IR) injury. The main culprit enzymes that have been suggested are intracellular matrix metalloproteinases (MMPs), calpains, and caspases.

MMP-2 is the main cardiac member of this Zn-dependant family of 25 endopeptidases[55]. As its name suggests, it was originally found to digest the extracellular matrix. However, intracellular localization and intracellular targets have since been demonstrated as well[56]. MMP-2 is involved in both normal cardiac development and pathological states. Being produced as an inactive zymogen, it requires activation by either proteolytic removal of its pro-peptide domain or post-translational modification by oxidative stress to remove an inhibitory cysteine sulfhydryl group from the catalytic zinc ion[57]. Both processes likely occur in IR injury, myocardial ischemia, and heart failure. Increased MMP-2 activity has been correlated with myocardial dysfunction and has been reported in various animal models for aging hearts, hypertension, and severe

tachyarrhythmia[58,59]. In addition, it was shown to be activated as early as 1 minute after releasing the aortic cross clamp in patients undergoing coronary artery bypass grafting (CABG)[60]. Thus, MMP-2 appears to be an important intracellular protease activated in a variety of pathological conditions.

cTnT and cTnI, but not cTnC, were shown to be degraded by MMP-2 in a concentration dependent manner and inhibited by MMP inhibitors[56]. Inhibiting MMP-2 with doxycycline or O-phenanthroline improved myocardial recovery from IR injury in rat hearts[61] which correlated with prevention of IR-induced cTnI degradation[56].

Calpains are a family of 15 calcium-dependent proteases that are mainly localised to the cytosol and mitochondria[62]. Two isoforms have been linked to ischemia and IR injury; μ-calpain and M-calpain. They are mainly activated by increased intracellular calcium concentrations[63,64]. In many cardiac pathologies like ischemia and IR injury, cellular calcium handling is altered leading to elevated cytosolic calcium levels and calpain activation[64]. Calpain is known to mediate proteolysis of many sarcomeric proteins including cTnI and cTnT[65,66].

Stunned myocardium and skinned trabeculae incubated with calpain both showed a cTnI degradation band that was prevented by calpastatin[67]. In isolated rat hearts, even though calpain was translocated to the membrane during ischemia, it was not activated until the pH was normalized upon reperfusion. Myocardial protection was achieved with calpain inhibitor MDL-28170 early in reperfusion, significantly reducing infarct size[68]. This observation was confirmed in porcine hearts using a different inhibitor, A-705253, 15 minutes before ischemia and during reperfusion. Reduced infarct size and improved hemodynamics and contractility were observed in the intervention pigs compared to the control ones[69]. Notably, μ-calpain seems to rapidly

proteolyse cTnT and cTnI in purified cTn complex[70] more than in the intact myofibril, where μ-calpain effect is more pronounced in Z-line proteins like desmin [71], which might rather explain the functional deterioration after reversible injury attributed to calpain.

Caspases (or cysteine aspartases) are a family of twelve endoproteases that are secreted as zymogens and require activation to attain their catalytic activity[72]. They play a crucial role in regulating cellular homeostasis, apoptosis, and inflammatory responses. Caspases act mainly by hydrolysing the peptide bonds following aspartic acid residues[73]. Caspase inhibitors showed promising effects in the reduction of brain IR injury after stroke in neonatal rats[74]. Caspase-1 expression was upregulated in a rat heart failure model[75], while deletion of the same endogenous caspase ameliorated post-MI heart failure. In addition, caspase knockout mice had smaller infarct sizes after myocardial IR injury[75]. These beneficial effects were explained in terms of inhibiting apoptosis. One study examining troponins as a direct substrate for caspases showed cTnT fragmentation after incubation of the cTn complex, though not the individual subunits, and rat cardiac myofilaments with caspase-3[76]. Moreover, caspase inhibitors abolished cTnT proteolysis. More studies are needed to further explore the role of caspases in proteolyzing myofibrillar proteins beside its role in apoptosis.

1.4.1 Myocardial ischemia and ischemia reperfusion injury [mainly cTnI C-terminal degradation and cTnT N-terminal degradation]

In global IR injury in rat hearts, cTnI was found to be partially proteolysed[67,77]. The degraded fragments' molecular weights were between 12 and 23.5 KDa, while higher MW fragments were observed and thought to be due to covalent attachment to cTnT and cTnC, though this was not confirmed. These modifications, especially proteolysis, correlated with myofibrillar dysfunction.

In addition, *in vivo* cTnI C-terminal degradation was shown to correlate with prolongation of ischemia in rat hearts, with a proposed cut site between 188-199[77]. With more severe ischemia - enough to cause necrosis - followed by reperfusion, more extensive degradation was noted in cTnI and other myofilament proteins, with a specific truncation estimated to remove the C-terminal 17 a.a residues of cTnI[78]. This truncation was shown to lead to functional impairment of the heart in *in vivo* and *in vitro* studies and decreasing the maximal response to calcium[40,42]. This degradation pattern was proposed to be the main contributor to the impaired cardiac function seen in stunning [15 min ischemia and 45 min reperfusion]. Other studies have also correlated cTnI degradation with a decline in functional performance, and protease inhibition prevented stunning[56,79,80].

One study found that proteolysis of the cTnI C-terminal tail was affected by phosphorylation. Pseudophosphorylation at Ser199 by mutating the Ser to Asp [phosphorylation-mimic] or Ala [dephosphorylation-mimic] caused altered cTnI susceptibility to preoteolysis and enhanced myofilament Ca sensitivity[65]. Moreover, μ-calpain was found to strongly proteolyse cTnT and cTnI, not cTnC, in both purified protein form and in myocardial cryosections, an action that was modified by different phosphorylation enzymes like PKA and PKC[70]. Further studies are needed to clarify the underlying mechanisms of cTnI phosphorylation-proteolysis cross-talk.

However, many subsequent studies questioned the role of cTnI proteolysis in IR injury[81]. No *in vivo* degradation of cTnI was associated with ischemia or IR injury in swine models[82,83]. In rabbit hearts, only minimal cTnI degradation was observed after extensive ischemia, which did not vary with functional recovery of the stunned hearts[84]. Furthermore, canine hearts displayed differential cTnT degradation, but not cTnI degradation, after ischemia[85], which again did not correlate with the cardiac dysfunction. In addition, some authors believe that cTnI degradation in the context of

IR injury is mainly due to increased preload. Eliminating elevations in preload after global ischemia-induced stunning prevented cTnI degradation[86]. It was concluded that elevations in preload produced in the isovolumetric heart preparations rather than the effect of reversible ischemia was independently responsible for cTnI degradation. In this study, increased preload in isolated rat hearts was associated with the appearance of cTnI degradation products which seemed to be due to calpain cleavage. Inhibiting calpain with calpeptin led to improved ventricular function.

Studies of myocardial tissue samples from elective cardiac bypass surgery patients did not show consistent patterns of cTnI proteolysis occurring during periods of ischemia followed by reperfusion[87]. cTnI proteolysis was observed in many patients, but the degraded band did not show a consistent pattern before and after cross clamping (degradation appeared in 10, disappeared in 12, and did not change in 12 patients). Perhaps degradation implies an underlying cardiac ischemic condition.

Several *in vivo* experimental models demonstrated that the structural integrity of cTnT in cardiac myocytes is determined by its incorporation into myofilaments. In adult dog hearts, cTnT undergoes rapid turnover, and the half-life of cTnT is estimated to be approximately 3.5 days[88]. It was determined that cTnT that is not associated with the myofilament is rapidly degraded in cardiomyocytes[89]. This potent degradation of non-myofilament-associated cTnT might be critical for maintaining normal protein stoichiometry of the myofilament regulatory system[90]. Without myofilament incorporation, the conserved C-terminal and middle regions of cTnT induced cell apoptosis, whereas the N-terminal variable region did not exhibit any apoptotic effects[89]. Proteolytic cleavage of cTnT by activated caspase-3 was shown in apoptotic rat cardiomyocytes to remove 92 amino acids from the N-terminal variable region and a part of the middle conserved

region, producing a 25 kDa truncated cTnT fragment[76]. Caspase-3 mediated cleavage was shown to have deleterious effects on cardiac muscle contractile function, myofibril force generation, and myosin ATPase activity[18].

The variable N-terminal region of cTnT is highly susceptible to proteolysis by μ-calpain during myocardial IR injury[91]. During acute myocardial IR injury and left ventricular pressure overload *in vitro*, myofilament associated μ-calpain selectively cleaves the N-terminal variable region (amino acids 1-71) in mouse, rat, and pig hearts[91]. This proteolysis selectively removes the entire N-terminal variable region, but preserves the conserved region of cTnT, unlike caspase-3-mediated cleavage, as discussed above[18,91]. The removal of the N-terminal region has no significant effect on the binding affinity of cTnT for tropomyosin. Extending the deletion from the N-terminal 1-71 to 1-91 amino acids (getting into the conserved middle region) results in increased calcium sensitivity of the troponin complex and weakened binding affinity for tropomyosin[92,93].

1.4.2 Microgravity [Mainly cTnI N-terminal degradation]

The microgravity model exerts stress on the cardiovascular system by redistributing blood volume towards the head[94]. In humans, this state is achieved in astronauts and objects floating in space. On Earth, this condition could be transiently experienced in a free-fall situation, like going over a big hill. It has drawn extensive interest because of the cardiovascular changes that occur in astronauts[95]. Neurohormonal adaptation mechanisms during microgravity lead to an decreased indices of cardiac function like stroke volume and left ventricular end diastolic volume[96]. Although the underlying molecular changes are not fully elucidated, contractile proteins are structurally and functionally modified in cardiac adaptation to microgravity. In a 14-day tail-suspended rats simulating microgravity, cardiac contractile force was decreased compared to

control rats, despite no changes in calcium sensitivity[97]. However, the major finding of the study was upregulation of a ~22 kDa N-terminally truncated fragment of cTnI when the rats were tail suspended for four weeks. Sequencing revealed targeted cTnI proteolysis producing cTnI fragments 1-25, 1-26, and 1-29[97], which is consistent with the calpain cleavage sites that we have mapped. In another study of tail suspended rats, increased cTnI degradation was observed in the N-terminal end, which was associated with decreased myocardial response to the β stimulant, isoproterenol[98]. This was associated with decreased calcium sensitivity and PKA-induced phosphorylation. This was not surprising as proteolysis at this position would eliminate the phosphorylation site, the main site in cTnI affected by beta-adrenergic stimulation. Similarly, *ex vivo* hearts from 4-week suspended rats showed less enhanced contractility with isoproterenol infusion[99]. Evidence has also been accumulating about translocation and activation of M-calpain associated with microgravity[100,101], and cTn degradation in this animal model was partially inhibited by non-specific inhibitor PD150606[102], an alpha-mercaptoacrylic acid derivative that was found to inhibit both calpain and MMP-2[103, 104, 105].

1.4.3 Miscellaneous conditions

cTn degradation is well documented in cardiac injury, and the available clinical assays are able to detect both intact and degraded forms[106]. One study looked into cTnI degradation in the context of iatrogenic induction of myocardial necrosis in hypertrophic obstructive cardiomyopathy patients receiving percutaneous transluminal septal myocardial ablation[107]. The degradation pattern in this study matched that of STEMI patients[108] in addition to two more bands. cTnI degradation has been reported in the failing heart and was shown to be altered by other factors like when Ser199 is hyperphosphorylated[109]. Further studies in transgenic pseudophosphorylated mice revealed significantly less C-terminal proteolysis after IR injury[110].

In vivo experiments done by the same group, where the same pseudophosphorylation was introduced to human cardiac myofilaments resulted in significantly less μ-calpain induced percentage of proteolysed cTnI[65].

A few studies have described the underlying remodelling mechanisms that happen in atrial fibrillation including degradation of myofibrillar proteins. Decreased calcium uptake, lowered pH after relative atrial ischemia and increased calcium influx all lead to increased cytosolic calcium which in turn activates divalent dependant proteolytic enzymes, like calpain[111]. Attenuating cTn degradation and improving cardiac dysfunction was achieved using calpain inhibitors[112]. The calpain inhibitors used in the experiment have shown inhibitory effect on MMP-2 as well[103], so a role for MMP-2 cannot be excluded.

1.5 Role of Troponins as a Biomarker of Cardiac Injury

In the heart, prolonged ischemia can lead to irreversible cellular necrosis, a condition known as myocardial infarction (MI). Irreversible death of cardiomyocytes is accompanied by the release of many of its components, some of which are unique to the heart, including cardiac troponins. cTn is released into the bloodstream, where it is reliably detected, making the cTn assay the current gold standard for the detection of myocardial injury and diagnosis of MI. Given that cardiac and slow skeletal TnC are the same isoform, detection of cTnC in the bloodstream would not specifically indicate if the injured muscle is cardiac or slow skeletal. Currently available cTn commercial assays target cTnI or cTnT for diagnosing cardiac injury. Thus, cTnI and cTnT could potentially serve as useful probes of proteolysis and post-translational modifications that occur in the human heart during various disease processes.

Since the emergence of the first cTnI assay in 1987[113] followed by the first cTnT assay in 1989[114], further refinements have resulted in the development of high sensitivity assays. cTn assays have shown superiority in terms of specificity to all previously used biomarkers for diagnosing MI like LD, CK-MB and even ECG[115–117]. Enhancing the analytical sensitivity of the assay allows measurement of cTn even in apparently healthy individuals, raising issues of what are clinically significant cut-off levels. The current guidelines recommend using the high sensitivity assays to diagnose myocardial injury, now requiring only a small acute elevation of cTnI or cTnT above the 99th percentile upper reference limit for a healthy population[118]. These high sensitivity assays measure cTn concentrations fivefold to 100-fold lower than conventional ones, should be able to detect cTn concentrations below the 99th percentile in >50% of normal individuals, and should have imprecision measured as the coefficient of variation <10% at the 99th percentile value[119]. The pathological definition of MI encompasses irreversible necrosis of the cardiac muscle cells due to prolonged ischemia. The clinical definition, however, has evolved along with the evolution of cTnI and cTnT assays. The most current Fourth Universal Definition of MI [118,120] acknowledges that cTn elevations are possible in reversible cardiac conditions without actual infarction, challenging the traditional view that cTn elevations necessarily require necrosis. Moreover, the cTn elevations are not necessarily reflective of an acute injury as chronic conditions might lead to stable elevations, such as chronic kidney disease or structural heart disease[121]. A new category of “myocardial injury” has been suggested. Strenuous exercise[122], atrial pacing induced tachycardia[123], myocarditis[124], and pericarditis[125,126] are all conditions with documented cTn release of unknown mechanism, though many theories have been suggested. Damaged cell membranes that allow leaking of cTn, cytoplasmic blebbing and microparticle

formation, activated cellular apoptosis, sarcolemmal disruption by lysosomal membranes, and accelerated turnover of cardiomyocytes have all been suggested as possible mechanisms[127,128].

In patients with supraventricular tachycardia (SVT) without significant underlying coronary artery disease (CAD), almost a third exhibited elevated cTnT levels[129]. As the level only correlated with the maximum heart rate during the SVT episode, shortened diastole resulting in minor subendocardial ischemia was proposed as the underlying mechanism in these patients. Similarly, no significant differences in CAD diagnosis were observed in another cohort of SVT patients. However, with longer follow up of patients in the GISSI-AF trial, elevated cTnT was related to recurrent atrial fibrillation in patients who recovered from recent atrial fibrillation[130].

cTns are not only released in cardiac diseases, but also in a wide range of non-cardiac conditions that can cause myocardial injury. For instance, elevated cTn levels have been detected early in the course of acute ischemic stroke. Intact and seven degradation TnI fragments were found in serum samples from acute ischemic stroke patients[131]. In general, elevated cTnI in stroke patients was found to be associated with poorer short term prognosis[132] and even predictive of new onset of atrial fibrillation[133].

Examination of various human blood samples reveals extensive degradation of cTn. cTn in the blood of MI patients was found to be comprised of a heterogeneous mixture of free cTnT, binary cTnC-cTnI complexes, and ternary cTnC-cTnI-cTnT complexes, in addition to proteolytic fragments of different MWs[134,135]. cTnT cleavage was also detected in human sera, whether in samples drawn from MI patients or after incubating cTnT in sera from controls[136]. Extensive proteolysis has been shown in MI patients using gel filtration chromatography[135,137]and by immunoblots[134]. In the cardiomyocyte cTnT is mainly proteolysed by μ-calpain between R68 and

S69 producing a 29 kDa fragment, and that cleavage is modulated by PKA-mediated phosphorylation[70]. However, it was demonstrated in a more recent study that thrombin also cleaves at this particular site, which is prevented by incubation in heparin plasma[136]. In fact, the intact form was shown to quickly disappear from serum samples within 12 hours after MI, with only degradation fragments being detected afterwards[138]. A western blot analysis in a similar patient cohort confirmed these observations and showed the time dependence of degradation[139]. A more recent study on human serum samples from human MI patients identified an additional cleavage site in cTnT between Gln189 and Lys190[140].

In a longitudinal study, up to 100% of end stage renal disease patients at some time points were found to have elevated cTnT levels and higher cTn levels were related to higher incidence of adverse events[141]. Examining the sera of chronic kidney disease (CKD) patients undergoing dialysis revealed extensive cTnT fragmentation[142]. It is believed that cardiac troponin is too big to be excreted through the kidney. However, isolated cTnT or fragments thereof might be candidates for renal clearance. Thus, the observation of elevated levels of fragmented cTnT in CKD patients would explain its elevation in the serum due to impaired renal clearance in the absence of apparent cardiac conditions. This issue is most pronounced for cTnT, which showed higher concentrations than cTnI in CKD patients with a history of cardiac MI[143]. However, both cTnI and cTnT show elevated levels in CKD patients, and these correlated with left ventricular mass and estimated GFR, and not with coronary artery calcification as measured by CT.

Since cTnT is readily cleaved by thrombin in the serum, and since its cleavage products are cleared by the kidney, serum cTnI may be a better probe of intracellular proteolysis in humans. In contrast to cTnT, for which there are only two available commercial assays (Roche and the more recent Radiometer assay), there are many different cTnI assays, which use different

antibody epitopes for capture and detection. There is currently no universal standardisation for the cTnI assays[144]. The heterogeneous mixture of proteolytic fragments released into the blood likely contributes to major discrepancies between different commercial assays[134] (epitopes detected by different commercial assays can be can be viewed in this IFCC document: http://www.ifcc.org/media/276661/IFCC%20Troponin%20Tables%20ng_L%20DRAFT%20Update%20NOVEMBER%202014.pdf).

Factors that might affect cTnI degradation are infarct zone size, reperfusion rate, time elapsed between injury onset and sample collection, and other biochemical features, like traumatic sample collection and sample handling methods that affect protease load in the sample[106]. However, recent studies (including chapter 3 of this thesis) have suggested that proteolytic degradation of cTnI is an accurate reflection of its state in the cardiomyocyte[145,146].

Given the complexity of the cTn complex structure, and the wide variety of modifications that occur in different regions of its components, detecting the different fragments can be challenging and the interpretation of its signal might become confusing and misleading when clinicians try to fit it into the clinical context. Better characterization of the modifications in cTn and unraveling the underlying mechanisms of the modifications has potential for enhancing their utility in cardiac diagnostics. In one study, the authors detected extensive degradation of cTnI after incubation in necrotic cardiac tissue and in AMI patients' sera at the N- and C-termini, while the most stable part was noted to lie between 30-110[106], which corresponds roughly to the well-structured region of cTnI is made up of residues 39-134. In a more recent study examining STEMI patient serum samples over the first 36 hours from symptom onset, extensive proteolysis of both N- and C-terminal tails[145]. We recently examined (in chapter 3 of this thesis) cTnI fragments released in the sera of serum troponin-positive patients with a variety of underlying

conditions[146]. A modified assay was developed to quantify cTnI using antibodies that detect the N-terminal tail, structured core, or C-terminal tail, thus distinguishing between intact cTnI and cTnI that was proteolyzed. Our study showed that the degree of proteolysis, particularly at the C-terminal tail, increased with increasing severity of ischemia, with the highest degree of proteolysis observed in STEMI patients, and lower degrees observed in NSTEMI patients and type 2 MI patients. The study suggested that benign causes for elevated cTnI (like peri-procedural elevations detected incidentally) can give abnormally high readings by the traditional assay, since intact non-degraded troponin is more readily detected by most commercial assays (which make use of N- or C-terminal epitopes for antibody binding). On the other hand, a severe infarct could be underestimated by the cTnI level due to extensive proteolysis of the cTnI N- or C-terminus. Thus, accounting for troponin degradation should give a more reliable indication of infarct severity than the troponin levels measured by the conventional assays. As well, our study suggests that it may be possible to derive important clinical information about the disease process impacting the cardiomyocyte from which the cTnI was released.

A crucial area for future research is mapping the exact cleavage sites. Mass spectrometry could be ideal to identify the degradation patterns under different pathological condition. Additionally, identifying the responsible proteases with unbiased experiments is needed.

Cardiomyocyte intracellular proteases like MMP-2 or calpain are plausible therapeutic targets to prevent or attenuate ischemia-reperfusion injury in MI patients. Despite there being more than two dozen MMP inhibitors available, none of them are used in clinical practice due to a variety of side effects[147]. In this regard, it is interesting to note that doxycycline , a commonly used antibiotic that is also a weak inhibitor of MMP-2, showed promising effects on imaging like

reduced end-diastolic volumes index, infarct size, and infarct severity[148], in a recent Italian clinical trial (TIPTOP) [149].

1.1 Objectives and Hypotheses:

Within proteins, intrinsically disordered regions (IDRs) are highly exposed and susceptible to protein-protein interactions, making them highly important for function and regulation. The C-terminal tail of cTnI is an example of an important IDR, alternating between binding partners, actin and cardiac troponin C, to control the cardiac cycle. My overall hypothesis for the thesis is as follows:

- As an IDR that forms critical protein-protein interactions, the C-terminal tail of cTnI (135-209) would be expected to be susceptible to enzymatic proteolysis. Because increasing severity of cardiac injury leads to progressively greater activation of proteases, the proteolytic digestion pattern of cTnI (or lack thereof) will inform us about the severity of the underlying injury. This has implications for the physiologic function of cTnI as well as its use as a biomarker for cardiac injury.

1.1.1 Combining a PagP fusion protein system with nickel ion-catalyzed cleavage to produce intrinsically disordered proteins in E. coli.

As intrinsically disordered regions (IDRs) are solvent-exposed and potentially very susceptible to proteolysis, it can be exceptionally difficult to express and purify them in the lab. We have been developing the use of the integral membrane protein, PagP, as a novel fusion partner to

direct the expression of IDRs into inclusion bodies, protecting them from proteolysis. The target IDR is connected to PagP by a short linker containing the sequence: SRHW. This sequence was shown to be particularly susceptible to nickel ion-catalyzed peptide bond hydrolysis under denaturing conditions. Chapter 2 tested the following hypothesis:

- The novel fusion protein, PagP, combined with nickel ion-assisted hydrolysis, is an effective method for producing the disordered C-terminal tail of cTnI in *E. coli* bacteria.

Chapter 2 sought to achieve the following objectives:

1. Protein expression and purification of the cTnI disordered C-terminal tail (135-209) fused to PagP. We demonstrate that our fusion protein is more than 95% pure after nickel affinity chromatography.
2. Nickel ion-catalysed removal of cTnI (135-209) from its fusion partner. We demonstrate efficient and specific cleavage only at the N-terminal side of the target sequence SRHW (no additional fragments were observed).
3. Isolation of cTnI (135-209) revealed a final yield of 15 mg from 1 L M9 minimal media. Characterisation by MALDI-TOF mass spectrometry and NMR spectroscopy confirmed the target protein MW with no additional amino acid modifications to the protein.

1.1.2 Degradation of serum cTnI C-terminal tail as a more specific marker for the severity of myocardial infarction

The cTn assay is the current gold standard for diagnosing MI. However, it is not entirely specific for the focal necrosis produced by a type I MI, a life-threatening condition that entails abrupt and

focal loss of blood supply causing a region of cellular necrosis. cTn elevations have been detected in reversible cardiac injury without radiologically detectable infarct. As previous studies have shown that cell death activates intracellular proteases, Chapter 3 tested the following hypothesis:

- It has already been established that serum cTnI is proteolytically degraded in the setting of MI. We postulate that cTnI released in focal infarct will be more proteolytically degraded than that released by milder ischemic processes.

1.1.3 Determining the structure of cTnI C-terminal tail (135-209) alone and in the presence of actin using NMR spectroscopy

Chapter 4 tested the following hypothesis:

- The C-terminal tail of cTnI(135-209) is intrinsically disordered and acquires a more structured form upon interacting with actin

Producing pure amounts of the C-terminal tail of cTnI (135-209) as described in chapter 2 enabled us to use solution NMR to achieve the following objectives of chapter 4:

1. Examining the structure of free cTnI (135-209) using solution NMR confirmed the disordered nature of this region. Secondary structure analysis using the chemical shift analysis program δ2D revealed α helical propensity especially in the residues (150-159).
2. Investigating the structure of the C-terminal tail in the presence of monomeric actin-DNase I demonstrated rigidification along its entire length, but especially in the region

corresponding to the inhibitory region, switch region, and “second actin binding site” (residues 135-177).

Chapter 2. Combining a PagP fusion protein system with nickel ion-catalyzed cleavage to produce intrinsically disordered proteins in *E. coli*

2.1 Abstract

Many proteins contain intrinsically disordered regions that are highly solvent-exposed and susceptible to post-translational modifications. Studying these protein segments is critical to understanding their physiologic regulation, but proteolytic degradation can make them difficult to express and purify. We have designed a new protein expression vector that fuses the target protein to the N-terminus of the integral membrane protein, PagP. The two proteins are connected by a short linker containing the sequence SRHW, previously shown to be optimal for nickel ion-catalyzed cleavage. The methodology is demonstrated for an intrinsically disordered segment of cardiac troponin I. cTnI[135-209]-SRHW-PagP-His_6 fusion protein was overexpressed in *E. coli*, accumulating in insoluble inclusion bodies. The protein was solubilized, purified using nickel affinity chromatography, and then cleaved with 0.5 mM $NiSO_4$ at pH 9.0 and 50°C, all in 6 M guanidine. Nickel ion-catalyzed peptide bond hydrolysis is an effective chemical cleavage technique under denaturing conditions that preclude the use of proteases. Moreover, nickel-catalyzed cleavage is more specific than the most commonly used agent, cyanogen bromide, which cleaves C-terminal to methionine residues. We were able to

produce 15 mg of purified cTnI[135-209] from 1 L of M9 minimal media using this protocol. The methodology is more generally applicable to the production of intrinsically disordered protein segments.

2.2 Introduction

Intrinsically disordered regions (IDRs) are protein segments that lack a fixed three-dimensional structure under physiologic conditions. Genomic analyses indicate that >30% of eukaryotic proteins contain at least one disordered region spanning 50 residues or more[150]. IDRs are solvent-exposed and susceptible to post-translational modifications such as phosphorylation and proteolysis. Thus, they are highly important in the regulation of numerous biological processes and cellular signal transduction[151].

It is of great interest to determine how post-translational modifications of IDRs gives rise to changes in function, but the structural malleability of IDRs can make biophysical characterization difficult[152]. Producing large quantities of pure intrinsically disordered proteins can also be challenging due to their susceptibility to proteolytic digestion both during expression and purification stages[153]. One solution is to target IDRs to inclusion bodies, an old method that is used to mass-produce a number of clinically important peptides like insulin[154]. Inclusion bodies are dense particles of aggregated (and usually misfolded) protein, a form that is largely protected from proteolytic enzymes[155]. The strategy allows for easy purification, since inclusion bodies can be separated from other cellular components through centrifugation. The primary disadvantage of producing proteins from inclusion bodies is that they are misfolded and have to be reconstituted into an active folded form[156]. Of course, this is not an issue for IDRs, suggesting that it might be an ideal strategy for their production.

Many proteins have been used as fusion partners to direct the expression of target proteins into inclusion bodies[157]. We previously developed a new fusion system based on PagP for this purpose[158]. PagP is a β-barrel integral membrane protein found in the outer membranes of many pathogenic Gram-negative bacteria[159]. It is directed to the outer membrane by a signal sequence, but when the signal sequence is deleted using recombinant DNA techniques, the misdirected protein accumulates in cytoplasmic inclusion bodies[160]. We used our PagP fusion protein to produce large amounts of a fragment of human cardiac troponin I, cTnI[1-71], which contains a large intrinsically disordered region spanning residues 1-38[12]. Our PagP fusion protein was more effective at targeting large constructs into inclusion bodies than the commercially available fusion protein system based on ketosteroid isomerase (KSI) as a fusion partner, making feasible isotopic enrichment and multinuclear multidimensional NMR studies of cTnI[1-71][12].

One challenge of using fusion proteins for protein expression is that the fusion partner must be cleaved and removed from the target protein. This is especially challenging in the case of inclusion body-targeted expression, because the inclusion bodies are usually solubilized in harsh denaturants or detergents[161], so that enzymatic cleavage (for example, with TEV protease or thrombin) is not possible. Cyanogen bromide (CNBr) is the most commonly used chemical cleavage technique[158], given that it is specific and highly effective even at room temperature. Cyanogen bromide cleaves peptide bonds C-terminal to methionine residues[162], though with reduced efficiency when the methionine is preceded by serine or threonine. The main disadvantage of CNBr cleavage is that the target protein of interest cannot contain internal methionine residues.

In our previous work expressing PagP-cTnI[1-71]-His_6 fusion protein, we used CNBr as the peptide bond-cleaving agent[158]. Achieving near-100% cleavage was challenging, but cleavage

was more complete when steps were taken to ensure that methionine residues were fully reduced. Another issue was that CNBr predictably cleaved PagP at multiple methionine-containing sites, yielding multiple fragments. This did not create any issues for our construct, which had a C-terminal His-tag that facilitated purification of cTnI[1-71]-His6 from fragments of PagP.

One research group has recently discovered that aqueous nickel ions can be used to selectively cleave the peptide bond N-terminal to the sequence S/T-X-H-Z, where "S/T" can be serine or threonine and "H" is histidine. The cleavage is most effective when "X" is a positively charged residue (R or K) and "Z" is I, K, L, R, or W[163]. The reaction is favoured by high temperatures, high Ni^{2+} concentrations, and alkaline conditions. It was demonstrated that incorporation of the sequence $SRHWAPH_6$ into the C-terminus of recombinant SPI2 protein yielded a His-tag that could be purified via immobilized metal affinity chromatography and then removed by Ni^{2+}-catalyzed cleavage [164].

In the current study we combine our previous work with PagP as a fusion protein partner with nickel ion-catalyzed cleavage. Nickel ion-catalyzed cleavage is ideally suited to the PagP fusion protein system because it can be carried out under denaturing conditions. Moreover, the cleavage reaction is selective for sequences in the form S/T-X-H-Z, which is less common in protein sequences than the individual methionine residues targeted by CNBr. Thus, our system should be readily applicable to any intrinsically disordered protein segment, including those that include internal methionine residues. We demonstrate the utility of our new construct in producing an unstructured fragment of cardiac troponin I, cTnI[135-209], which contains three internal methionine residues.

2.3 Materials and Methods

2.3.1 Design of PagP fusion partner plasmid

A novel plasmid, pELECTRA-PagP-His_6, was developed with DNA 2.0 for expressing target proteins fused to PagP-His_6. In contrast to our previous system[158] , the current plasmid fuses the C-terminus of the target protein to the N-terminus of PagP. Thus, when a nickel cleavage-sensitive SRHW site is added to the target protein C-terminus, nickel-mediated proteolysis will yield the target protein with its native C-terminus (see Figure 2 -3 A). The SRHW site was not included in pELECTRA-PagP-His_6, so that any cleavage site (whether for chemical or enzymatic cleavage) could be introduced onto the C-terminus of the target protein through recombinant DNA methods and inserted into the pELECTRA-PagP-His_6 plasmid. Because of this, all the internal methionine residues in PagP were also mutated to other residues (corresponding to other residues found in other Gram-negative bacterial homologues, see Figure 2-1B), so that a methionine residue could also be included in the linker sequence, allowing separation via cyanogen bromide cleavage without fragmentation of the PagP-His_6 fusion partner (although this strategy was not used in the current study).

(A)

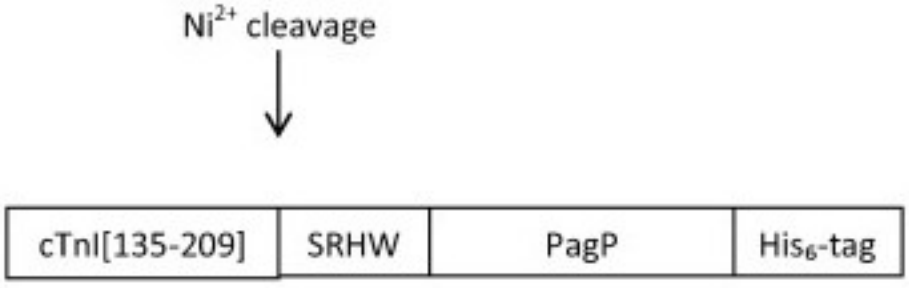

(B)

```
MRGKFKRPTL RRVRISADAM MQALLGARAK ESLDLRAHLK QVKKEDTEKE NREVGDWRKN

        70         80         90        100        110        120

IDALSGMEGR KKKFESSRHW GNADEWLTTF RENIAQTWQQ PEHYDLYIPA ITWHARFAYD

       130        140        150        160        170        180

KEKTDRYNER PWGGGFGLSR WDEKGNWHGL YAIAFKDSWN KWEPIAGYGW ESTWRPLADE
```

Figure 2-3 (A) The cTnI[135-209]-SRHW-PagP-His$_6$ fusion protein. The SRHW sequence allows for nickel-catalyzed peptide bond cleavage N-terminal to the serine residue, allowing separation of the cTnI[135-209] target protein from SRHW-PagP-His$_6$.
(B) Amino acid sequence of cTnI[135-209]-SRHW-PagP-His$_6$. The nickel-sensitive SRHW sequence, His$_6$ tag, and former methionine residues in PagP mutated to other residues are highlighted in red.

The pELECTRA-PagP-His$_6$ plasmid contains a lacI repressor gene and a T5 promoter flanked with lacO sites, allowing for IPTG-inducible expression in any *E. coli* host (the T5 promoter utilizes native *E. coli* RNA polymerase). It also incorporates ampicillin selection, a high copy number origin of replication, and a strong ribosome binding site (Figure 2 -4). The pELECTRA –PagP-His$_6$ plasmid is designed to allow insertion of any target sequence using the patented Electra cloning system of DNA 2.0 (see DNA 2.0 website: https://www.dna20.com/products/expression-vectors/electra-system#2). The double-stranded target sequence must have a 5'-ATG overhang at one end corresponding to the start codon (coding for methionine) and 5'-ACC overhang at the other end corresponding to the anti-sense codon of a C-terminal glycine residue (which is thus the last residue in the insert). The target sequence (in this case, cTnI[135-209]-SRHW) was synthesized by DNA 2.0 and inserted into the pELECTRA-PagP-His$_6$ plasmid, generating the sequence shown in Figure 2 -3 B and the cTnI[135-209]-SRHW-PagP-His$_6$ plasmid shown in Figure 2 -4.

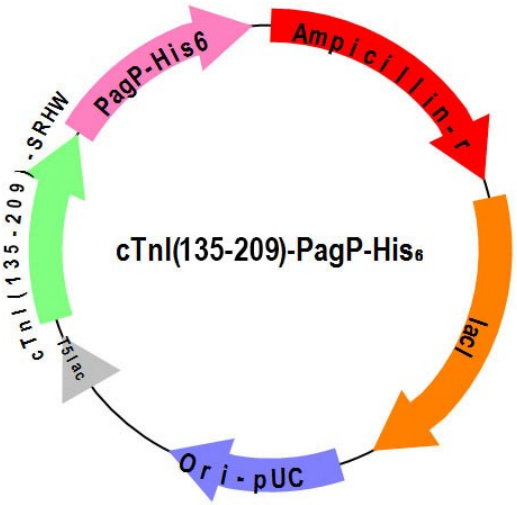

Figure 2-4 A map of the cTnI[135-209]-SRHW-PagP-His$_6$ expression plasmid. The graphic was produced using the website: http://www.premierbiosoft.com/plasmid_maps/index.html, using the SimVector application

2.3.2 Protein expression and purification

The cTnI[135-209]-PagP-His$_6$ plasmid was transformed into calcium chloride-treated competent BL21(DE3) cells (though we did not need the T7 polymerase encoded by BL21(DE3) strain). A few transformed colonies were inoculated into 10 mL LB media containing 100 mg/L ampicillin. After reaching an A_{600} of about 1.0, the cells were diluted into M9 minimal media and allowed to grow overnight at 25°C until A600 ~ 0.9. The cells were then induced with 200 mg of Isopropyl β-D-1-thiogalactopyranoside (IPTG) and grown for an additional 6 hours at 37°C. The cells were harvested at 4,500 x g for 10 minutes. The wet weight of the pellet was 5.3 g from a 1 L growth.

The cell pellet was resuspended in a total volume of 20 mL lysis buffer: 50 mM Tris, pH 8.0, 10 mM MgSO4, and 10 µg/mL DNAse I. Then, 200 mg deoxycholic acid and 20 mg lysozyme, each predissolved in 1 mL of distilled water, were added to the sample, which was then thoroughly mixed and incubated at room temperature for 20 minutes. The cell lysate was

centrifuged at 27,000 x g for 10 minutes, and the pellet was resuspended with 20 mL of 1% Triton X-100 solution containing 5 mM EDTA, and vigorously stirred for an hour, followed by repeat centrifugation at 27,000 x g for 10 minutes. The pellet was washed with water and then dissolved in denaturing nickel column binding buffer: 6 M guanidine-HCl, 20 mM Tris-HCl, 0.3 M NaCl, and 10 mM imidazole, pH 7.9. The sample was applied to a Ni-NTA column, which was further washed with binding buffer and then with wash buffer, which was identical to the binding buffer except that 33 mM imidazole was used. Finally, the fusion protein-target protein was eluted with the elution buffer, which contained 250 mM imidazole. Fractions were assessed by UV-vis spectrophotometry at 280 nm and SDS-PAGE.

2.3.3 Nickel cleavage and final purification

Purified cTnI[135-209]-PagP-His_6 protein at 0.1 mM was cleaved with 0.5 mM $NiSO_4$ in 6 M Gdn-HCl, 50 mM HEPES buffer under different conditions of pH and temperature. The pH corresponds to that of a 1 M stock solution of HEPES buffer. No attempt was made to measure the final pH of the solutions containing 6 M Gdn-HCl, since the high concentrations of Gdn-HCl complicates pH measurement[165].

After the cleavage, our sample protein was then dialysed against water 3 times for 4 hours each, then overnight to get rid of the Guanidine and PagP, causing PagP to precipitate, while the target protein remained soluble. PagP was removed by centrifugation. Finally, the sample was lyophilized and then stored at 4°C.

2.4 Results

2.4.1 Protein expression and purification

cTnI[135-209]-PagP-His_6 was robustly produced in *E. coli* following induction with IPTG (Figure 2 -5). The predicted molecular weight of the fusion protein is 29.4 kDa, and there is a corresponding band appearing on the SDS-PAGE gel post-IPTG induction (Figure 2 -5, lane 2). Another band is seen at ~24 kDa, corresponding to folded PagP. PagP typically migrates as a double band in SDS-PAGE, with one band corresponding to a folded (β-barrel) form and the other corresponding to an unfolded form. This unusual behavior stems from the fact that PagP, unlike most other proteins, is an integral membrane protein that is capable of forming a folded structure even within an SDS micelle[166]. Depending on the composition of the SDS-PAGE gel, sometimes the folded form of PagP migrates slower and sometimes faster than the unfolded form.

Almost all of the cTnI[135-209]-PagP-His_6 fusion protein appeared in the insoluble fraction (Figure 2 -5, lane 4) and not in the soluble fraction (lane 3), as expected for PagP protein on its own. However, the insoluble fraction was not as pure as when PagP is expressed on its own or with other PagP fusion constructs[158], suggesting that the cTnI[135-209] protein sequence may drag other protein contaminants into inclusion bodies. The cTnI[135-209]-PagP-His_6 fusion protein was purified to >95% purity by nickel affinity chromatography, as judged by SDS-PAGE.

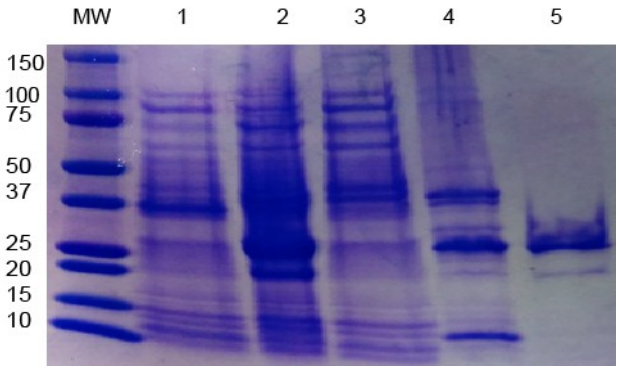

Figure 2-5 SDS-PAGE gel stained with Coomassie Brilliant Blue, showing production and purification of cTnI[135-209]-PagP-His6 protein. Lane 1: whole cells prior to induction. Lane 2: whole cells 6 hours post-induction with IPTG. Lane 3: cell lysate, soluble fraction. Lane 4: cell lysate, insoluble fraction. Lane 5: insoluble fraction dissolved in 6 M Gdn-HCl and purified on a Ni-NTA column under denaturing conditions.

2.4.2 Nickel ion-catalyzed cleavage

Ni^{2+}-catalyzed cleavage is predicted to generate two fragments, the target protein cTnI[135-209] with a molecular weight of 8.8 kDa, and the fusion partner, SRHWG-PagP-His_6 with a molecular weight of 20.5 kDa. The cleavage reaction produced two fragments, although on SDS-PAGE, SRHWG-PagP-His6 ran as a doublet at about 20 kDa, corresponding to folded and unfolded forms, and cTnI[135-209] ran as a band at about 12 kDa (see Figure 2 -6). It is possible that the positively charged nature of cTnI[135-209] caused it to migrate slower than expected, and its true mass was confirmed by MALDI-TOF (see below). No additional cleavage products were observed. The sequence most similar SRHW in our fusion construct was noted to be ^{112}TWHA (see Figure 2 -3 B), though a previous study of combinatorial peptide libraries predicted that 0% cleavage would occur at this site[163]. Indeed, no additional fragments corresponding to this potential cleavage site were observed.

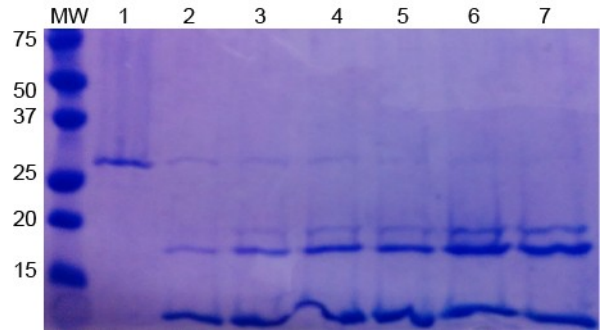

Figure 2-6 Nickel cleavage time course. Lane 1: Purified fusion protein before cleavage. Lane 2: After 30 minutes. Lane 3: 60 minutes. Lane 4: 90 minutes. Lane 5: 2 hours. Lane 6: 3 hours. Lane 7: 4 hours.

Previous work had demonstrated that nickel-catalyzed cleavage required high temperatures and high pH. We found near-complete cleavage after 4 hours at 45°C and pH 9.0. Figure 2 -7 shows partial cleavage under milder temperatures and pH conditions. At pH 9.0 and above, nickel hydroxide precipitate was apparent by the end of the incubation.

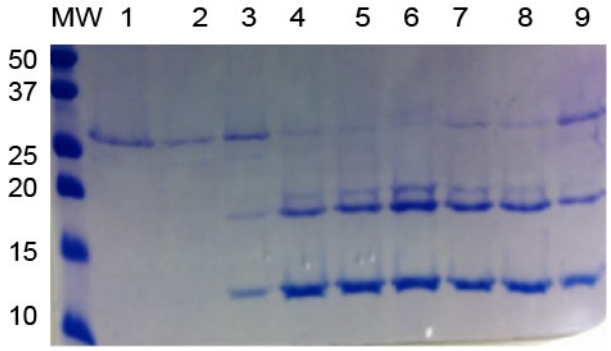

Figure 2-7 Different conditions for Nickel cleavage of cTnI[135-209]-PagP-His$_6$, all taken after 4 hours. Lane 1: Purified protein before cleavage. Lane 2: pH 7.0 at 45°C. Lane3: pH 7.5 at 45°C. Lane 3: pH 8.0 at 45°C. Lane 4: pH 8.5, at 45°C. Lane 5: pH 9.0, at 45°C. Lane 6: pH 9.0 at 37°C. Lane 7: pH 9.0 at 30°C. Lane 8: pH 9.0 at 25°C.

2.4.3 Isolation and characterization of final product

After nickel-catalyzed cleavage, an excess of 15 mM EDTA and 55 mM sodium acetate, pH 4.0 was added, and the reaction mixture was incubated at 50°C for an additional 2 hours. The

prolonged incubation under acidic conditions and elevated temperature was necessary to chelate Ni^{2+} that had precipitated out as nickel hydroxide. Following this, the sample was extensively dialyzed against water (for a minimum of 3 days and at least five 4 L changes). This caused PagP and any uncleaved fusion protein to precipitate out of solution, and this was removed by centrifugation. The remaining supernatant consisted mainly of cTnI[135-209] then was syringe filtered through a 0.45 μm filter. Thus, cTnI[135-209] retained its solubility in the presence of insoluble PagP. The purification protocol had also been performed without the prolonged incubation with EDTA under acidic conditions at 50°C. This step was not always needed for the current construct, though other constructs for expressing other fusion partners required this step, since separation from PagP required repeat nickel affinity chromatography (results not shown).

The final product, cTnI[135-209] was lyophilized and stored long-term at 4°C. Amino acid quantitation showed the expected amino acid composition and a final yield of 15 mg from 1 L M9 minimal media. MALDI-TOF mass spectrometry showed that the molecular weight of the final product was 8850, close to the expected molecular weight of 8842 (Figure 2 -8). An additional minor peak of unknown significance at 8948 was also observed, though this could be a sulfate ion (added to the cleavage reaction in the form of nickel sulfate).

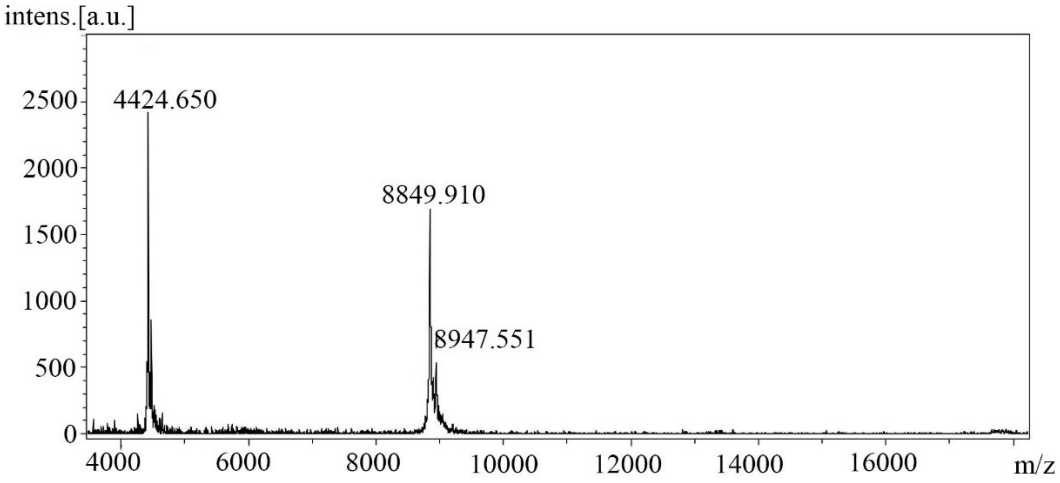

Figure 2-8 Matrix-assisted laser desorption/ionization time-of-flight (MALDI-TOF) mass spectrometry of final purified cTnI[135-209] product.

Protein production procedures were also repeated using M9 minimal media supplemented with $^{15}NH_4Cl$ and uniformly ^{13}C-labeled glucose to produce double ^{13}C,^{15}N-labeled cTnI[135-209]. We were able to assign almost all ^{1}H, ^{13}C, and ^{15}N atom NMR resonances for the sample in aqueous conditions, suggesting that there were no chemical modifications for any of the amino acid residues. Moreover, there were only single NMR resonances for every atom and no multiple peaks suggestive of heterogeneity. As a side note, NMR studies revealed that EDTA [that was added to 15mM to chelate nickel and stop the nickel-catalysed cleavage] was still present in the final product despite extensive dialysis. It is well known but not well documented that EDTA is not readily removed by dialysis for unknown reasons. Extending dialysis times to a week could eventually remove EDTA.

2.5 Discussion

We have previously demonstrated the utility of PagP as an N-terminal fusion partner for directing target proteins into inclusion bodies[158]. In the current study, we demonstrate that PagP

is also effective at targeting proteins to inclusion bodies as a C-terminal fusion partner, so it does not seem to matter that the target protein is translated by the ribosome before PagP. The PagP protein sequence used in the current study also has a C-terminal histidine tag with all internal methionine residues mutated out, and these changes do not appear to disrupt the ability of PagP to direct fusion partners into inclusion bodies. Use of PagP as a C-terminal fusion partner is advantageous when combined with an SRHW sequence-containing linker region, because Ni^{2+}-catalyzed cleavage N-terminal to the serine residue leaves the SRHW sequence attached to PagP, leaving the native C-terminus of the target protein intact.

A previous study identified SRHW as the optimal sequence for Ni^{2+}-catalyzed cleavage[163]. However, the influence of residues N-terminal to this sequence has not been studied, and it is possible that certain amino acid types could inhibit or facilitate the reaction. Solvent exposure of the target sequence is another important factor affecting cleavage efficiency. This is more of a concern under physiologic conditions than in the harsh denaturant used in the current study. However, solubility could be an issue even in 6 M Gdn-HCl. We have found that some fusion partners are difficult to solubilize, and this may be a function of metal ion binding sites. Our fusion protein construct contains at least two metal ion binding sites, SRHW and HHHHHH. Additional Cys, His, Ser, Thr, Gln/Glu, or Asn/Asp residues could potentially contribute additional weak metal ion binding sites leading to metal-ion-bridged aggregation and poor cleavage efficiencies. We have found that nickel-catalyzed cleavage efficiency varies with the nature of the fusion partner. The construct used in the current study was unusual in that it required only 4 hours to achieve near-complete cleavage. Other constructs we have studied required overnight or even 48-hour incubations (data not shown).

Another factor limiting nickel-catalyzed cleavage efficiency is the inherent instability of the reaction mixture. The solubility product, K_{sp}, of $Ni(OH)_2$ at 25°C is only 5.48 x 10^{-16} [167], so that the cleavage reaction could not be substantially enhanced by addition of more Ni^{2+} or base. Under the reaction conditions employed in this study, $Ni(OH)_2$ precipitate is invariably present at the end of the reaction. Care must be taken to ensure that $Ni(OH)_2$ does not precipitate at the beginning of the reaction, as can occur if concentrated $Ni(OH)_2$ stock solution is added to a pH 9.0 solution (thus, $NiSO_4$ should be diluted before alkaline buffer is added). We note that the pKa of HEPES buffer, used in the current study as well as in the original nickel cleavage study using recombinant protein[164], is only 7.5, so that one would expect the pH to drop significantly as $Ni(OH)_2$ precipitates out of solution, since a pH above 8.0 is beyond the optimal buffering capacity of HEPES. The drop in pH would be expected to directly slow the rate of nickel-catalyzed hydrolysis, but it would also help to keep more Ni^{2+} in solution. A buffer with pK_a > 9.0 would be expected to better maintain the pH of the reaction mixture and use of CHES buffer (pK_a 9.3) was found to yield slightly better peptide hydrolysis rates. Finally, certain buffers with Ni^{2+}-coordinating activity do prevent the formation of $Ni(OH)_2$ precipitate (like imidazole and Tris), but these also interfered with the peptide hydrolysis reaction (inhibition by imidazole >> Tris).

The primary concern about Ni^{2+}-catalyzed peptide bond hydrolysis is the possible effects of high temperature and pH on amino acid sidechains[168 169 170]. There was no evidence of oxidation from MALDI-TOF mass spectrometry or multinuclear NMR spectroscopy. In particular, there was no evidence of modification of Phe, Trp, His, or Met, the amino acid residues in cTnI[135-209] that are most sensitive to oxidation. Moreover, NMR analysis found no evidence for hydrolysis of Asn or Gln residues to Asp/Glu, modifications that would not be detectable by MALDI-TOF.

There are no Tyr or Cys residues present in cTnI[135-209]. Cys residues would be inevitably oxidized in the presence of Ni^{2+} and alkaline pH. Thus, they would either need to be protected before the cleavage reaction or reduced afterwards.

Our study further confirms the utility of nickel ion-catalyzed cleavage as a method for cleaving specifically designed linkers for fusion protein expression. We suggest that the technique is most useful in the setting of protein expression from inclusion bodies, where the high concentrations of denaturant employed precludes the use of proteases. The technique is generally applicable, but further experience with a wide range of systems is needed to better define its limitations. Further refinements are needed to allow for less harsh conditions in terms of pH and temperature. Interestingly, other group 10 element ions besides nickel, namely palladium and platinum, have been found to be useful for the cleavage of peptide bonds [171 172]. A complete exploration of these agents, their mechanism of action, amino acid sequence specificity, and effect of co-ordinating small molecules can be expected to further improve upon the current strategy.

Chapter 3. Proteolytic digestion of serum cardiac troponin I as a marker of ischemic severity

3.1 Abstract

Background

The cardiac troponin assay is the biochemical gold standard for detecting myocardial infarction (MI). A major diagnostic issue is that troponin levels can rise with reversible injuries in the absence of radiologically detectable infarct.

Hypothesis

Since cell death activates intracellular proteases, troponin released by irreversible infarct will be more proteolyzed than that released by milder processes. Our goal was to quantitate proteolytic digestion of cardiac troponin I in patients with varying degrees of myocardial injury.

Methods

Serum or plasma samples from 29 patients with cardiac troponin I elevations were analyzed for proteolytic degradation, using three different sandwich ELISA assays designed to specifically detect the N-terminal, core, or C-terminal regions of cardiac troponin I, respectively.

Results

As predicted, the degree of proteolytic digestion increased with increasing severity of injury, as estimated by the total troponin level, and this trend was more pronounced for C-terminal (versus N-terminal) degradation. The highest degree of proteolytic digestion was observed in patients with ST-elevation MI, and the least in type 2 MI (supply-demand ischemia rather than acute thrombus formation).

Conclusions

The proteolytic degradation pattern of cardiac troponin I may be a better indicator of clinically significant MI than total serum troponin level. Distinguishing between intact and degraded forms of troponin may be useful for: 1) identifying those patients with clinically significant infarct in need of revascularization, 2) monitoring intracellular proteolysis as a possible target for therapeutic intervention, and 3) providing an impetus for standardizing the epitopes used in the troponin I assay.

IMPACT STATEMENT

The gold standard diagnostic test for myocardial infarction is the cardiac troponin assay. However, serum troponin elevations do not always correlate with clinically significant infarct, creating uncertainty in the management of troponin-positive patients. We demonstrate that severe infarct releases cardiac troponin I that is more proteolytically digested than that released by milder ischemic conditions. Quantifying troponin degradation products might lead to the development of a novel biomarker that better informs about the underlying cardiac pathology.

3.2 Introduction

The 2012 Third Universal Definition defines myocardial infarction (MI) as myocardial necrosis in the setting of ischemia[120], divided into 5 distinct sub-types. Type 1 MI is the classic "heart attack", in which a coronary vessel is occluded by acute thrombus. Type 1 MI can be further subdivided into ST-elevation MI (STEMI) and non-ST-elevation MI (NSTEMI), based on the electrocardiogram. STEMI is associated with complete major vessel occlusion[173], necessitating urgent revascularization using thrombolytics or invasive procedures[174]. Management of NSTEMI, associated with partial vessel occlusion, is less clear-cut. An early invasive strategy is favored in high-risk patients, while a more conservative ischemia-guided approach is reserved for low-risk patients[175].

In clinical practice, myocardial necrosis is detected using serum biomarkers, of which cardiac troponin has emerged as the gold standard[120,176]. However, recent observations have questioned whether serum troponin elevations necessarily indicate irreversible myocardial cell death[177,178]. Troponin elevations can occur in the absence of infarct detectable by cardiac MRI (the gold standard for imaging)[179] and in healthy individuals following strenuous exercise[180] or atrial pacing-induced tachycardia[123]. Moreover, any condition that creates a vascular supply-demand imbalance (tachyarrhythmias, anemia, or shock) can cause a troponin elevation, a situation classified as a type 2 MI[181]. In the seriously ill patient, it is vitally important to distinguish whether an observed troponin elevation is due to generalized cardiac strain or a critically stenotic lesion in need of urgent revascularization.

The problem with the conventional blood troponin measurement is that it does not distinguish between a focal area of intense infarct and more diffuse injury. It is known that troponin is

proteolytically degraded in the setting of ischemia and/or infarction[56,106] through the activity of proteases[182] like caspases[183], calpains[184], and intracellular matrix metalloproteinase-2[185]. Furthermore, the degradation of the cardiac troponin I subunit (cTnI) in particular is known to produce a heterogeneous mixture of degradation products that complicates its standardization and measurement[106]. We hypothesize that the degree of proteolysis correlates with severity of ischemic injury. We therefore propose to quantitate degradation of cTnI as a marker of the ischemic state (ranging from mild injury to irreversible necrosis) of the cells from which it originated.

3.3 Methods

3.3.1 Design of troponin I degradation assay

To quantify proteolytic degradation of cardiac troponin I (cTnI), we designed a series of three sandwich enzyme-linked immunosorbent assays (ELISAs) employing commonly used antibodies (HyTest Inc. Finland): 19C7 (targeting troponin I core residues 41-49) as the capture antibody and as detection antibodies, M18 (N-terminal residues 18-28), 560 (core residues 83-93), and MF4 (C-terminal residues 190-196) (see Figure 3 -9)

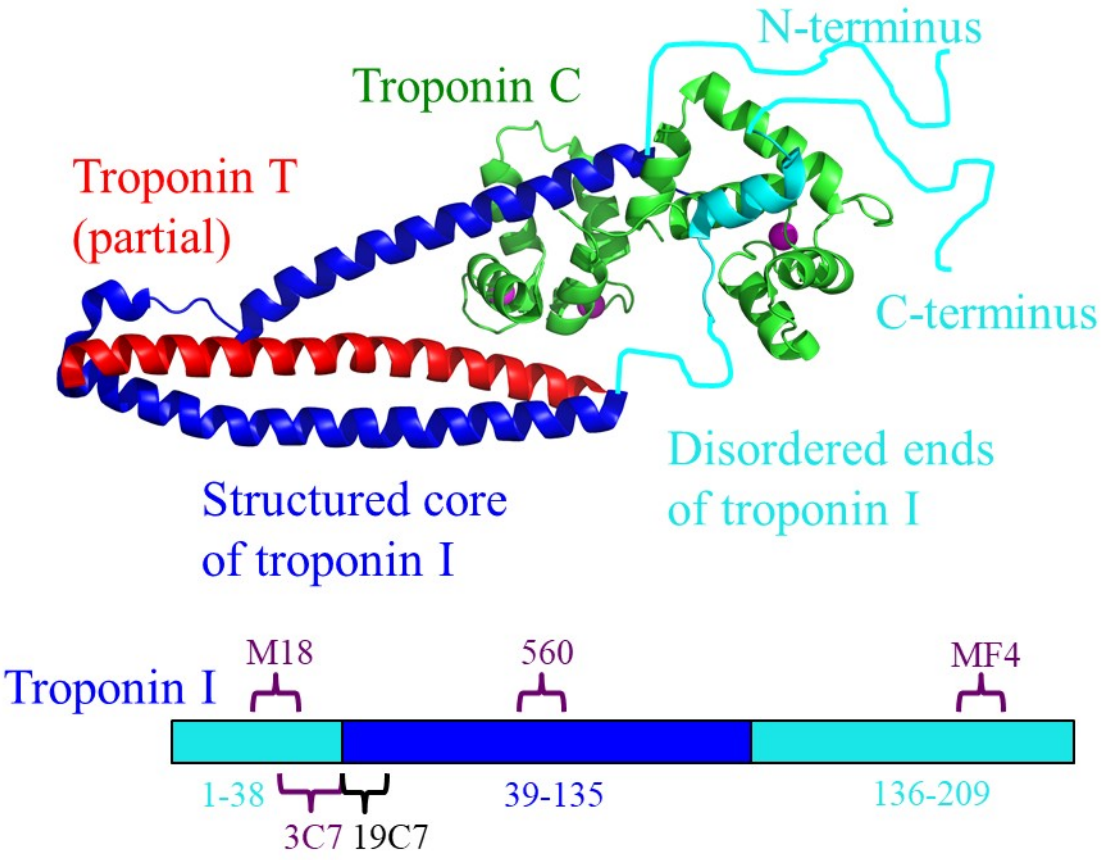

Figure 3-9 Ribbon diagram of the human cardiac troponin complex (PDB code 1J1E). The unstructured ends of troponin I have been drawn in as squiggles and are highlighted in cyan. These are solvent-exposed and susceptible to proteolytic degradation. Antibodies used in this study and their epitopes in cardiac troponin I are shown below. In the current study, antibody 19C7 is used as the capture antibody, while antibodies M18, 560, and MF4 detect the N-terminal, core, and C-terminal regions, respectively. The Beckman Access system uses antibodies that bind epitopes that correspond to 19C7 for capture and 3C7 for detection.

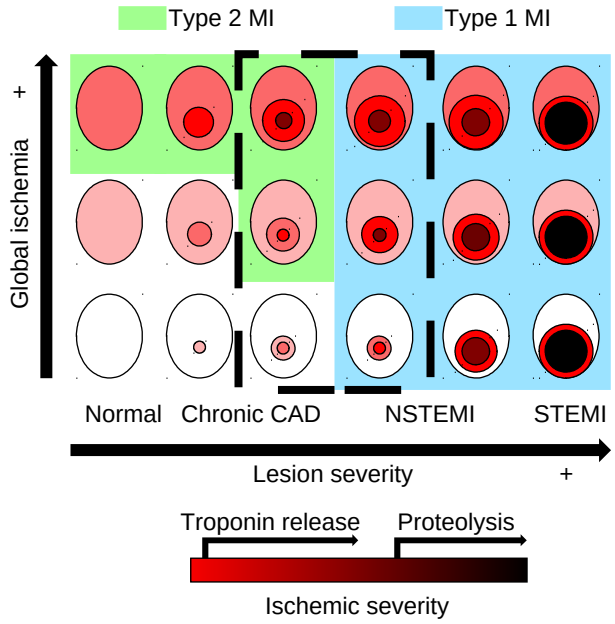

Figure 3-10 Schematic showing the impact of increasing severity of focal atherosclerotic lesions (along x-axis) and generalized cardiac strain (along y-axis) on infarct size in the heart (shown as circles on an oval-shaped heart). Both the quantity of troponin released, and its degree of proteolytic degradation increase with increasing ischemic severity. The boxed area with dashed border highlights situations in which the decision of whether or not to proceed with angiography is debatable.

Polystyrene 96-well plates were coated with 2 µg/mL 19C7 antibody in phosphate-buffered saline (PBS) overnight at 4°C, then blocked with 7% skim milk in PBS for one hour. Patient plasma or serum samples were added undiluted or at 2-fold, 5-fold, or 10-fold dilution, and incubated at room temperature for two hours. 2-4 µg/mL biotin-conjugated detection antibodies (EZ-link™ biotinylation kit, Thermo Fisher Scientific) in Superblock (TBS, Tris-buffered saline) blocking buffer (Thermo Fisher Scientific) were then added and incubated for 90 minutes at room temperature. Detection was achieved using NeutrAvidin-horseradish peroxidase conjugate (Thermo Fisher Scientific) and 3,3′,5,5′-tetramethylbenzidine substrate (Sigma-Aldrich). Extensive washing (5 times) with PBS-0.05% Tween 20 buffer was performed between every step. Every patient sample was run in duplicate for every capture-detect antibody pairing.

As a control, cTnI levels were measured on all clinical specimens using the Beckman Access system. A fundamental issue with all troponin I assays is the lack of universal standardization[186]. Inter-assay measurements on a single sample can differ by over an order of magnitude[187]. One major reason for this is heterogeneity caused by post-translational modifications to troponin I[109,188], especially proteolytic digestion[78,134,189]. Attempts to standardize our assays against a previously proposed reference material, SRM 2921[190], failed to yield consistent relationships between our three sandwich ELISAs. Thus, in keeping with the recommendation of the International Federation of Clinical Chemistry and Laboratory Medicine (IFCC) Troponin Standardization Committee to normalize readings against pooled troponin-positive human serum[186], we normalized readings so that the average troponin level for non-STEMI patients matched that obtained by the Beckman Coulter Access system. (STEMI patients were excluded from the normalization process because they showed extensive proteolytic degradation, see Results section.) Assaying all samples in a single run minimized variation, facilitating consistent comparisons across all patient samples.

3.3.2 Patient sample collection

All patients provided written informed consent and all protocols were approved by the University of Alberta Health Research Ethics Board. Patients with positive plasma cTnI readings >1 ng/mL were identified. The most recent (<24 hours old) plasma sample for each study patient was pulled from the hospital lab and frozen at -80°C. An additional serum sample from each patient was collected with the next scheduled blood draw. This strategy resulted in the collection of patient samples from a wide range of time points in their clinical trajectory for this pilot study. A future study will have to address how cTnI degradation levels vary as a function of time for

different patients. cTnI levels were read using the Beckman Coulter Access system. For each patient, the sample with the higher reading, serum or plasma, was used and reported in this study.

3.4 Results

3.4.1 Patients

We assayed cTnI degradation in a total of 29 patients classified by the hospital admitting service or cardiology consult service independently of the study investigators as follows: 12 had a STEMI, 5 were classified as NSTEMI, 1 patient had a type 4a MI following an elective percutaneous coronary intervention for chronic stable angina, while another patient had myocarditis (confirmed by cardiac MRI), and 10 patients were considered to have type 2 MI (Table 3 -1).

Table 3-1 Clinical presentation and characteristics of study patients classified as having type 2 MI. (Abbrevations: Hgb, hemoglobin; pCO2, partial pressure carbon dioxide; COPD, chronic obstructive pulmonary disease)

Patient	Clinical presentation and characteristics
24	Decompensated acute heart failure; angiogram showing ectatic right coronary artery with old stent, 70-90% occlusions
35	Melena over 2 weeks, Hgb 59; chest pain and ECG changes resolved with transfusion of 3 units packed red blood cells
26	Multiple embolic strokes due to culture-negative endocarditis (1.6 cm vegetation on mitral valve); normal left ventricular function on echocardiogram; ST-segment elevations on ECG attributed to stroke
22	Takotsubo cardiomyopathy, with angiogram showing only moderate, non-occlusive coronary artery disease; hypercarbic (pCO_2 70mm Hg) respiratory failure, acute exacerbation of COPD
32	New onset atrial fibrillation, heart rate 130s; severe aortic stenosis; decompensated acute heart failure
23	Chest pain with ventricular tachycardia (heart rate 185), resolved with cardioversion; echocardiogram showing aneurysm in left ventricle inferoposterior wall; angiogram showing extensive multi-vessel disease and old grafts, but no change from previous
6	Diabetic ketoacidosis; normal left ventricular function on echocardiogram
28	On day 3 of admission for decompensated acute heart failure, collapsed with chest pain, blood pressure 80/50, bigeminy on ECG; chronic peritoneal dialysis; angiogram showing a single tight (90% occluded) ostial lesion in

Patient	Clinical presentation and characteristics
	the obtuse marginal branch of the left circumflex artery
9	Tibia fracture post-op day 3, embolic pontine stroke coinciding with troponin elevation; angiogram showing 80-90% occlusions of the distal left circumflex artery
7	Rhinovirus-positive upper respiratory tract infection; akinetic apex and ejection fraction 30-35% on echocardiogram, adverse changes from 2014; progressively worsening pulmonary edema and cardiorenal syndrome, died after one month in hospital

3.4.2 cTnI is extensively degraded in STEMI patients

Three sandwich ELISAs using three different detection antibodies yielded troponin readings that correlated well with the Beckman Access system (correlation coefficient, r=0.92-0.96).

Figure 3 -11 shows that as cTnI levels increase in type 1 MI patients, there is proportionately less detection by MF4 antibody at the C-terminal region compared to detection by 560 antibody at the core region, suggesting that the C-terminal degradation of cTnI increases with increasing infarct severity. (Compare this with the less consistent degradation at the N-terminus by the M18 antibody in Figure 3 -12). Thus, the remainder of our analysis will center on C-terminal degradation of cTnI.

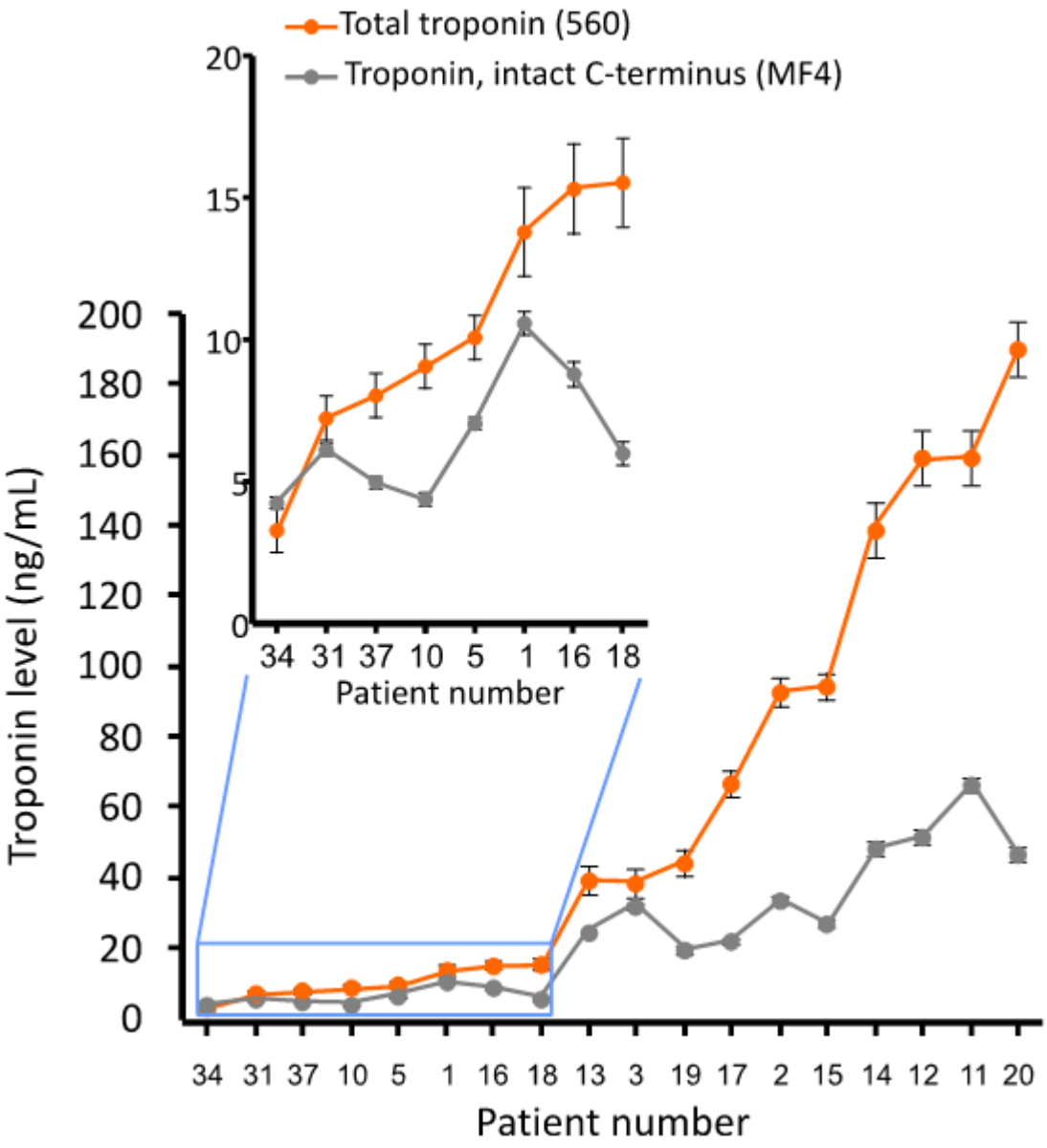

Figure 3-11 Plasma/serum troponin I levels in patients with type 1 MI (plus one patient, 37, with myocarditis. Troponin levels measured using two different detection antibodies: 560 (core region) versus MF4 (C-terminal region). Error bars represent the average standard deviation between duplicate measurements.

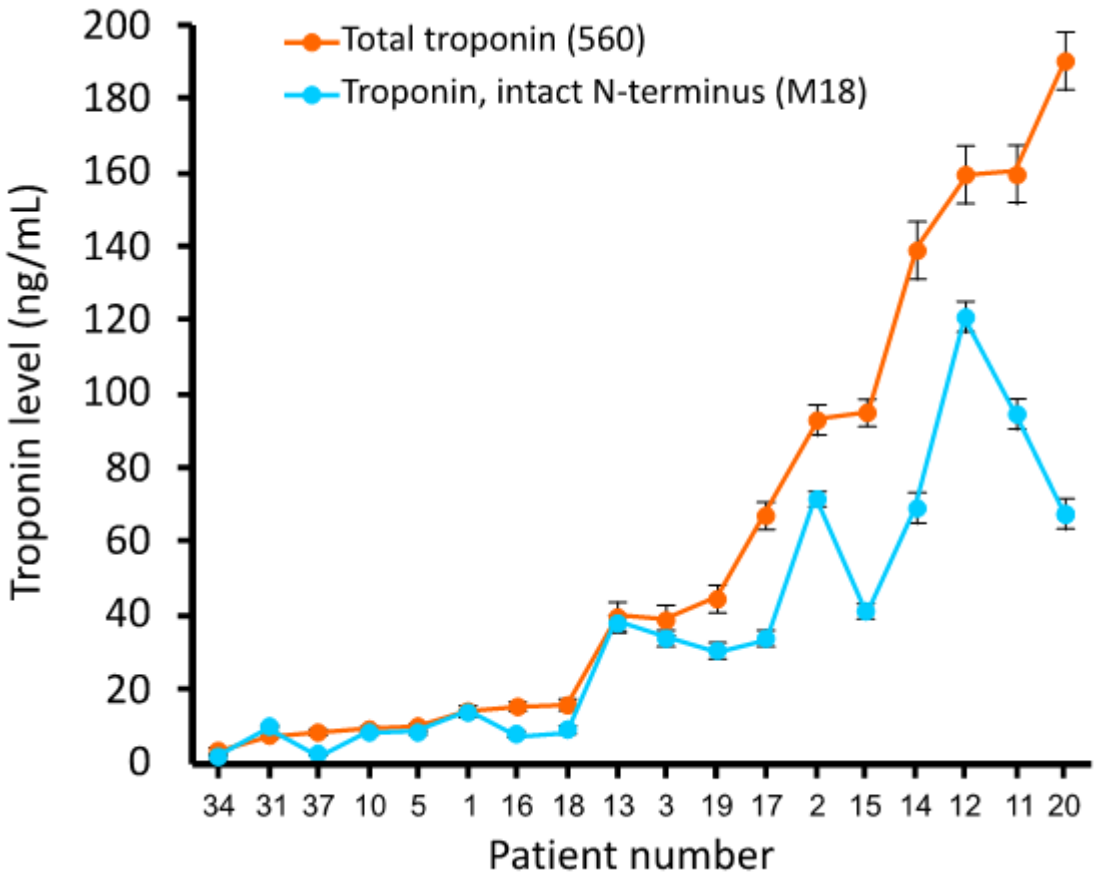

Figure 3-12 Plasma/serum troponin I levels in patients with type 1 MI (plus one patient, 37, with myocarditis). Troponin levels measured using two different detection antibodies: 560 detects the core region of troponin I, while M18 detects the N-terminal region.

NSTEMI patients (patients 34, 31, 5, 1, and 3) showed a lesser degree of cTnI degradation than STEMI patients, consistent with the expectation that complete vessel occlusion leads to a more focal and intense area of infarction and proteolytic degradation. As shown in Figure 3 -13, STEMI patients tend to have higher cTnI levels, but the total cTnI level does not reliably differentiate between STEMI and NSTEMI. In contrast, when patients are ordered according to the proportion of intact (versus proteolytically degraded) cTnI, a clear distinction between STEMI and NSTEMI can be seen Figure 3 -13. Of note, the lone patient in our study with acute myocarditis (patient 37) showed cTnI degradation levels comparable to STEMI patients. Possible

mechanisms could be: direct injury of the cardiomyocytes by the lytic enzymes' load of the viruses[191–193] and indirect injury whether by the release of cytokines as part of the inflammatory process that would eventually lead to activating proteolytic enzymes like MMP-2[194] or by the autoimmune mechanisms involved in the pathogenesis of viral myocarditis[195]. Further studies are needed to confirm this interesting observation and disclose its underlying mechanisms.

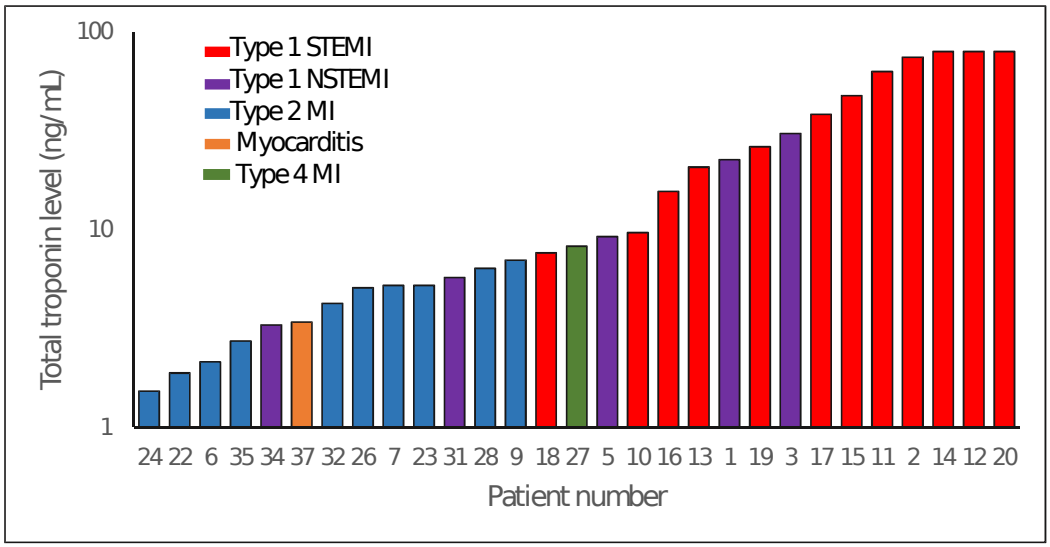

(A)

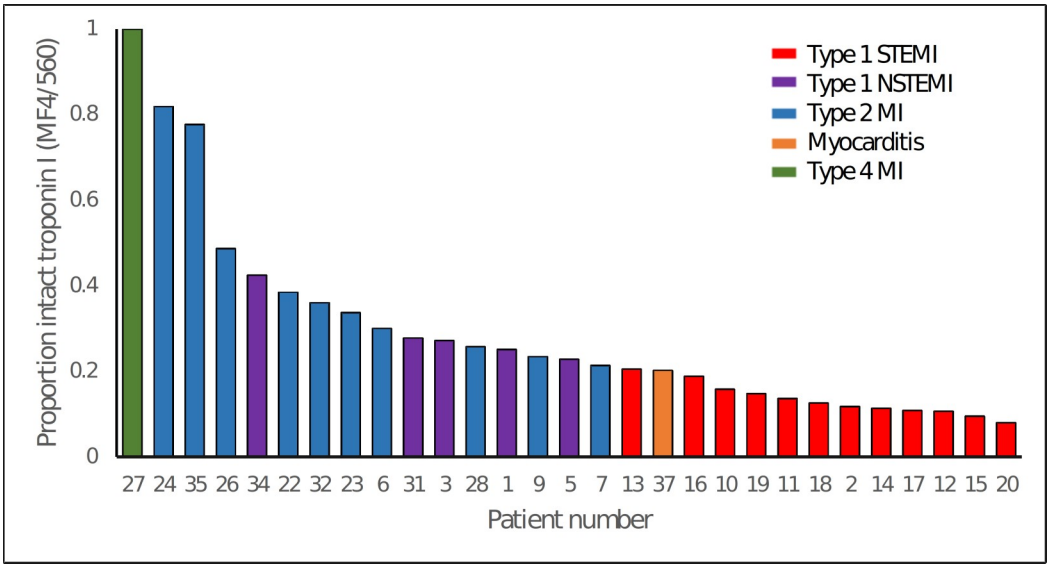

(B)

Figure 3-13 ***(A):*** *Patients ordered according to total troponin level (measured by the Beckman Access system).* ***(B)*** *Patients ordered according to the proportion of troponin I degraded, determined by the*

ratio of troponin level determined using MF4 detection antibody (corresponding to intact troponin) to that determined using 560 detection antibody (corresponding to total troponin). The ratios were normalized to patient 27, assuming that the patient that showed the least amount of degradation had no degradation.

3.4.3 Degradation of cTnI is variable in Type 2 MI patients

Type 2 MI patients consistently showed less cTnI degradation than type 1 STEMI patients (Figure 3 -14). However, a clear distinction could not be made between NSTEMI and type 2 MI, though there was a trend towards less degradation in type 2 MI patients (compare purple and blue bars, Figure 3 -13).

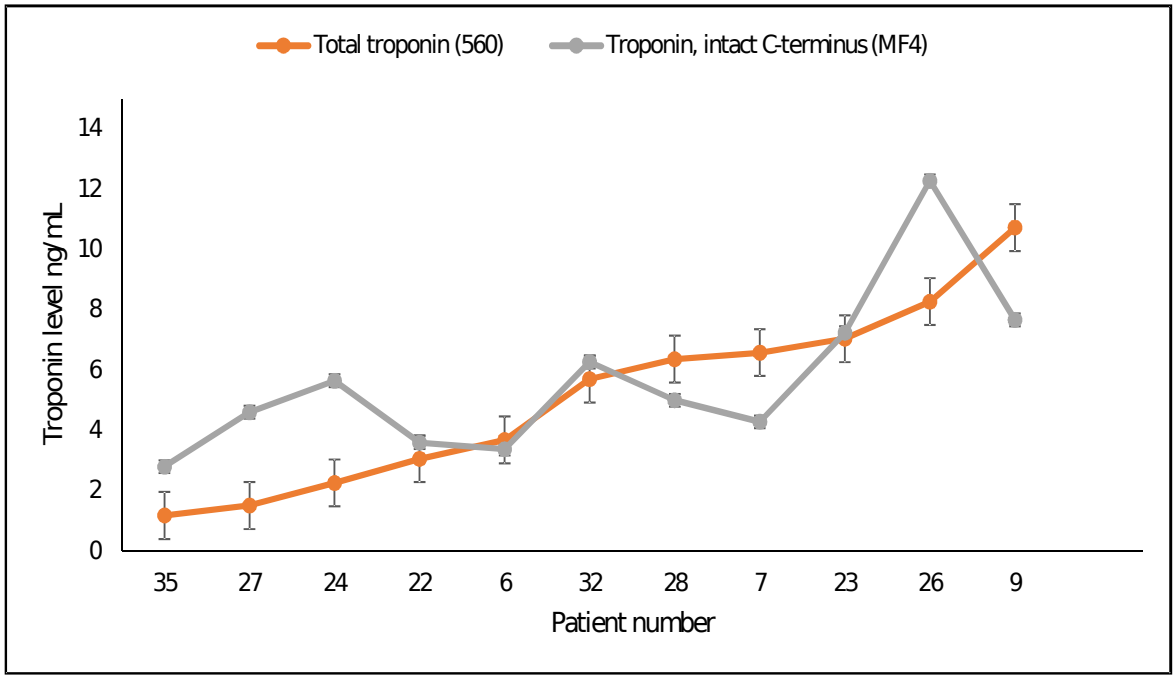

Figure 3-14 Patients with potential type 2 MI. Comparison between troponin levels detected by antibody 560 (core region) and MF4 (C-terminal region).

The lone type 4a MI patient, patient 27, showed significant improvement of chronic angina and improved exercise capacity post-PCI, suggesting that the observed post-procedural cTnI

elevation was benign. This patient showed the least cTnI degradation out of all study patients (see Figure 3 -13), though the conventional cTnI test could not differentiate the clinical situation from a more serious type 1 MI.

3.5 Discussion

According to our pilot study, proteolytic degradation of cTnI appears to correlate with ischemic severity, with type 1 STEMI patients showing the highest degree of degradation, followed by NSTEMI patients. Consistent with clinical experience, patients labeled as having type 2 MI were a heterogeneous group showing varying degrees of degradation. Those with severe medical illness and non-critical atherosclerotic disease show the release of relatively intact cTnI, while those with more severe underlying atherosclerotic lesions had cTnI degradation levels comparable to type 1 NSTEMI patients (Table 3 -1).

Our study suggests that most commercial cTnI assays, which utilize at least one N- or C-terminal epitope, may favor detection of more intact forms of cTnI released by milder injuries. This may explain the observation that total troponin levels correlate poorly with radiologically determined infarct size in NSTEMI patients[196]. Further studies are needed to determine whether specific quantitation of degraded troponin would lead to improved correlation with infarct size.

Thus, accurate quantitation of degraded troponin may be more useful in guiding clinical management than a single troponin level obtained by a conventional assay. Our proposed cTnI degradation assay can be easily implemented, since it employs antibodies that are already routinely used. One potential side benefit of measuring cTnI degradation and standardizing the epitopes used for its quantitation is that it may also become possible to achieve universal standardization of cTnI assays[144,197].

Chapter 4. Structure and proteolytic susceptibility of the inhibitory C-terminal tail of cardiac troponin I

4.1 Abstract

Background

Cardiac troponin I (cTnI) has two flexible tails that control the cardiac cycle. The C-terminal tail, $cTnI_{135-209}$, binds actin to shut off cardiac muscle contraction, whereas the competing calcium-dependent binding of the switch region, $cTnI_{146-158}$, by cardiac troponin C (cTnC) triggers contraction. The N-terminal tail, $cTnI_{1-37}$, regulates the calcium affinity of cTnC. cTnI is known to be susceptible to proteolytic cleavage by matrix metalloproteinase-2 (MMP-2) and calpain, two intracellular proteases implicated in ischemia-reperfusion injury.

Methods

Soluble fragments of cTnI containing its N- and C-terminal tails, $cTnI_{1-77}$ and $cTnI_{135-209}$, were highly expressed and purified from *E. coli*, allowing structural studies using solution NMR and *in vitro* proteolysis studies using liquid chromatography-mass spectrometry (LC-MS).

Results

$cTnI_{135-209}$ is intrinsically disordered, though it contains three regions with helical propensity (including the switch region) that rigidify upon actin binding. We identified three precise MMP-

2 cleavage sites at cTnI P17-I18, A156-L157, and G199-M200. In contrast, calpain-2 has numerous cleavage sites throughout Y25-T30 and A152-A160. The critical cTnI switch region is targeted by both proteases, though it is partially protected when bound to cTnC or actin.

Conclusions

Both N- and C-terminal tails of cTnI are intrinsically disordered, but only the C-terminal tail acquires rigid structure when bound to cTnC or actin. Still, both remain susceptible to cleavage by MMP-2 and calpain.

General Significance

cTnI is an important probe of cardiomyocyte intracellular proteolysis, given its many protease-specific cut sites, high natural abundance, indispensable functional role, and clinical use as gold standard biomarker of myocardial injury.

4.2 Introduction

The cardiac troponin complex (cTn) links cyclic Ca^{2+} fluctuations to cardiac muscle contraction and relaxation[198,199]. It is comprised of three subunits[2]: cTnC binds calcium; cTnT anchors the complex to tropomyosin; and cTnI is the inhibitory subunit (Figure 4 -15**)**. Cardiac troponin I (cTnI) has two flexible tails that are critical to its function. The N-terminal tail, $cTnI_{1\text{-}38}$, interacts with the regulatory domain of cTnC (cNTnC) to enhance its calcium affinity. This effect is attenuated by phosphorylation of cTnI Ser22/Ser23[200], the primary post-translational modification regulating the calcium sensitivity of cardiac muscle contraction in humans[201].

The C-terminal tail, $cTnI_{135\text{-}209}$, binds actin to anchor the troponin-tropomyosin complex to a "blocked" position that prevents actin-myosin cross-bridging during diastole (the ventricular

relaxation phase of the cardiac cycle). During systole (the ventricular contraction phase), cNTnC binds the cTnI switch region, $cTnI_{146-158}$, in a calcium-dependent manner, to release the inhibitory effect of $cTnI_{135-209}$. Thus, the $cTnI_{135-209}$ C-terminal tail cycles back and forth between actin and cTnC during diastole and systole, respectively, driving the cardiac cycle. The interactions between cTnI and cTnC have been well established by X-ray crystallography and NMR spectroscopy[5,17,202], but very little is known about the interaction between cTnI and actin.

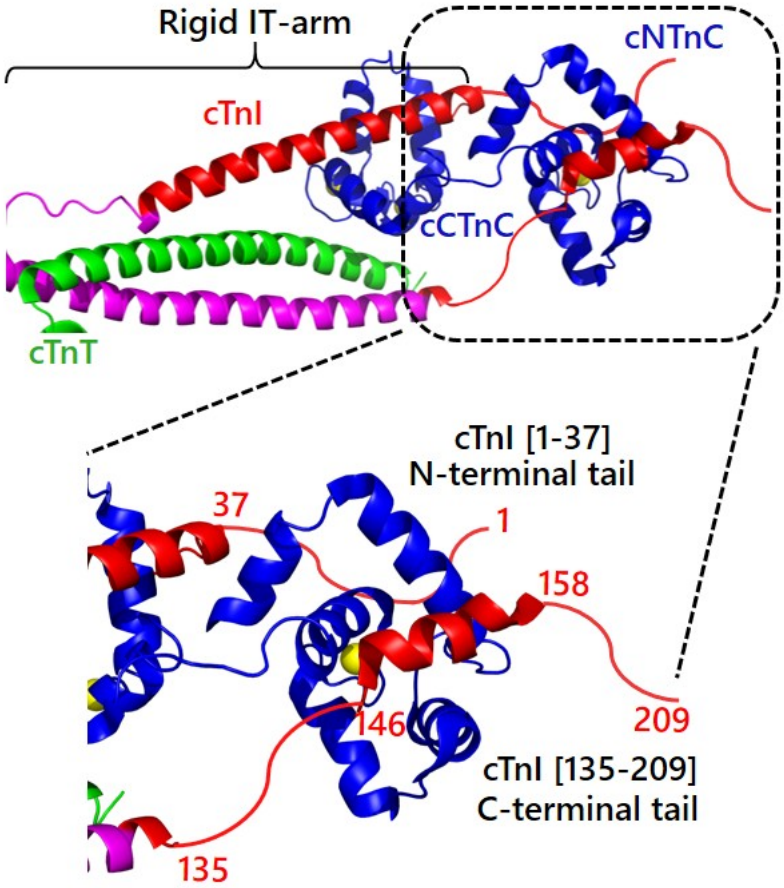

Figure 4-15 Calcium-saturated cardiac troponin complex. Cardiac troponin C (cTnC) is shown in blue and consists of an N-terminal domain (cNTnC) and a C-terminal domain (cCTnC). Troponin I (cTnI) is shown in magenta and red, with the red regions corresponding to the two constructs used in this study: $cTnI_{1-77}$ and $cTnI_{135-209}$. The inset highlights the N- and C-terminal tails of cTnI, with intrinsically disordered drawn manually as squiggles. Figure prepared using PyMOL and structure 4Y99 (PDB code). At resting calcium concentrations, cNTnC releases calcium (yellow sphere), adopts a closed conformation, and $cTnI_{135-209}$ binds to actin.

The N-terminal and C-terminal tails of cTnI are flexible, solvent-exposed, and susceptible to post-translational modifications like proteolysis[203,204]. Western blot analysis of serum cTnI in myocardial infarction patients demonstrates multiple cut sites within the cTnI N- and C-terminal tails[205]. In animal models, proteolytic digestion of cTnI has been demonstrated to occur in myocardial ischemia-reperfusion injury[56,78,206]. Two major mechanisms are known to contribute to ischemia-reperfusion injury: generation of excess reactive oxygen-nitrogen species (RONS)[207,208] and calcium overload[209,210]. Both processes activate downstream proteases that can compromise structural integrity and promote cell death.

Matrix metalloproteinases (MMPs) were originally identified as extracellular proteases but were subsequently found to localize to intracellular compartments as well[56,211], with matrix metalloproteinase-2 (MMP-2) being the predominant isoform in cardiomyocytes. MMPs are synthesized as inactive zymogens, with an inhibitory cysteine residue in the pro-peptide domain complexing the catalytic zinc ion. MMPs are activated by proteolytic removal of the pro-peptide domain or by chemical modification of the inhibitory cysteine sulfhydryl group, as occurs when reactive oxygen-nitrogen species, particularly peroxynitrite[212], are generated during ischemia-reperfusion injury[213–215].

Calpains are a family of calcium-dependent cysteine proteases that are involved in cytoskeletal remodeling, signal transduction, and cell death[216,217]. Calpain-1 (μ-calpain) and calpain-2 (m-calpain) are ubiquitously expressed and are activated by elevated intracellular Ca^{2+} concentrations[63,209,210,218,219]. These calpains have nearly indistinguishable substrate specificities[220,221] but differ in the concentration of calcium required for activation.

Both MMP-2 and calpain have been shown to cleave cTnI in animal models of ischemia-reperfusion injury[56,79]. Small molecule inhibition of MMP-2[56,61] or calpain[184,222,223] has been shown to attenuate ischemia-reperfusion injury in animal models.

The structured "IT-arm" core of cTnI (residues 39-134) is known to be relatively resistant to proteolytic digestion[106]. Moreover, since full-length cTnI misfolds and aggregates on its own, we generated two soluble fragments of cTnI containing its flexible protease-susceptible N- and C-terminal tails, $cTnI_{1-77}$ and $cTnI_{135-209}$, respectively. Using purified proteins and mass spectrometry, we have mapped out the precise cTnI cleavage sites for MMP-2 and calpain-2. Since cTnI interacts primarily with cTnC and actin *in vivo*, we also examine its proteolysis in the presence of these binding partners.

Given the extensive biophysical characterization of the troponin complex over the past six decades, it is possible to understand the proteolytic susceptibility of cTnI in terms of its structure. However, relatively little is known about the structure of the critical C-terminal tail bound to the actin, because the intrinsic disorder of the tail, combined with the filamentous nature of actin, is difficult for any one biophysical technique to tackle comprehensively. In the current study, we use solution NMR spectroscopy to probe the structure of the C-terminal $cTnI_{135-209}$ tail alone and in the presence of actin maintained in a monomeric form by its complex with DNase I (so that it can be studied by solution NMR).

4.3 Materials and methods

4.3.1 Protein expression and purification

Soluble recombinant human cTnI proteins, $cTnI_{1-77}$ and $cTnI_{135-209,}$ were expressed in *Escherichia coli* and purified as described previously[158,224]. Briefly, both recombinant proteins were expressed

as fusions to the β-barrel membrane protein, PagP. This causes the fusion protein to accumulate in insoluble inclusion bodies, which can be harvested by centrifugation, solubilized in 6 M guanidine-HCl, and then purified by nickel affinity chromatography. $cTnI_{1-77}$ was separated from PagP via cyanogen bromide cleavage in 0.1 M HCl[12,158], while $cTnI_{135-209}$ was separated using nickel ion-catalyzed cleavage[224]. $cTnI_{135-209}$ was produced with ^{15}N- and/or ^{13}C-isotope enrichment for solution NMR studies.

4.3.2 NMR Spectroscopy

All NMR data used in this study were generated at 30°C using a Varian Inova 500 MHz spectrometer equipped with a triple resonance probe and pulsed field gradients. NMR samples contained 500 µl of aqueous NMR buffer consisting of 10 mM imidazole, 0.5 mM 2,2-dimethyl-2-silapentane-5-sulfonate-d6 sodium salt (d_6-DSS), and 0.01 % NaN_3 in 90% H_2O, 10% D_2O or 100 % D_2O at pH 6.8. Three-dimensional HNCACB and CBCA(CO)NH experiments were carried out to obtain backbone ^1H, ^{15}N, ^{13}C chemical shift assignments for a sample of 2.8 mg $cTnI_{135-209}$ dissolved in NMR buffer. In addition, both (H)C(CO)NH-TOCSY and H(C)(CO)NH-TOCSY experiments were conducted to obtain side-chain ^1H and ^{13}C chemical shift assignments. 3D ^{15}N-edited and ^{13}C-edited homonuclear ^1H-^1H NOESY experiments were also performed and analyzed to obtain NOE information. All two- and three-dimensional NMR data were processed using NMRPipe/NMRDraw software[225]. NMRviewJ[226] from One Moon Scientific (http://www.onemoonscientific.com/nmrviewj) was used to further visualize and analyse spectra. The δ2D program[227] (http://www-mvsoftware.ch.cam.ac.uk/) was used to quantitate secondary structure propensities (α-helix, β-strand and random coil) using backbone chemical shift assignments[228].

Recombinant bovine cardiac muscle actin (>99% pure, Cat. # AD99-A) was purchased from Cytoskeleton, Inc (U.S.A). RNase-free and protease-free deoxyribonuclease I (DNase I) was purchased from Worthington Biochemical Corporation. Actin was maintained in a monomeric form through its tight binding to DNase I, thereby inhibiting polymerization[229].

^{15}N-labeled cTnI$_{135-209}$ (1.1 mg) was dissolved in 500 µL NMR buffer with an additional 10 mM DTT. A baseline (^{1}H, ^{15}N)-HSQC spectrum was recorded of this sample. Next, 1 mg of actin was dissolved in 200 µL NMR buffer + 10 mM DTT and then added to 1 mg DNase I, and the mixture was added to the 500 µL solution of ^{15}N-labeled cTnI$_{135-209.}$ The (^{1}H, ^{15}N)-HSQC spectrum was repeated, and a comparison of peak intensities before and after addition of monomeric actin-DNase I was obtained.

4.3.3 SDS-PAGE analysis of *in vitro* proteolysis

Purified human recombinant MMP-2 (72 kDa) (200 µg/ml) was activated chemically by 1 mM of 4-aminophenylmercuric acetate (APMA) in activation buffer (100 mM Tris-HCl, 10 mM $CaCl_2$, pH 7.6), as previously described[230]. Recombinant rat calpain-2 was expressed and purified as previously described[231]. APMA-activated recombinant human MMP-2 was incubated with cTnI$_{1-77}$ (0.1 µg/ µl) or cTnI$_{135-209}$ (0.1 µg/ µl) in incubation buffer (50 mM Tris-HCl, 5 mM $CaCl_2$, 150 mM NaCl, pH 7.6) for 2 h at 37˚C. Similarly, recombinant rat calpain-2 was also incubated with cTnI$_{1-77}$ (0.1 µg/ µl) or cTnI$_{135-209}$ (0.1 µg/ µl) in incubation buffer (50 mM Tris-HCl, 5 mM $CaCl_2$, 150 mM NaCl, 10 mM beta mercaptoethanol, 10 mM DTT, pH 7.6) for 2 h at 37 ˚C. Proteolytic assays were carried out with enzyme-to-substrate molar ratios ranging from 1:500 to 1:10000 and 1:250 to 1:5000 for MMP-2:cTnI and calpain-2:cTnI respectively. As controls, 2-[((1, 1'-Biphenyl)-4-ylsulfonyl)-(1-methylethoxy) amino]-N-hydroxyacetamide (ARP-100) and MDL-28170 inhibitors [Cayman Chemical, USA] were used to block MMP-2 and calpain-2

activity, respectively. The products of all proteolysis assays were separated by electrophoresis in 16% Tris-Tricine gels and visualized by Coomassie Blue staining.

In an additional set of experiments, activated MMP-2 or calpain-2 were incubated with $cTnI_{1-77}$ or $cTnI_{135-209}$ in the presence or absence of cTnC or actin. cTnC binds to cTnI with a 1:1 stoichiometry, so 0.32 µg/µl cTnC was used [produced in our lab], corresponding to a 1.5:1 cTnC:cTnI ratio (excess cTnC). For actin, a 1:1 stoichiometry was suspected (discussed further in the Results section), therefore actin was added at a concentration of 0.50 µg/ µl, corresponding to a 1:1 molar ratio. The actin concentration was then serially diluted two-fold to yield molar ratios ranging from 1:1 to 0.0625:1. Note that under these conditions, actin is predominantly in the filamentous F-actin form, though at the lowest concentrations used, there would be a more significant proportion of monomeric G-actin[232].

4.3.4 Mass spectrometric analysis of *in vitro* proteolysis

A cocktail of MMP-2 (1 ng/µL) with cTnI1-77 (0.43 µg/µl) or MMP-2 (1 ng/µL) with cTnI135-209 (0.44 µg/µl), each at 1:5000 molar ratio, was incubated at 37˚C for a time course study from 0 min to 24 h. The same time course study was applied to calpain-2 (4 ng/µL) with cTnI1-77 (0.43 µg/µl) and calpain-2 (4 ng/µL) with cTnI135-209 (0.44 µg/µl), each incubated at 1:1000 molar ratio at 37 ˚C. Formic acid (1% v/v) was used to denature the proteins and stop the reaction, and the samples were immediately flash frozen with liquid nitrogen. For protein molecular weight determination reverse phase high performance liquid chromatography followed by mass spectrometry (RP-HPLC-MS) was performed using an Agilent 1200 SL HPLC System with a Poroshell 300SB-C8, 5-micron particle size, 75x0.5mm column (Agilent Technologies, USA), with Opti-pak trap cartridge kit, 5µL BED, C8, thermostated at 60 °C or a Phenomenex Aeris 3.6um, WIDEPORE XB-C8, 200Å, 2.1x50 mm with guard column, thermostated at 50 °C.

For the Poroshell column a buffer gradient system composed 0.1% formic acid in water as mobile phase A and 0.1% formic acid in acetonitrile (ACN) as mobile phase B was used. An aliquot of 5 µL of sample was loaded onto the column at a flow rate of 0.15 ml/min and an initial buffer composition of 95% mobile phase A and 5% mobile phase B. After injection, the column was washed using the initial loading conditions for 3 min to effectively remove salts. Elution of the proteins was done by using a linear gradient from 5% to 50% mobile phase B for 10 min, 50% to 95% mobile phase B for 2 min, 95% to 98% mobile phase B for 4 min and back to 5% mobile phase B for of 1 min.

For the Phenomenex Aeris column following gradient was used: the column was washed after loading of the sample using a 0.4 ml/min flow rate and 5% mobile phase B for 2 min to effectively remove salts. Elution of the proteins was done by using a linear gradient from 5% to 65% mobile phase B for 8 min, 65% to 98% mobile phase B over a period of 2 minute, kept at 98% mobile phase B for 2 min and back to 5% mobile phase B for 1 min.

Mass spectra were acquired in positive mode of ionization using an Agilent 6220 Accurate-Mass TOF HPLC/MS system (Santa Clara, CA, USA) equipped with a dual sprayer electrospray ionization source with the second sprayer providing a reference mass solution. Mass correction was performed for every individual spectrum using peaks at m/z 121.0509 and 922.0098 from the reference solution. Mass spectrometric conditions were drying gas 10 L/min at 325 °C, nebulizer 20 psi, mass range 100-3000 Da, acquisition rate of ~1.03 spectra/sec, fragmentor 200 V, skimmer 65 V, capillary 3200 V, instrument state 4 GHz High Resolution. Data analysis was performed using the Agilent MassHunter Qualitative Analysis software package version B.03.01 SP3. From the masses, the proteolysis fragments from both recombinant proteins were determined by using the online bioinformatics tool FindPept from the ExPASy server[233], (http://

web.expasy.org/findpept/). SequenceEditor (Build 5.65) from Bruker Daltonics Biotools 3.2 SR3 (https://www.bruker.com/service/support-upgrades/software-downloads/mass-spectrometry.html) was also used to analyse the peptide masses.

4.4 Results

4.4.1 Structure of free $cTnI_{135-209}$ by NMR spectroscopy

The ^{1}H-^{15}N HSQC spectrum of $cTnI_{135-209}$ alone shows narrow and intense peaks with poor chemical shift dispersion, suggestive of intrinsically disordered regions. Some peaks are weak due to rapid backbone amide-solvent exchange (becoming more visible at more acidic pH due to the slowing of base-catalyzed solvent exchange), especially peaks corresponding to inhibitory region residues, 135-147. Near-complete chemical shift assignments of backbone and side chain resonances were obtained (deposited in the Biological Magnetic Resonance Bank, **BMRB# 27476**).

Secondary structure analysis showed predominantly random coil structure, using the chemical shift analysis program δ2D, which determines the percentage of secondary structure based on HN, N, Hα, Cα, CO, and Cβ chemical shifts on a per residue basis. cTnI residues 150-159 are known to form an alpha helix when the switch region binds cNTnC, and δ2D indicates that this region has the highest helical propensity (up to 50%) in $cTnI_{135-209}$ in the absence of cTnC (Figure 4 -16 A). Some helical character extends beyond the switch region out to residue 172, though this is not observed in X-ray or NMR structures[5,17]. Helical propensity was also observed from residues 189 to 202 (though only up to ~10%). There was no significant β-sheet propensity anywhere in the $cTnI_{135-209}$ sequence.

Regions with helical propensity indicated by δ2D also had corroborating NOEs obtained from ^{13}C- and ^{15}N-edited NOESY-HSQC experiments. Figure 4 -16 B shows medium range $d_{\alpha\beta}$ (*i, i + 3*) NOEs that correspond to the helical regions identified by chemical shift analysis. The strongest helical NOEs were observed in the switch region, as shown in Figure 4 -16 C**,** which shows 6 strip plots extracted from ^{15}N- and ^{13}C-edited NOESY spectra. The NOE pattern confirms nascent helix formation in residues 149-159, 165-172 and 187-197.

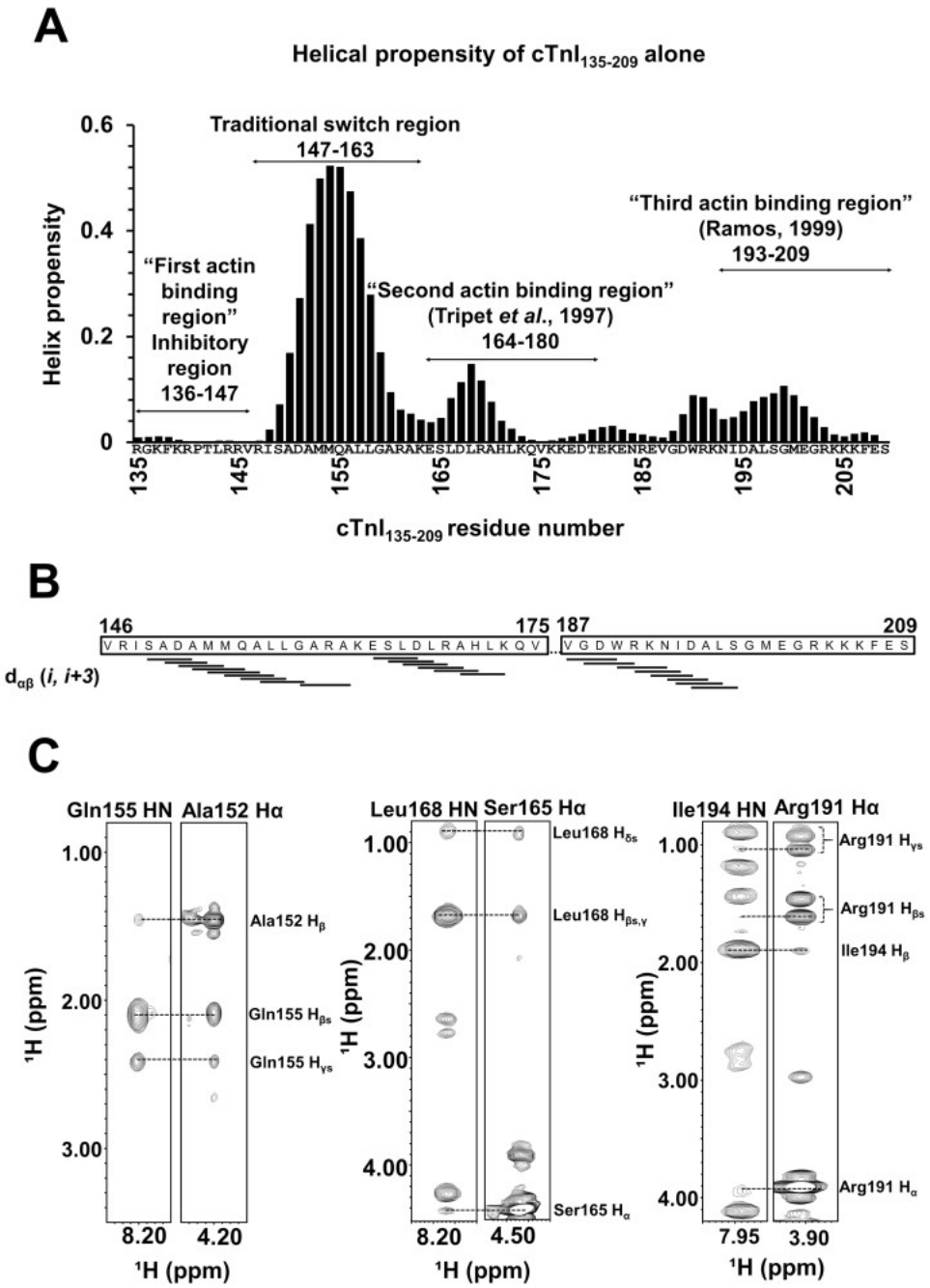

Figure 4-16 ***(A)*** *Residue-specific secondary structure of $cTnI_{135-209}$ calculated by the program δ2D using backbone NMR chemical shifts. The functional regions shown highlight the results of limited binding studies in the past, rather than exact boundaries determined from structure.* ***(B)*** *Summary of medium-range NOE connectivities $d_{\alpha\beta\ (i,\ i+3)}$ that are specific for alpha helix.* ***(C)*** *Representative strip plots showing helical medium-range NOEs from 3D ^{15}N- edited NOESY-HSQC and 3D ^{13}C edited NOESY-HSQC.*

Our analysis of the cardiac troponin I C-terminal region is consistent with the results of Blumenschein et al.[234], who documented primarily disordered structure in the corresponding region in fast skeletal troponin I (though their analysis did not include the inhibitory and switch regions). Our findings also partially agree with the findings of Murakami et al.[235], who noted similar regions of alpha-helicity in fast skeletal troponin I. However, we could find no evidence to corroborate the "mobile domain" of Murakami et al., which would require packing of the C-terminal helix against a small anti-parallel β-sheet extending from residues 175 to 186, for which we found no supportive NOEs or chemical shift data.

4.4.2 Rigidification of $cTnI_{135-209}$ in the presence of monomeric actin-DNase I

Many intrinsically disordered segments of proteins acquire structure upon binding to a protein partner. However, we previously found that $cTnI_{1-37}$ does not acquire any rigid secondary structure upon binding the cNTnC domain through predominantly electrostatic interactions[12]. In contrast, the hydrophobic binding of $cTnI_{146-158}$ to cTnC is associated with formation of a rigid alpha helix comprising cTnI residues 150-158[5,17].

When we added $cTnI_{135-209}$ to filamentous F-actin, all NMR signals broadened out beyond detection, consistent with a molecular tumbling rate too slow to allow the use of solution NMR spectroscopy. We, therefore, added DNase I to actin to maintain it in a monomeric form, with the total molecular weight of the complex ~74 kDa. Addition of a 10% molar ratio of actin-DNase I to $cTnI_{135-209}$ caused sequence-specific broadening of $cTnI_{135-209}$ **(Figure 4 -17** A), indicating that the kinetics of $cTnI_{135-209}$ binding to actin-DNase I occur within the fast exchange regime with respect to the NMR signal frequency differences between free and bound states. (If binding were in the slow exchange regime, binding of a 1:10 ratio actin-DNase I to $cTnI_{135-209}$ could at most

obliterate 10% of the signal.) The degree of signal attenuation provides a rough estimate of which regions of $cTnI_{135-209}$ become rigidly structured upon interacting with actin-DNase I, with more tightly bound residues having a greater degree of signal broadening due to the slower molecular tumbling of the complex and a larger chemical shift difference between free and bound states.

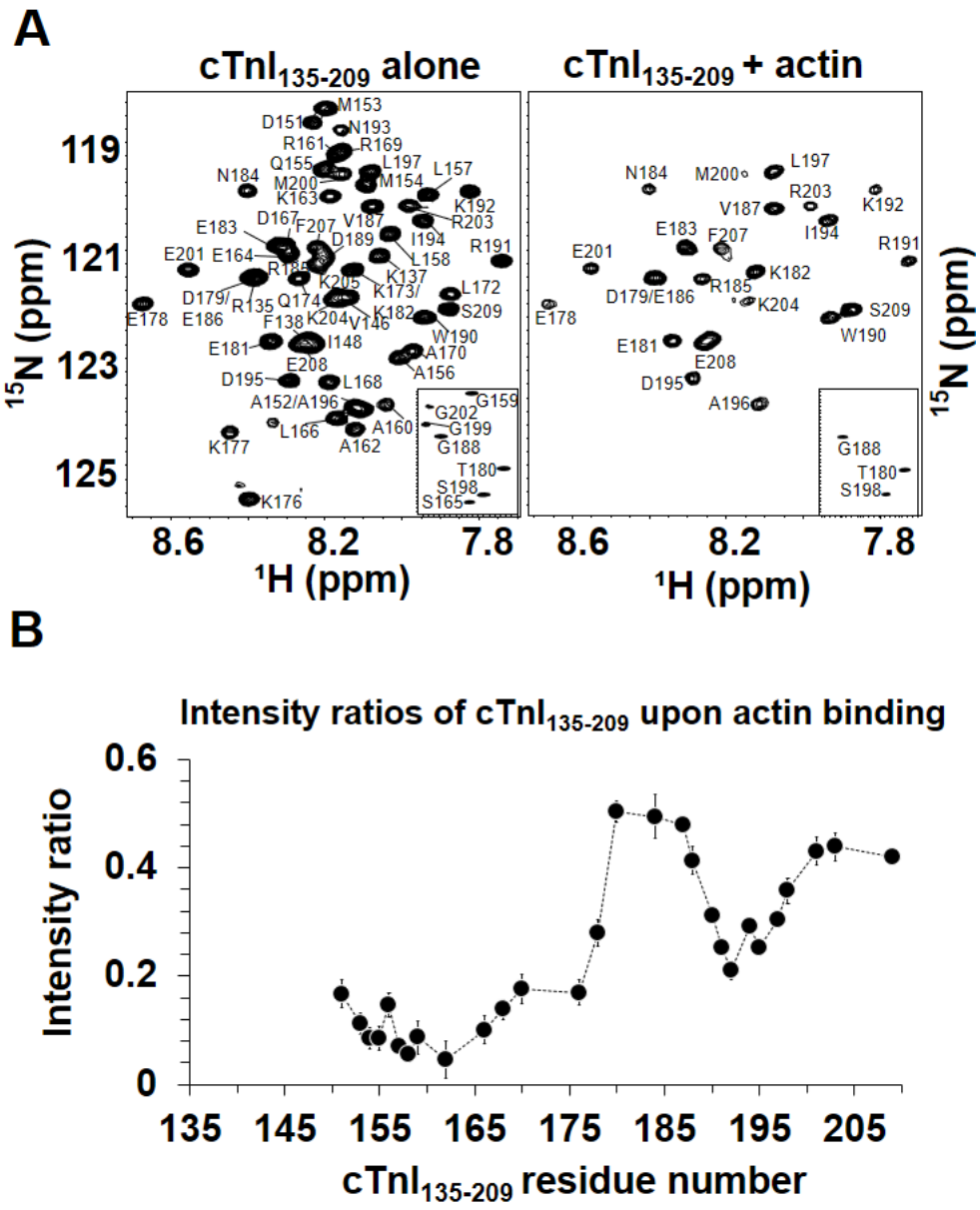

*Figure 4-17 2D [^{1}H, ^{15}N]-HSQC NMR spectra of $cTnI_{135-209}$. **(A)** $cTnI_{135-209}$ alone (left) or with actin (right). The insets show the ^{15}N-upfield region of the spectrum containing, Gly, Ser, and Thr residues. Addition*

of a small amount of monomeric actin-DNase I complex into $cTnI_{135-209}$ causes differential signal broadening (right). ***(B)*** *The observed reduction in signal intensities in the 2D [^{1}H, ^{15}N]-HSQC signals of $cTnI_{135-209}$ when actin-DNase I complex is added. Overlapped signals or signals with weak intensity were excluded.*

In the 2D ^{1}H-^{15}N spectrum of $cTnI_{135-209}$ alone, the inhibitory region, residues 135-147, contain weak signals that became undetectable upon addition of actin-DNase I, confirming that the region interacts with actin, as expected (Figure 4 -17A). A small peptide consisting of only cTnI residues 136-147 alone is capable of completely inhibiting actin-myosin cross-bridging, demonstrating this to be the minimal actin-binding inhibitory region[10]. Residues 147-177, which includes the switch region, broaden considerably upon addition of actin-DNase I, suggesting substantial rigidification upon binding to actin-DNase I. This finding is consistent with the work of Tripet *et al*.[11], which showed a "second actin-binding region" within a region corresponding to cTnI residues 164-180. In summary, our data indicate that residues 135-177, comprising the inhibitory region, switch region, and second actin-binding region, acquires rigid structure upon interaction with actin-DNase I.

The rest of the C-terminal tail of cTnI, residues 178-209, appear to be more loosely tethered to actin-DNase I than residues 135-177 (Figure 4 -17 B). However, the helical C-terminal region from residues 190-198 appears to be more tightly bound than adjacent segments. This is consistent with the study of Ramos[14], who found that the last 17 residues of chicken skeletal troponin I (corresponding to residues 193-209 in the current construct) also contribute to a third actin-interacting region in cTnI.

It is noteworthy that the regions of $cTnI_{135-209}$ that become the most structured upon binding actin-DNase I are the same regions found to possess alpha-helical propensity (Figure 4 -17 B),

with the exception of the inhibitory region $cTnI_{135-147}$. It is therefore quite possible that the same regions acquire helical structure when bound to actin. In contrast, residues 178-192 and 201-209 have negligible intrinsic helical propensity and do not appear to become as structured upon binding actin (which suggests that the folded "mobile domain" detected by Murakami et al.[235] could be formed by cTnI residues 135-177, rather than 164-209, as originally proposed). Nevertheless, it is important to note that all residues in $cTnI_{135-209}$ broaden upon binding actin-DNase I, including the less structured regions, which may represent flexible loops that bind to actin through predominantly electrostatic interactions. In fact, mutations associated with hypertrophic or restrictive cardiomyopathy are found throughout the sequence of $cTnI_{135-209}$ [45], suggesting that residues along its entire length are important to interactions with the actin thin filament.

4.4.3 *In vitro* proteolysis of cTnI by MMP-2 and calpain-2

Proteolytic cleavage of purified recombinant human cardiac troponin constructs, $cTnI_{1-77}$ and $cTnI_{135-209}$, was monitored by SDS-PAGE. $cTnI_{1-77}$ runs as a single 16 kDa band, which is higher than its actual (mass spectrometry-confirmed) weight of 8.6 kDa, likely due to its high proportion of positively charged residues. $cTnI_{135-209}$ similarly runs slower than predicted on SDS-PAGE. $cTnI_{1-77}$ and $cTnI_{135-209}$ were readily proteolysed by MMP-2, and this was almost entirely abolished by the MMP inhibitor, ARP-100 (Figure 4 -18 A&B). Similarly, calpain-2 readily cleaved $cTnI_{1-77}$ and $cTnI_{135-209}$, and this was blocked by the calpain inhibitor, MDL-28710. **(**Figure 4 -18 C&D). The pattern of bands on the gels in Figure 4 -18 is explained by mass spectrometry in the next section.

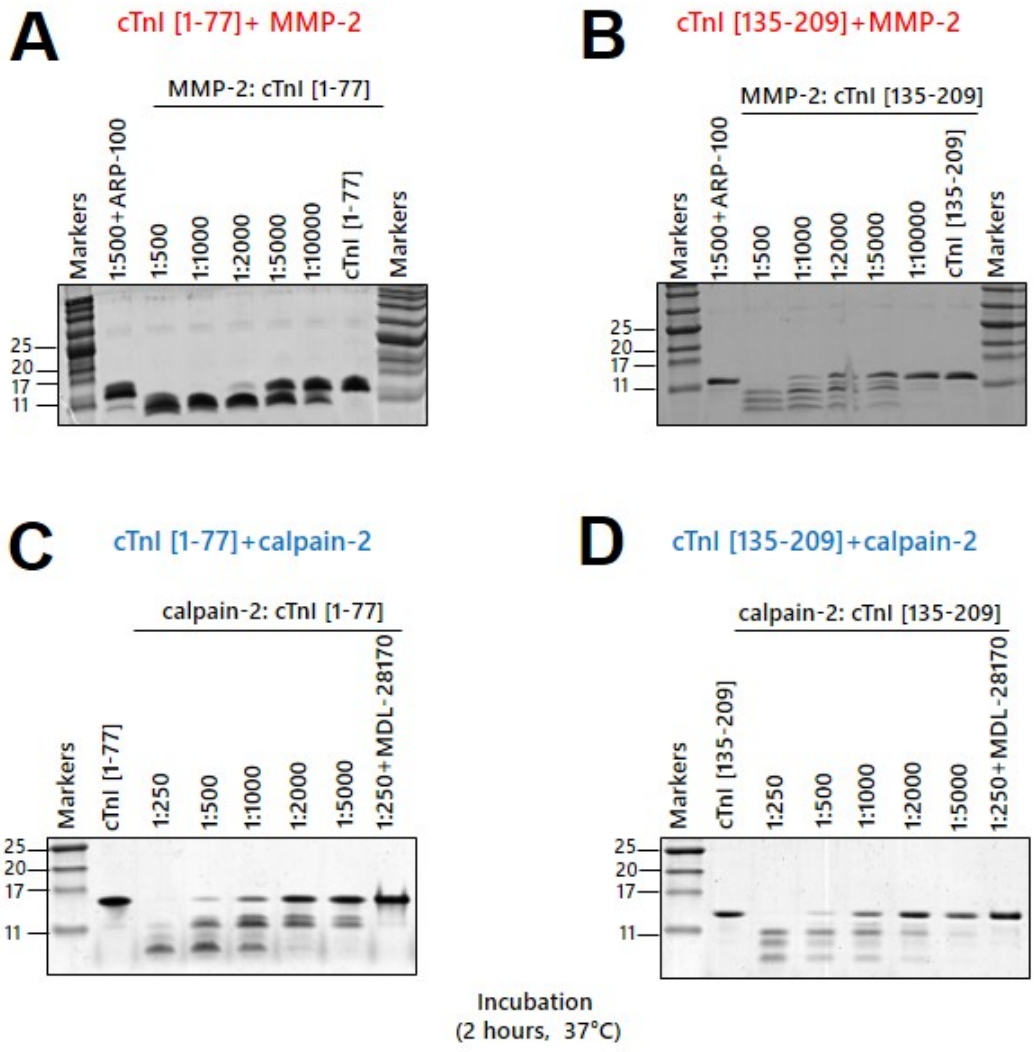

Figure 4-18 Representative Coomassie Blue-stained 16% Tris-Tricine gels illustrating in vitro proteolysis of $cTnI_{1-77}$ or $cTnI_{135-209}$ by proteases MMP-2 or calpain-2 (N=3). Molar protease-to-substrate are shown above each gel. 2 µg of cTnI was loaded in every reaction lane. Incubations were 2 h at 37 °C. Inhibition of MMP-2 and calpain-2 activities by ARP-100 and MDL-28710, respectively, is also shown.

4.4.4 Mass spectrometric identification of MMP-2 cleavage sites of cTnI

Reversed-phase high-performance liquid chromatography-mass spectrometry was used to identify MMP-2-derived cleavage sites in $cTnI_{1-77}$ and $cTnI_{135-209}$. We observed cleavage products

after incubation with MMP-2 for 0 min, 10 min, 30 min, 2 h, 6 h and 24 h **(see Appendix A, Appendix B, Appendix C** and **Figure 4 -19)**. At 0 min, intact $cTnI_{1-77}$ appeared at its expected molecular weight, 8627 Da. Within 10 min of incubation, cleavage products were formed corresponding to $cTnI_{1-17}$ (1663.8 Da) and $cTnI_{18-77}$ (6980.9 Da) **(Appendix A)**, and these continued to predominate even after 24 h of digestion. Thus, there appears to be a single main cleavage site for MMP-2 within $cTnI_{1-77}$ at ^{12}RPAPAP-IRRRSS^{23}.

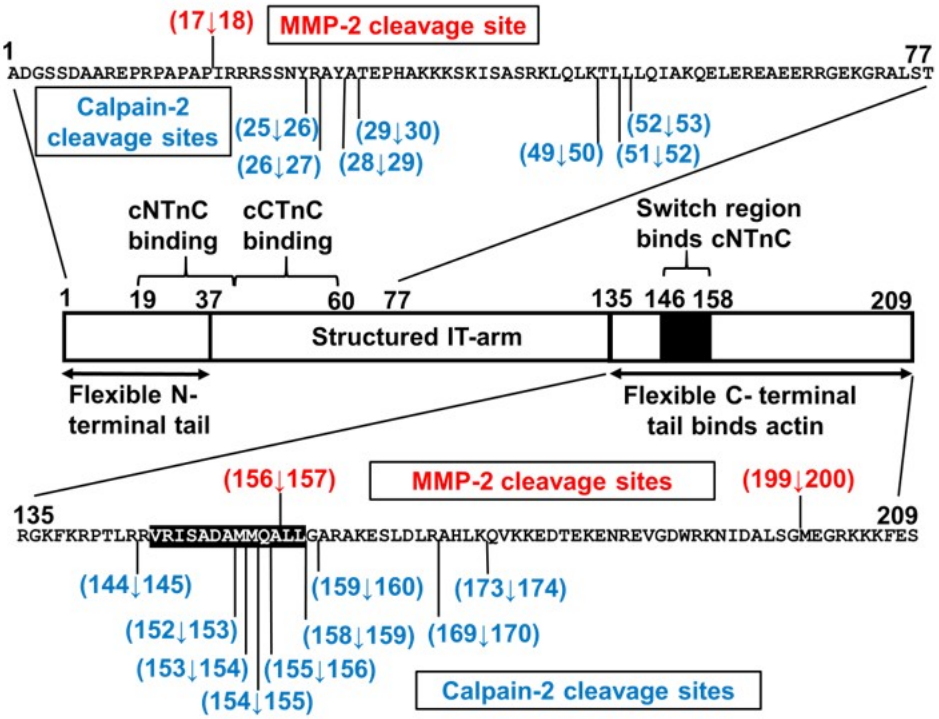

Figure 4-19 Summary of mass spectrometric analysis identifying MMP-2 and calpain-2 cleavage sites within $cTnI_{1-77}$ and $cTnI_{135-209}$. Note that our numbering of cTnI excludes the N-terminal methionine, which is removed and replaced by an acetyl group in post-translational processing.

MMP-2-mediated cleavage of $cTnI_{135-209}$ occurs at two sites that were apparent after 10 min of digestion: ^{151}DAMMQA-LLGARAK^{163} and ^{194}IDALSG-MEGRKK^{205} **(Appendix A).** The cleavage site at A156-L157 is preferred, because it is entirely cleaved at 2 h, whereas the more

C-terminal site at G199-M200 is not entirely cleaved, even after 24 h. (Note that $cTnI_{135-209}$ was ^{15}N-labeled for NMR studies, so its molecular mass was increased by the amount expected from replacing the naturally occurring ^{14}N isotope with ^{15}N).

The MMP-2 cleavage sites identified within $cTnI_{1-77}$ and $cTnI_{135-209}$ are consistent with computer-aided prediction of MMP-2 cleavage sites http://cleavpredict.sanfordburnham.org/ [236] and consensus sequences derived from MMP-2-catalyzed cleavage of peptide libraries[237–239], which show a strong preference for a hydrophobic residue (particularly leucine, isoleucine, methionine) in the P1' site (the residue immediately C-terminal to the cleavage site), as well as a proline or hydrophobic β-branched residue (valine or isoleucine) at P3 (the third residue N-terminal to the cleavage site). A feature that is somewhat unique to MMP-2 is its predilection for small amino acid residues like glycine, alanine, or serine at positions P2, P1, and P3'.

4.4.5 Mass spectrometric identification of calpain-2 cleavage sites of cTnI

We also mapped calpain-2 specific cleavage sites within $cTnI_{1-77}$ and $cTnI_{135-209}$ using mass spectrometry (Appendix A, Appendix B, and Appendix C). We identified calpain-2-mediated $cTnI_{1-77}$ and $cTnI_{135-209}$ cleavage products after 0 min, 10 min, 2 h, 6 h and 24 h (Appendix B and Appendix C**)**. At 0 min, intact $cTnI_{1-77}$ is observed at its expected molecular weight 8627 Da, though cleavage products have already appeared, with the most prominent fragments being $cTnI_{1-28}$ (3088 Da), $cTnI_{1-29}$ (3159 Da), $cTnI_{29-77}$ (5557 Da), $cTnI_{30-77}$ (5486 Da), and $cTnI_{50-77}$ (3225 Da), suggesting rapid proteolysis even before the reaction is immediately stopped by adding 1% v/v formic acid and the reaction vial frozen in liquid nitrogen. Thus, calpain-2-mediated proteolysis of cTnI occurs at a much faster rate than that observed with MMP-2. By 10 min, intermediate cleavage products like $cTnI_{1-49}$ (5419.9 Da) and $cTnI_{30-77}$ (5486.1 Da) are

disappearing, while smaller cleavage fragments begin to predominate: $cTnI_{1-25}$ (2697.4 Da), $cTnI_{1-28}$ (3087.6 Da), $cTnI_{1-29}$ (3158.6 Da), $cTnI_{27-49}$ (2583 Da), $cTnI_{26-49}$ (2739.6 Da), $cTnI_{50-77}$ (3224.8 Da), and $cTnI_{53-77}$ (2897.6 Da). These terminal products are still present after 24 h, suggesting that the major cleavage sites for calpain are all clustered around cTnI residues 25-30 and 49-53.

For calpain-2 digestion of $cTnI_{135-209}$, we identified intact ^{15}N labelled $cTnI_{135-209}$ with expected molecular weight 8964.4 Da at 0 min (See supplementary file 3). Similar to $cTnI_{1-77}$, the major cleavage products of $cTnI_{135-209}$ can also be detected from 0 min. After 10 min incubation, numerous major cleavage sites are apparent. Strikingly the calpain-2 activity localizes predominantly to the hydrophobic switch region, with a total of 6 different sites located between residues 152 and 160 (Figure 4 -19). This is consistent with the known sequence preferences of calpains-1 and -2. Of note is the cleavage site at ^{156}ALL-GAR^{161}, which has a striking similarity to the optimal calpain cleavage sequence PLF-AAR determined by peptide library analysis[240] and alanine scanning mutation[221], with hydrophobic residues on either side of the central scissile bond. Additional calpain cleavage sites are located N-terminal to residues R145, A170, and Q174.

In contrast to the very specific cut sites of MMP-2, calpain-2 appears to possess much broader substrate specificity, having multiple cleavage sites within $cTnI_{1-77}$ and $cTnI_{135-209}$ **(Figure 4 -19)**. Remarkably, calpain cut sites occur in all cTnI segments that are involved in protein-protein interactions. It seems as though calpain targets protein regions above a certain threshold of hydrophobicity, and these tend to be the same segments involved in protein-protein interactions: $cTnI_{25-30}$ contains four calpain cleavage sites and is the most hydrophobic segment of $cTnI_{19-37}$, which binds electrostatically to the N-terminal domain of cTnC; $cTnI_{49-53}$ contains three calpain

cleavage sites and is the most hydrophobic segment of $cTnI_{39-60}$, which forms an alpha helix that binds tightly to C-terminal domain of cTnC; and $cTnI_{152-160}$ contains six calpain cleavage sites and includes the most hydrophobic segment of the cTnI switch region, $cTnI_{146-158}$. Full activation of calpain would have a devastating effect on cardiac troponin I function, severely disabling calcium-mediated excitation-contraction coupling. However, it is necessary to determine which physiologic protein-protein interactions protect cTnI from proteolysis, as detailed in the sections below.

4.4.6 *In vitro* proteolysis of $cTnI_{1-77}$ in the presence of cTnC

We therefore examined proteolysis of $cTnI_{1-77}$ in the presence of its only known binding partner, cTnC. $cTnI_{1-77}$ interacts with both globular domains of cTnC in two distinct ways. cTnI residues 39-60 bind tightly to the C-terminal domain of cTnC (cCTnC) as a well-structured alpha helix that extends down to residue 79[5]. In contrast, $cTnI_{1-37}$ is intrinsically disordered, with $cTnI_{19-37}$ interacting with the cNTnC domain through predominantly electrostatic interactions[12].

There was no observable proteolysis of cTnC itself in the presence of MMP-2 or calpain-2 (Figure 4 -20). cTnC binding had virtually no effect on MMP-2-mediated digestion of $cTnI_{1-77}$ (Figure 4 -20 A), which occurs between residues 17 and 18 **(Figure 4 -19)**. This cut site lies just N-terminal to $cTnI_{19-37}$, which interacts with cNTnC[12]. Calpain-2-mediated digestion of $cTnI_{1-77}$ yields two partially digested intermediate fragments at 11 and 12 kDa on SDS-PAGE corresponding roughly to fragments $cTnI_{30-77}$ and $cTnI_{1-49}$, respectively. Upon addition of cTnC, the larger fragment corresponding to residues 1-49 disappears completely (Figure 4 -20 C), which makes sense because the cut sites between residues 49 and 53 lie exactly in the middle of the alpha helix (cTnI residues 39-60) that binds very tightly to cCTnC. Thus, formation of a rigid alpha helix precludes calpain-mediated proteolysis at this site in its native biologic context. In

contrast, when $cTnI_{19-37}$ binds electrostatically to the cTnC N-terminal domain, cTnI residues 25-31 display a partial restriction in mobility, but retain an intrinsically disordered random coil state[12]. Apparently, this interaction provides only partial protection from calpain-mediated proteolysis, as suggested by Figure 4 -20 C (that is, digestion at this site still produces a prominent 11 kDa band in the presence of cTnC).

Based on earlier biophysical studies, proteolytic removal of the first 17 residues of cTnI by MMP-2 would be expected to slightly decrease the calcium sensitivity of the troponin complex, but not to the same extent as the physiologic phosphorylation of Ser22 and Ser23 [38]. Hence, while cTnI is vulnerable to MMP-2 digestion at residues 17-18 when in complex with cTnC, proteolytic cleavage at this site would not be expected to have a devastating impact on cardiac function. In contrast, cleavage at cTnI residues 25-30 by calpain would remove more of the N-terminal tail and have a much bigger calcium desensitizing effect[38]. In addition, removing this region might negatively interfere with the diagnostic accuracy of many of the available commercial assays that target this region for detection. Examples include assays that use epitope 24-40 for either capturer or detection, whether point of care assays like Abott AxSYM ADV, Beckman Access AccuTnI, Ortho Vitros ECi ES or high sensitivity assays like Abbott ARCHITECT and Beckman Access[241].

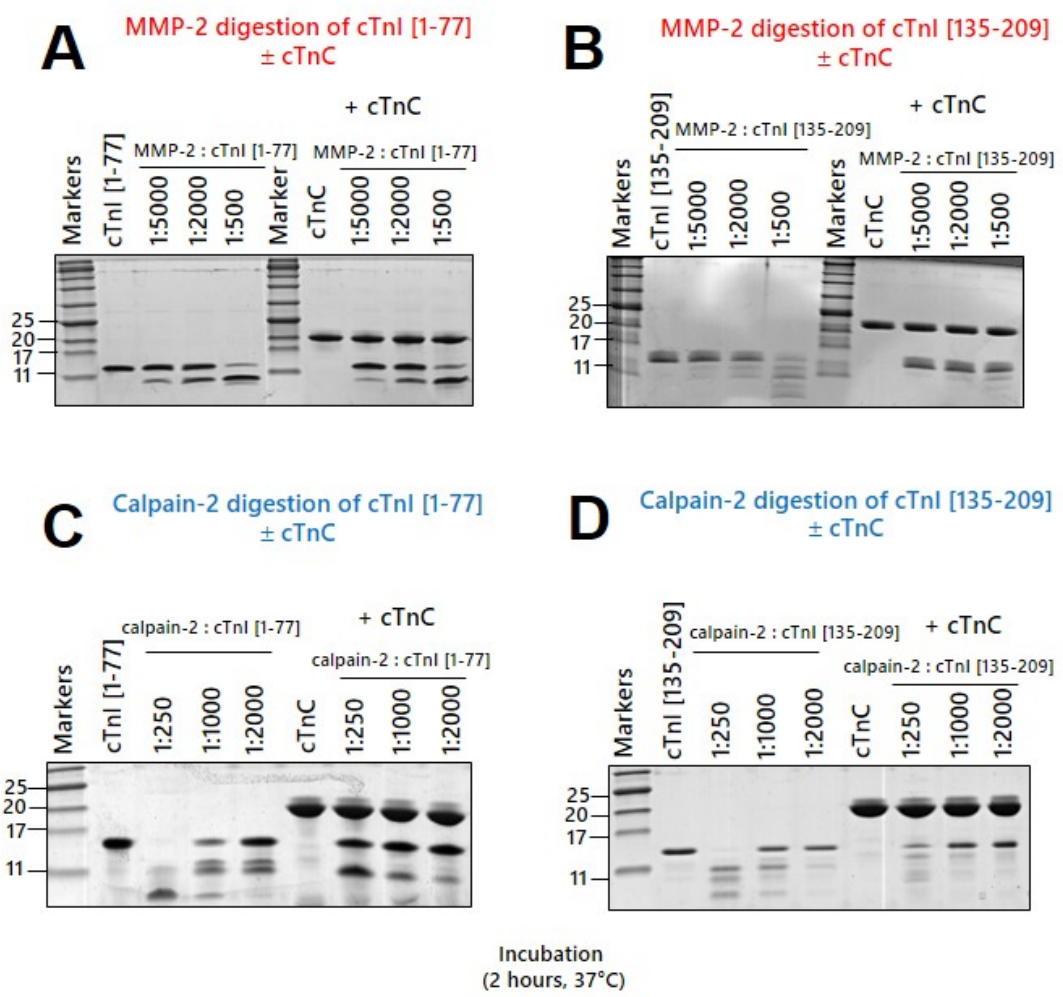

Figure 4-20 Comparison of in vitro proteolysis of $cTnI_{1-77}$ and $cTnI_{135-209}$ in the presence or absence of cTnC by MMP-2 ***(A, B)*** *and calpain-2 (****C, D****) in representative Coomassie Blue-stained SDS–PAGE gel (N=3). Cardiac troponin C is not susceptible to either MMP-2 or calpain-2 proteolysis and appears intact as a single band at ~21 KDa****.*** *2 µg of cTnI was loaded in every reaction lane. Molar cTnI-to-cTnC ratio was 1 to 1. The incubation period was 2 h at 37 °C.*

4.4.7 *In vitro* proteolysis of $cTnI_{135-209}$ in the presence of cTnC

Note that MMP-2 has only two cut sites (between residues 156-157 and 199-200) in $cTnI_{135-209}$, leading to the production of five different degradation products, producing a surprisingly complex appearance on the SDS-PAGE gels for so few cut sites (Figures 4-6 and 4-7). cTnC binding to $cTnI_{135-209}$ resulted in proteolytic protection against MMP-2 (Figure 4 -20 B) primarily

at the cut site between residues 156 and 157. This results from the binding of the switch region, $cTnI_{146-158}$, to cNTnC, with an alpha helix extending from residues 150-159. In contrast, the C-terminal cut site between cTnI residues 199 and 200, which is not known to form any interaction with cTnC, remains exposed to MMP-2 cleavage. Thus, in the presence of cTnC, this C-terminal locus becomes the preferred MMP-2 cut site in $cTnI_{135-209}$.

Binding of $cTnI_{135-209}$ to cTnC significantly changes its proteolysis pattern by calpain (Figure 4 - 20 D). In the absence of cTnC, the most favoured cut sites are distributed throughout the switch region, between residues 152 and 160, yielding a fragment at about 11 kDa ($cTnI_{153-209}$) on the SDS-PAGE gel and a smaller fragment that runs at the bottom ($cTnI_{135-152}$). However, binding of the $cTnI_{146-158}$ switch region to cNTnC shields it from cleavage, making the cut sites flanking the switch region more probable and altering the pattern of SDS-PAGE-visible proteolytic fragments.

Cleavage of the switch region would be expected to have a devastating effect on cardiac function, making it impossible to activate cardiac muscle contraction. However, it is apparent that binding of $cTnI_{135-209}$ to cTnC specifically protects the switch region against proteolytic digestion by MMP-2 and calpain, as would be expected.

4.4.8 *In vitro* proteolysis of $cTnI_{135-209}$ in the presence of actin

We next examined the proteolysis of $cTnI_{135-209}$ in the presence of actin. The current NMR study of $cTnI_{135-209}$ suggests a partial rigidification throughout its entire length upon interaction with actin. Incubation of $cTnI_{135-209}$ with actin showed pronounced concentration-dependent inhibition of MMP-2 proteolytic activity, almost completely inhibiting cTnI proteolysis at the highest concentration of actin studied, at a molar ratio of $cTnI_{135-209}$ to actin of 1:1 **(**Figure 4 -21 A**)**.

However, even at this concentration of actin, some residual proteolysis at both MMP-2 cut sites are still evident.

Calpain-2-mediated digestion of $cTnI_{135-209}$ in the presence of actin at a 1:1 molar ratio showed partial proteolytic protection of all cut sites, leading to significant preservation of intact $cTnI_{135-209}$ (Figure 4 -21 B). The degradation band at 11 kDa, corresponding to cleavage of the switch region, remains prominent in the presence of actin. This suggests that actin binding does not protect the switch region to the same extent as binding to cTnC.

It should be noted that within the sarcomere, the stoichiometry of cTnI:actin is 1:7. However, this is the result of a single troponin complex being associated with a single tropomyosin coiled-coil that lies along seven actin monomers. Presumably, in the absence of tropomyosin, the binding site for cTnI is limited to a single actin monomer. The protection of $cTnI_{135-209}$ by a 1:1 molar ratio of actin is suggestive of a 1:1 stoichiometry of binding, as expected.

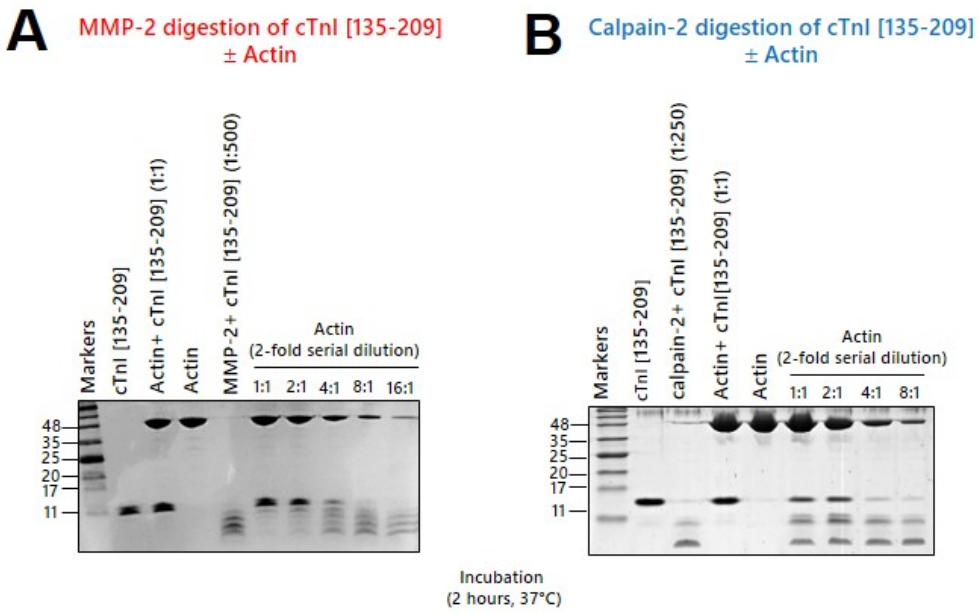

*Figure 4-21 Representative Coomassie Blue-stained SDS–PAGE gels showing in vitro proteolysis of $cTnI_{135-209}$ in the presence of **A)** MMP-2 (N=3) or **B)** calpain-2 (N=3). Molar actin:cTnI ratios are indicated above the gel. Incubation duration was 2 h at 37°C. 2 µg of cTnI was loaded in every reaction lane. MMP-2-to-cTnI ratio was 1:500, and calpain-2-to-cTnI ratio was 1:250.*

4.5 Discussion

Our study demonstrates that the C-terminal tail of cTnI contains three regions with intrinsic helical propensity, corresponding to the critical switch region that binds to cNTnC, the "second actin binding region"[11], and the "third actin binding region"[14]. We further show that all of these regions become more rigid in the presence of actin, and it would not be unreasonable to postulate that they acquire more helical character. Finally, we demonstrate that the C-terminal tail is susceptible to cleavage by MMP-2 and calpain-2, two intracellular proteases that are activated in ischemia-reperfusion injury[56,184,211,219,223].

Numerous studies in different animal model systems have attempted to address the issue of cTnI proteolysis in ischemia-reperfusion injury[40,56,67,78–80,83,85,110]. A fundamental question is which

proteases are activated, and at what degree of ischemic injury. The severity of ischemic injury depends on the degree and duration of ischemic insult, and one can envision a full spectrum of ischemia-reperfusion injury ranging from immediate recovery of function to irreversible cell death. Even with cell death, there is a spectrum of functional impairment ranging from ventricular wall akinesis to aneurysm to wall rupture. Central to the understanding of structural damage is the activation of intracellular proteases, of which MMP-2, calpains, and caspases have been identified as major players. (Caspase was found to not digest cTnI in an earlier study[76]).

"Myocardial stunning" is a form of reversible injury[242] in which restoration of blood flow relieves ischemia, but the viable, post-ischemic myocardium does not recover full contractile function immediately, sometimes requiring hours to days for full restoration[243,244]. The exact mechanism behind stunning remains a mystery, though the stunned cardiomyocyte is believed to be structurally and metabolically intact[207,245]. Most investigations have indicated that calcium handling is unperturbed, but there is decreased maximum force generation and either decreased or unchanged calcium sensitivity[77,246–249].

Proteolytic digestion of cTnI has previously been proposed as an explanation for myocardial stunning. Past studies focused on a 17-residue C-terminal truncation of cTnI, $cTnI_{1\text{-}193}$, that was associated with decreased Ca^{2+} sensitivity and myocardial stunning[42]. Separate biochemical analyses of this cleavage product demonstrated increased, rather than decreased, Ca^{2+} sensitivity[39,42]. We found no evidence to suggest that $cTnI_{1\text{-}193}$ is generated by either MMP-2- or calpain cleavage. On the other hand, we have determined that **within the C-terminal tail of cTnI, the critical switch region is most susceptible to cleavage,** both by MMP-2 and calpain**,** and cleavage at this site would provide the simplest possible explanation for the phenomenon of myocardial stunning.

The cTnI switch region is partially protected from proteolytic cleavage as it cycles between cNTnC and actin to control cardiac contraction, although severe myocardial ischemia creates additional factors that could release it from both: 1) formation of the actomyosin “rigor” state due to depletion of ATP[250]; and 2) intracellular acidosis causing calcium desensitization of the cNTnC domain. (It should be noted that acidosis would also compromise the calcium-dependent activity of calpains, however.) The necessary convergence of multiple factors under sub-lethal conditions is a possible explanation for why myocardial stunning is not universally observed in all experimental and clinical settings involving ischemia-reperfusion injury.

The proteolytic cleavage of cTnI residues C-terminal to the switch region would likely also have a negative impact on cardiac function. The importance of C-terminal residues is underscored by the existence of many hypertrophic cardiomyopathy-associated mutations that extend all the way to Glu208[45]. A recent case study of a 30-year-old man with progressive heart failure associated with restrictive cardiomyopathy identified a 15-residue (D195-S209) deletion from the C-terminus of cTnI[49].

Another recent study in transgenic mice found that the pseudophosphorylation mutation S198D decreased formation of a proteolyzed form of cTnI following 30 min of global ischemia and 1 h of reperfusion[110]. A S198A mutation did not attenuate proteolytic digestion. The simplest explanation is that the cTnI S198D mutation abolishes the MMP-2 cleavage site, whereas the S198A mutation does not, as suggested by MMP-2 cleavage site amino acid preferences at position P2[237].

Proteolytic digestion of cTnI during myocardial ischemia has clinical consequences beyond impairment of cardiac function. Proteolytic cleavage results in the generation of heterogeneous

fragments of cTnI that are released into the bloodstream and used in the detection and diagnosis of myocardial infarction[120,176]. In a recently published study, we demonstrate that the degree of proteolysis in cTnI depends on the severity of ischemic injury, with the highest degree of digestion observed in patients with ST-elevation myocardial infarct and lesser degrees of digestion seen in supply-demand ischemia[146]. It is thus quite possible that the pattern of cTnI proteolysis could be used to differentiate between different mechanisms of myocardial injury.

In summary, cardiac troponin I contains intrinsically disordered tails that are key to its function but are also sensitive to proteolysis by the proteases purported to be active during ischemia-reperfusion injury. Proteolytic digestion of cTnI has important implications for cardiac muscle function, as well as for the clinical diagnosis of myocardial infarction.

Chapter 5. Conclusions

Christian Anfinsen's studies of protein folding in the 1960s, awarded with a Nobel prize in 1972, led to his proposal that a protein's primary amino acid sequence determined its unique secondary and tertiary structures[251]. This assertion has proven to be essentially correct, but it is now known that a given amino acid sequence can adopt different structures in different contexts. As well, many intrinsically disordered regions [IDRs] do not adopt a well-defined structure until they are bound to a binding partner, and some never adopt a fixed structure. Despite the lack of structure, many of these IDRs are indispensable for function. Given their high adaptability and solvent accessibility, IDRs are highly susceptible to posttranslational modifications, and there has been a great deal of research focusing on how such modifications modulate cellular function.

The same factors that make IDRs susceptible to protein-protein interactions and post-translational modifications can make them extremely difficult to produce in large enough quantities for biophysical studies. We have overcome this problem by attaching the IDR-containing protein of interest to a fusion partner to direct its cellular expression into inclusion bodies, protecting it from proteolytic degradation. Subsequent purification steps are also carried out in strong denaturant, which also protects against proteolytic digestion. Our lab has been able to produce large amounts of pure IDRs from a number of different proteins using the bacterial membrane protein, PagP, as a fusion partner (as mentioned in chapters 2 and 4).

PagP is removed from the IDR of interest using nickel ion-assisted hydrolysis, which can be carried out under denaturing conditions. Even though this protocol has enabled us to produce a wide variety of important IDRs, it does have some limitations. First, there is wide variability in

the efficacy of the nickel-catalyzed cleavage. This seems to be construct-dependent and likely depends on the amino acid sequence surrounding the nickel ion-susceptible SRHW amino acid sequence. Further research into the ideal sequence for nickel-catalyzed cleavage would be useful. Secondly, even under ideal conditions, the nickel catalysed cleavage requires harsh pH and temperature conditions that might inadvertently lead to modification of the protein of interest. In particular, cysteine residues are likely to be oxidized (favoured by high pH and the presence of metal ions), and none of the protein constructs we have produced using this approach contain cysteine. Thus, it will be important to explore other cleavage techniques like acid-catalysed hydrolysis, to overcome these limitations. Currently, it is known that the amino acid sequence DP (Asp-Pro) is particularly susceptible to acid-catalysed peptide bond hydrolysis[157], but besides this, the optimal sequence has not been elucidated to the same extent as was done for nickel-catalyzed hydrolysis to obtain the SRHW sequence[164].

IDRs are believed to comprise more than 40% of any eukaryotic proteome[252]. Our main protein of interest, cardiac troponin I (cTnI), is made up of >50% IDRs that are crucial for its regulatory function, making it susceptible to post-translational modifications like phosphorylation and proteolytic degradation. The N-terminal IDR of cTnI is essential for stabilising the inter-domain orientation of the regulatory N-terminal domain of troponin C and regulating its calcium binding affinity. The C-terminal IDR plays the essential role of controlling every single heartbeat by alternatively binding to troponin C during systole (ventricular contraction) and actin during diastole (ventricular relaxation). While the structure of this region bound bound to troponin C is well known, very little was known about its structure while bound to actin. Our solution NMR work indicates that there are some regions with helical propensity that rigidify upon interaction with actin, but solving the atomic resolution structure by NMR would be extremely difficult. To

this end, we have started a collaboration with Dr. Stefan Raunser[253] at the Max Planck Institute in Germany to determine the cryo-electron microscopy structure of cTnI[135-209] bound to the actin thin filament.

We have used our PagP fusion protein system to produce full-length cTnI and cTnT, as well as fragments thereof. In contrast, cTnC expresses well on its own as a soluble globular protein. Interestingly, PagP alone was not effective in targeting full-length cTnI and cTnT into inclusion bodies, and effective expression required fusion to another inclusion body-directing tag in addition to PagP. Our ultimate goal is to produce, purify, and then refold all of the cTn complex components together to produce a highly pure, soluble and stable end product that can be used to solve the cryo-electron microscopic structure of intact thin filament. As a first step towards this goal, I tested many different conditions for optimal folding and/or stability of reconstituted troponin complex using the protein thermal shift assay. Briefly, the method uses a qPCR machine to measure protein thermal denaturation curves. Denaturation is detected by an increase of fluorescence caused by the binding of hydrophobic fluorescent probes that bind non-specifically to hydrophobic segments of a protein when it unfolds. I discovered that magnesium ions surprisingly have a stabilizing effect on the complex (increasing its temperature of unfolding), whereas calcium had a destabilizing effect. This was somewhat unexpected, given the preference of cTnC for binding calcium.

Besides using our purified reconstituted troponin complex for biophysical studies, it will also be used as a calibration standard for our serum cardiac troponin proteolysis assay (see Chapter 3), which requires a protein standard containing all of the relevant epitopes detected by the antibodies used for the ELISA-based assays.

As highlighted by the most recent definitions of myocardial infarction (MI)[118], the cTnI and cTnT assays have become a cornerstone in diagnosing MI, due to the reliable release of these proteins and their very high cardiac tissue specificity. Despite its status as the gold standard biomarker for MI, there are a number of serious limitations associated with its use.

One major challenge in interpreting blood troponin concentrations is that an elevated level does not necessarily indicate the presence of a myocardial infarct. Troponin elevations are observed after healthy runners complete a marathon[122] (without cardiac complication), as well as after pacemaker-induced tachycardia[123]. Moreover, even when there is a true infarct present, the magnitude of troponin elevation appears to correlate poorly with infarct size determined by imaging, particularly in the case of NSTEMI patients[179]. These observations challenge the traditional dogma that troponins are released only as a result of cellular necrosis – irreversible cell death. However, it appears reversible cellular injury, either as a result of mechanical strain or sub-lethal injuries due to ischemia or inflammation, can also result in elevated cardiac troponin concentrations. Our troponin proteolysis study suggests that these milder injuries may release less proteolyzed troponins, which are more readily detected by commercially available cTnI assays. Moreover, the degree of proteolytic degradation in cTnI correlates with the severity of ischemic injury, with the most severe degradation observed in STEMI patients and the least degradation observed in type 2 MI patients. Thus, we hypothesize that proteolyzed cTnI fragments may correlate better with true infarct size than total troponin I levels, which would contain a mixture of intact and proteolyzed forms. Future clinical studies should be undertaken to measure the correlation between proteolyzed cTnI levels and infarct size, as measured by cardiac MRI (the current clinical gold standard for measuring infarct size[254]). It would be clinically advantageous to be able to estimate infarct size with a convenient biomarker. Cardiac MRI is a

limited and expensive resource. Acute NSTEMI patients with larger evolving infarcts may be more likely to benefit from invasive revascularization[255]. Current management of NSTEMI patients does not have clear guidelines as to when to pursue invasive revascularization, in contrast to STEMI patients.

Another area of controversy surrounding the cardiac troponin assay is how to make the distinction between type 1 NSTEMI and type 2 MI. The treatment of these conditions is very different, with NSTEMI patients treated with antiplatelet agents and anticoagulants and potentially invasive revascularization for the more unstable patients, in order to treat an acute coronary artery blockage due to thrombosis[256]. In contrast, type 2 MI patients do not have an acute thrombus and would not benefit from such a treatment[118]. Our clinical study of cardiac troponin I proteolysis suggested a trend towards less proteolysis in type 2 MI patients, but there was considerable overlap between the NSTEMI patients and type 2 MI patients in relation to the degree of troponin I proteolysis observed. This is most likely due to the clinical ambiguity that exists between the two conditions – that is, an inability to distinguish between the two conditions with no gold standard. Some of the patients classified as having an NSTEMI probably in fact had an element of type 2 MI, while other patients classified as having type 2 MI were probably having an NSTEMI. In many clinical situations, there is no way to distinguish between the two conditions. However, we note that in unambiguous cases, there was a clear distinction in degradation patterns between type 2 MI patients and NSTEMI patients. For example, a patient with a clear type 2 MI (a troponin elevation associated with acute gastrointestinal bleeding and a hemoglobin level less than 60 g/L, with complete clinical resolution of ischemia after receiving blood transfusions) had very low levels of troponin degradation compared to a patient with a clear type 1 MI (no other physiologic stressors and a clear lesion on angiography, along with

resolution of symptoms post-stenting). Thus, it would be valuable to conduct a larger study that selected only patients with very clear-cut type 2 MI versus those with clear-cut type 1 NSTEMI to test whether a clear distinction can be made on the basis of cTnI proteolysis. Establishing the utility of this test under known conditions would make it useful in cases where there is more diagnostic uncertainty.

In the era of high sensitivity cTn assays and with the incorporation of delta levels into the diagnostic criteria of MI[118], it is necessary to recognise that any elevated cTn concentration above the predetermined 99th percentile level is concerning and necessitates medical management because it reflects cardiac injury that is significant enough to cause the respective elevation. Intervening in these patients has been shown to improve patients' outcomes[257]. Generally, we expect to observe relatively low amounts of cTn degradation in these patients with very small cTn elevations (since the degree of cardiac injury is milder, so there would be less cell death) if their samples were to be tested in our degradation assay, but more research is needed to improve the sensitivity our degradation assay to the level of modern high sensitivity cTn assays.

One of the interesting observations in our clinical study of troponin proteolysis was the degradation pattern observed in two unique patients. One was a young otherwise healthy patient with myocarditis, whose cTnI degradation pattern matched that of STEMI patients in terms of severity. In contrast, a type 4a MI patient (a relatively benign troponin elevation following uncomplicated elective cardiac stent placement) whose cTnI showed the least degradation out of all the patients in the study. Separate studies could target each of these categories to determine if patients with these conditions show similar cTnI degradation profiles.

As proteolysis of cardiac proteins is known to be part of a pathological sequence of events during myocardial ischemia and necrosis, targeting this process could be a plausible therapeutic option. Using compounds that are known to inhibit the well-studied proteases like MMP-2 or calpain or both as part of the early treatment regimen of acute coronary syndrome patients in a well-designed clinical trial might reveal valuable long-term health benefits. Such studies could also look into the extent of cTn degradation, if the levels are affected by the use of protease inhibitors like doxycycline, and whether the levels of proteolyzed cTnI correlate with future major adverse cardiovascular events (MACE).

One major limitation of our clinical study of cTnI proteolysis in patients is that it utilized only a single technique, sandwich ELISA, to detect cTnI. The basis of the technique (sandwich immunoassays) is used for almost all clinical chemistry tests, but it does not provide a complete profile of the degradation products present in the patient's serum. I attempted to combine immunoprecipitation with western blotting, which depends on using two different antibodies (one for immunoprecipitation and one for detection) to select for different epitopes on cTnI. The use of two antibodies, should in theory, provide relatively specific detection of cTnI, as in the case of sandwich ELISA. However, it was difficult to obtain reproducible results using this technique. One issue we encountered was the detection of intense bands at apparent molecular weights higher than that of intact cTnI. It is possible that this is due to cross-reactivity with another protein, though this would require both immunoprecipitation and detection antibodies to cross-react. We used a secondary detection antibody specific for non-denatured mouse antibody, so that light and heavy chains from the immunoprecipitation would not be detected, so it seems unlikely that the higher molecular weight bands came from immunoglobulin heavy chain. One possibility is that cTnI is cross-linked or covalently attached to another protein, which has been

suggested in other publications[78]. Very recently, Katrukha et al, working for the leading worldwide supplier of anti-cTnI antibodies in clinical use, Hytest Inc., presented a study of cTnI proteolytic degradation profiles from the serum of MI patients, using a wide range of detection antibodies[145]. The profiles are consistent with the MMP-2 and calpain cleavage sites we determined by our *in vitro* proteolysis studies. However, we note that the gels in this study were not displayed in their entirety, particularly at molecular weights higher than intact cTnI. It would be interesting to observe whether the authors of this publication also observed bands at high molecular weights greater than cTnI or not.

An even better technique to analyze proteolytic fragments would be mass spectrometry, which could identify exact protease cleavage sites. We made some initial attempts to analyze immunoprecipitated cTnI from plasma samples of STEMI patients using mass spectrometry. We were able to detect proteolytic fragments corresponding to cTnI after limited trypsin digestion, but no fragments indicative of intracellular proteolysis were identified. In collaboration with Dr. Olivier Julien, affiliated with the University of Alberta Department of Biochemistry with specialization in proteolysis, proteomics, and mass spectrometry, our lab intends to build upon our initial efforts to map the exact cleavage patterns in cTnI, both in animal models of ischemia-reperfusion injury (with collaborator and committee member, Dr. Richard Schulz) and plasma samples from patients with MI. Identifying biologically relevant cut sites in cTnI is an important step towards determining the culprit proteases most responsible for causing intracellular structural damage in the setting of ischemia-reperfusion injury. Based on the work of Dr. Schulz, we believe that MMP-2 will be one of the most important proteases activated early in the course of ischemia-reperfusion injury, while calpain activation will require more severe and prolonged ischemia. Hopefully, many other protease substrates will be identified from mass spectrometric

analysis of ischemia-reperfusion injury as well, giving a more complete of the extent of proteolytic digestion that is occurring in the cardiac muscle cell.

Bibliography

1. Ebashi, S. & Kodama, A. A new protein factor promoting aggregation of tropomyosin. *J. Biochem. (Tokyo)* **58**, 107–108 (1965).
2. Greaser, M. L. & Gergely, J. Purification and properties of the components from troponin. *J. Biol. Chem.* **248**, 2125–2133 (1973).
3. Park, K. C., Gaze, D. C., Collinson, P. O. & Marber, M. S. Cardiac troponins: from myocardial infarction to chronic disease. *Cardiovasc. Res.* **113**, 1708–1718 (2017).
4. Zabrouskov, V., Ge, Y., Schwartz, J. & Walker, J. W. Unraveling Molecular Complexity of Phosphorylated Human Cardiac Troponin I by Top Down Electron Capture Dissociation/Electron Transfer Dissociation Mass Spectrometry. *Mol. Cell. Proteomics* **7**, 1838–1849 (2008).
5. Takeda, S., Yamashita, A., Maeda, K. & Maéda, Y. Structure of the core domain of human cardiac troponin in the Ca2+-saturated form. *Nature* **424**, 35–41 (2003).
6. Takeda, S., Kobayashi, T., Taniguchi, H., Hayashi, H. & Maéda, Y. Structural and functional domains of the troponin complex revealed by limited digestion. *Eur. J. Biochem.* **246**, 611–617 (1997).
7. Tanokura, M., Tawada, Y., Ono, A. & Ohtsuki, I. Chymotryptic subfragments of troponin T from rabbit skeletal muscle. Interaction with tropomyosin, troponin I and troponin C. *J. Biochem. (Tokyo)* **93**, 331–337 (1983).
8. Lehman, W. Switching Muscles On and Off in Steps: The McKillop-Geeves Three-State Model of Muscle Regulation. *Biophys. J.* **112**, 2459–2466 (2017).
9. Narita, A., Yasunaga, T., Ishikawa, T., Mayanagi, K. & Wakabayashi, T. Ca(2+)-induced switching of troponin and tropomyosin on actin filaments as revealed by electron cryo-microscopy. *J. Mol. Biol.* **308**, 241–261 (2001).
10. Van Eyk, J. E., Thomas, L. T., Tripet, B., Wiesner, R. J., Pearlstone, J. R., Farah, C. S., Reinach, F. C. & Hodges, R. S. Distinct regions of troponin I regulate Ca2+-dependent activation and Ca2+ sensitivity of the acto-S1-TM ATPase activity of the thin filament. *J. Biol. Chem.* **272**, 10529–10537 (1997).
11. Tripet, B., Van Eyk, J. E. & Hodges, R. S. Mapping of a second actin-tropomyosin and a second troponin C binding site within the C terminus of troponin I, and their importance in the Ca2+-dependent regulation of muscle contraction11Edited by P. E Wright. *J. Mol. Biol.* **271**, 728–750 (1997).

12. Hwang, P. M., Cai, F., Pineda-Sanabria, S. E., Corson, D. C. & Sykes, B. D. The cardiac-specific N-terminal region of troponin I positions the regulatory domain of troponin C. *Proc. Natl. Acad. Sci. U. S. A.* **111**, 14412–14417 (2014).
13. Mahmud, Z. & Hwang, P. M. Cardiac Troponin Complex: Cardiac Troponin C (TNNC1), Cardiac Troponin I (TNNI3), and Cardiac Troponin T (TNNT2). in *Encyclopedia of Signaling Molecules* (ed. Choi, S.) 692–701 (Springer International Publishing, 2018). doi:10.1007/978-3-319-67199-4_101901
14. Ramos, C. H. Mapping subdomains in the C-terminal region of troponin I involved in its binding to troponin C and to thin filament. *J. Biol. Chem.* **274**, 18189–18195 (1999).
15. Solaro, R. J., Rosevear, P. & Kobayashi, T. The unique functions of cardiac troponin I in the control of cardiac muscle contraction and relaxation. *Biochem. Biophys. Res. Commun.* **369**, 82–87 (2008).
16. Tung, C. S., Wall, M. E., Gallagher, S. C. & Trewhella, J. A model of troponin-I in complex with troponin-C using hybrid experimental data: the inhibitory region is a beta-hairpin. *Protein Sci. Publ. Protein Soc.* **9**, 1312–1326 (2000).
17. Li, M. X., Spyracopoulos, L. & Sykes, B. D. Binding of cardiac troponin-I147-163 induces a structural opening in human cardiac troponin-C. *Biochemistry* **38**, 8289–8298 (1999).
18. Wei, B. & Jin, J.-P. TNNT1, TNNT2, and TNNT3: Isoform genes, regulation, and structure-function relationships. *Gene* **582**, 1–13 (2016).
19. Wang, J. & Jin, J. P. Conformational modulation of troponin T by configuration of the NH2-terminal variable region and functional effects. *Biochemistry* **37**, 14519–14528 (1998).
20. Jin, J.-P., Zhang, Z. & Bautista, J. A. Isoform diversity, regulation, and functional adaptation of troponin and calponin. *Crit. Rev. Eukaryot. Gene Expr.* **18**, 93–124 (2008).
21. Jin, J.-P. & Chong, S. M. Localization of the two tropomyosin-binding sites of troponin T. *Arch. Biochem. Biophys.* **500**, 144–150 (2010).
22. Murakami, K., Stewart, M., Nozawa, K., Tomii, K., Kudou, N., Igarashi, N., Shirakihara, Y., Wakatsuki, S., Yasunaga, T. & Wakabayashi, T. Structural basis for tropomyosin overlap in thin (actin) filaments and the generation of a molecular swivel by troponin-T. *Proc. Natl. Acad. Sci. U. S. A.* **105**, 7200–7205 (2008).
23. Ishii, Y. & Lehrer, S. S. Two-site attachment of troponin to pyrene-labeled tropomyosin. *J. Biol. Chem.* **266**, 6894–6903 (1991).
24. Oliveira, D. M., Nakaie, C. R., Sousa, A. D., Farah, C. S. & Reinach, F. C. Mapping the domain of troponin T responsible for the activation of actomyosin ATPase activity. Identification of residues involved in binding to actin. *J. Biol. Chem.* **275**, 27513–27519 (2000).

25. Franklin, A. J., Baxley, T., Kobayashi, T. & Chalovich, J. M. The C-Terminus of Troponin T Is Essential for Maintaining the Inactive State of Regulated Actin. *Biophys. J.* **102**, 2536–2544 (2012).
26. Murphy, R. T., Mogensen, J., Shaw, A., Kubo, T., Hughes, S. & McKenna, W. J. Novel mutation in cardiac troponin I in recessive idiopathic dilated cardiomyopathy. *Lancet Lond. Engl.* **363**, 371–372 (2004).
27. Sadayappan, S., Finley, N., Howarth, J. W., Osinska, H., Klevitsky, R., Lorenz, J. N., Rosevear, P. R. & Robbins, J. Role of the acidic N' region of cardiac troponin I in regulating myocardial function. *FASEB J. Off. Publ. Fed. Am. Soc. Exp. Biol.* **22**, 1246–1257 (2008).
28. Barbato, J. C., Huang, Q.-Q., Hossain, M. M., Bond, M. & Jin, J.-P. Proteolytic N-terminal truncation of cardiac troponin I enhances ventricular diastolic function. *J. Biol. Chem.* **280**, 6602–6609 (2005).
29. Fentzke, R. C., Buck, S. H., Patel, J. R., Lin, H., Wolska, B. M., Stojanovic, M. O., Martin, A. F., Solaro, R. J., Moss, R. L. & Leiden, J. M. Impaired cardiomyocyte relaxation and diastolic function in transgenic mice expressing slow skeletal troponin I in the heart. *J. Physiol.* **517 (Pt 1)**, 143–157 (1999).
30. Solaro, R. J., Moir, A. J. & Perry, S. V. Phosphorylation of troponin I and the inotropic effect of adrenaline in the perfused rabbit heart. *Nature* **262**, 615–617 (1976).
31. Ray, K. P. & England, P. J. Phosphorylation of the inhibitory subunit of troponin and its effect on the calcium dependence of cardiac myofibril adenosine triphosphatase. *FEBS Lett.* **70**, 11–16 (1976).
32. Kranias, E. G. & Solaro, R. J. Phosphorylation of troponin I and phospholamban during catecholamine stimulation of rabbit heart. *Nature* **298**, 182–184 (1982).
33. Reddy, Y. S. Phosphorylation of cardiac regulatory proteins by cyclic AMP-dependent protein kinase. *Am. J. Physiol.* **231**, 1330–1336 (1976).
34. Chandra, M., Dong, W. J., Pan, B. S., Cheung, H. C. & Solaro, R. J. Effects of protein kinase A phosphorylation on signaling between cardiac troponin I and the N-terminal domain of cardiac troponin C. *Biochemistry* **36**, 13305–13311 (1997).
35. Najafi, A., Sequeira, V., Kuster, D. W. D. & van der Velden, J. β-adrenergic receptor signalling and its functional consequences in the diseased heart. *Eur. J. Clin. Invest.* **46**, 362–374 (2016).
36. Gomes, A. V., Harada, K. & Potter, J. D. A mutation in the N-terminus of Troponin I that is associated with hypertrophic cardiomyopathy affects the Ca2+-sensitivity, phosphorylation kinetics and proteolytic susceptibility of troponin. *J. Mol. Cell. Cardiol.* **39**, 754–765 (2005).

37. Wang, Y., Pinto, J. R., Solis, R. S., Dweck, D., Liang, J., Diaz-Perez, Z., Ge, Y., Walker, J. W. & Potter, J. D. Generation and functional characterization of knock-in mice harboring the cardiac troponin I-R21C mutation associated with hypertrophic cardiomyopathy. *J. Biol. Chem.* **287**, 2156–2167 (2012).
38. Ward, D. G., Cornes, M. P. & Trayer, I. P. Structural Consequences of Cardiac Troponin I Phosphorylation. *J. Biol. Chem.* **277**, 41795–41801 (2002).
39. Rarick, H. M., Tu, X.-H., Solaro, R. J. & Martin, A. F. The C Terminus of Cardiac Troponin I Is Essential for Full Inhibitory Activity and Ca2+ Sensitivity of Rat Myofibrils. *J. Biol. Chem.* **272**, 26887–26892 (1997).
40. Murphy, A. M., Kögler, H., Georgakopoulos, D., McDonough, J. L., Kass, D. A., Van Eyk, J. E. & Marbán, E. Transgenic mouse model of stunned myocardium. *Science* **287**, 488–491 (2000).
41. Galińska, A., Hatch, V., Craig, R., Murphy, A. M., Eyk, J. E. V., Wang, C.-L. A., Lehman, W. & Foster, D. B. The C Terminus of Cardiac Troponin I Stabilizes the Ca2+-Activated State of Tropomyosin on Actin Filaments. *Circ. Res.* (2010).
42. Foster, D. B., Noguchi, T., VanBuren, P., Murphy, A. M. & Van Eyk, J. E. C-terminal truncation of cardiac troponin I causes divergent effects on ATPase and force: implications for the pathophysiology of myocardial stunning. *Circ. Res.* **93**, 917–924 (2003).
43. Kimura, A., Harada, H., Park, J. E., Nishi, H., Satoh, M., Takahashi, M., Hiroi, S., Sasaoka, T., Ohbuchi, N., Nakamura, T., Koyanagi, T., Hwang, T. H., Choo, J. A., Chung, K. S., Hasegawa, A., Nagai, R., Okazaki, O., Nakamura, H., Matsuzaki, M., Sakamoto, T., Toshima, H., Koga, Y., Imaizumi, T. & Sasazuki, T. Mutations in the cardiac troponin I gene associated with hypertrophic cardiomyopathy. *Nat. Genet.* **16**, 379–382 (1997).
44. Lu, Q.-W., Wu, X.-Y. & Morimoto, S. Inherited cardiomyopathies caused by troponin mutations. *J. Geriatr. Cardiol. JGC* **10**, 91–101 (2013).
45. Mogensen, J., Hey, T. & Lambrecht, S. A Systematic Review of Phenotypic Features Associated With Cardiac Troponin I Mutations in Hereditary Cardiomyopathies. *Can. J. Cardiol.* **31**, 1377–1385 (2015).
46. Liu, B., Tikunova, S. B., Kline, K. P., Siddiqui, J. K. & Davis, J. P. Disease-related cardiac troponins alter thin filament Ca2+ association and dissociation rates. *PloS One* **7**, e38259 (2012).
47. Takahashi-Yanaga, F., Morimoto, S., Harada, K., Minakami, R., Shiraishi, F., Ohta, M., Lu, Q. W., Sasaguri, T. & Ohtsuki, I. Functional consequences of the mutations in human cardiac troponin I gene found in familial hypertrophic cardiomyopathy. *J. Mol. Cell. Cardiol.* **33**, 2095–2107 (2001).

48. Ohtsuki, I. & Morimoto, S. Troponin: Regulatory function and disorders. *Biochem. Biophys. Res. Commun.* **369**, 62–73 (2008).
49. Shah, S., Yogasundaram, H., Basu, R., Wang, F., Paterson, D. I., Alastalo, T.-P. & Oudit, G. Y. Novel Dominant-Negative Mutation in Cardiac Troponin I Causes Severe Restrictive Cardiomyopathy. *Circ. Heart Fail.* **10**, (2017).
50. Willott, R. H., Gomes, A. V., Chang, A. N., Parvatiyar, M. S., Pinto, J. R. & Potter, J. D. Mutations in Troponin that cause HCM, DCM AND RCM: what can we learn about thin filament function? *J. Mol. Cell. Cardiol.* **48**, 882–892 (2010).
51. Mörner, S., Richard, P., Kazzam, E., Hainque, B., Schwartz, K. & Waldenström, A. Deletion in the cardiac troponin I gene in a family from northern Sweden with hypertrophic cardiomyopathy. *J. Mol. Cell. Cardiol.* **32**, 521–525 (2000).
52. Kostareva, A., Gudkova, A., Sjöberg, G., Mörner, S., Semernin, E., Krutikov, A., Shlyakhto, E. & Sejersen, T. Deletion in TNNI3 gene is associated with restrictive cardiomyopathy. *Int. J. Cardiol.* **131**, 410–412 (2009).
53. Zhang, Z., Feng, H.-Z. & Jin, J.-P. Structure of the NH2-terminal variable region of cardiac troponin T determines its sensitivity to restrictive cleavage in pathophysiological adaptation. *Arch. Biochem. Biophys.* **515**, 37–45 (2011).
54. Feng, H.-Z., Biesiadecki, B. J., Yu, Z.-B., Hossain, M. M. & Jin, J.-P. Restricted N-terminal truncation of cardiac troponin T: a novel mechanism for functional adaptation to energetic crisis. *J. Physiol.* **586**, 3537–3550 (2008).
55. Puente, X. S., Sánchez, L. M., Overall, C. M. & López-Otín, C. Human and mouse proteases: a comparative genomic approach. *Nat. Rev. Genet.* **4**, 544–558 (2003).
56. Wang, W., Schulze, C. J., Suarez-Pinzon, W. L., Dyck, J. R. B., Sawicki, G. & Schulz, R. Intracellular action of matrix metalloproteinase-2 accounts for acute myocardial ischemia and reperfusion injury. *Circulation* **106**, 1543–1549 (2002).
57. Ali, M. A. M. & Schulz, R. Activation of MMP-2 as a key event in oxidative stress injury to the heart. *Front. Biosci. Landmark Ed.* **14**, 699–716 (2009).
58. Mujumdar, V. S., Smiley, L. M. & Tyagi, S. C. Activation of matrix metalloproteinase dilates and decreases cardiac tensile strength. *Int. J. Cardiol.* **79**, 277–286 (2001).
59. King, M. K., Coker, M. L., Goldberg, A., McElmurray, J. H., Gunasinghe, H. R., Mukherjee, R., Zile, M. R., O'Neill, T. P. & Spinale, F. G. Selective matrix metalloproteinase inhibition with developing heart failure: effects on left ventricular function and structure. *Circ. Res.* **92**, 177–185 (2003).
60. Lalu, M. M., Pasini, E., Schulze, C. J., Ferrari-Vivaldi, M., Ferrari-Vivaldi, G., Bachetti, T. & Schulz, R. Ischaemia-reperfusion injury activates matrix metalloproteinases in the human heart. *Eur. Heart J.* **26**, 27–35 (2005).

61. Cheung, P. Y., Sawicki, G., Wozniak, M., Wang, W., Radomski, M. W. & Schulz, R. Matrix metalloproteinase-2 contributes to ischemia-reperfusion injury in the heart. *Circulation* **101**, 1833–1839 (2000).
62. Smith, M. A. & Schnellmann, R. G. Calpains, mitochondria, and apoptosis. *Cardiovasc. Res.* **96**, 32–37 (2012).
63. Goll, D. E., Thompson, V. F., Li, H., Wei, W. & Cong, J. The calpain system. *Physiol. Rev.* **83**, 731–801 (2003).
64. Garcia-Dorado, D., Ruiz-Meana, M., Inserte, J., Rodriguez-Sinovas, A. & Piper, H. M. Calcium-mediated cell death during myocardial reperfusion. *Cardiovasc. Res.* **94**, 168–180 (2012).
65. Wijnker, P. J. M., Li, Y., Zhang, P., Foster, D. B., Remedios, C. dos, Van Eyk, J. E., Stienen, G. J. M., Murphy, A. M. & van der Velden, J. A novel phosphorylation site, Serine 199, in the C-terminus of cardiac troponin I regulates calcium sensitivity and susceptibility to calpain-induced proteolysis. *J. Mol. Cell. Cardiol.* **82**, 93–103 (2015).
66. Martin-Garrido, A., Biesiadecki, B. J., Salhi, H. E., Shaifta, Y., Remedios, C. G. dos, Ayuz-Guner, S., Cai, W., Ge, Y., Avkiran, M. & Kentish, J. C. Monophosphorylation of cardiac troponin-I at Ser23/24 is sufficient to regulate cardiac myofibrillar Ca2+ sensitivity and calpain-induced proteolysis. *J. Biol. Chem.* jbc.RA117.001292 (2018). doi:10.1074/jbc.RA117.001292
67. Gao, W. D., Atar, D., Liu, Y., Perez, N. G., Murphy, A. M. & Marban, E. Role of troponin I proteolysis in the pathogenesis of stunned myocardium. *Circ. Res.* **80**, 393–399 (1997).
68. Hernando, V., Inserte, J., Sartório, C. L., Parra, V. M., Poncelas-Nozal, M. & Garcia-Dorado, D. Calpain translocation and activation as pharmacological targets during myocardial ischemia/reperfusion. *J. Mol. Cell. Cardiol.* **49**, 271–279 (2010).
69. Khalil, P. N., Neuhof, C., Huss, R., Pollhammer, M., Khalil, M. N., Neuhof, H., Fritz, H. & Siebeck, M. Calpain inhibition reduces infarct size and improves global hemodynamics and left ventricular contractility in a porcine myocardial ischemia/reperfusion model. *Eur. J. Pharmacol.* **528**, 124–131 (2005).
70. Di Lisa, F., De Tullio, R., Salamino, F., Barbato, R., Melloni, E., Siliprandi, N., Schiaffino, S. & Pontremoli, S. Specific degradation of troponin T and I by mu-calpain and its modulation by substrate phosphorylation. *Biochem. J.* **308 (Pt 1)**, 57–61 (1995).
71. Papp, Z., van der Velden, J. & Stienen, G. J. M. Calpain-I induced alterations in the cytoskeletal structure and impaired mechanical properties of single myocytes of rat heart. *Cardiovasc. Res.* **45**, 981–993 (2000).
72. McIlwain, D. R., Berger, T. & Mak, T. W. Caspase Functions in Cell Death and Disease. *Cold Spring Harb. Perspect. Biol.* **5**, a008656 (2013).

73. Seaman, J. E., Julien, O., Lee, P. S., Rettenmaier, T. J., Thomsen, N. D. & Wells, J. A. Cacidases: caspases can cleave after aspartate, glutamate and phosphoserine residues. *Cell Death Differ.* **23**, 1717–1726 (2016).
74. Renolleau, S., Fau, S., Goyenvalle, C., Joly, L.-M., Chauvier, D., Jacotot, E., Mariani, J. & Charriaut-Marlangue, C. Specific caspase inhibitor Q-VD-OPh prevents neonatal stroke in P7 rat: a role for gender. *J. Neurochem.* **100**, 1062–1071 (2007).
75. Merkle, S., Frantz, S., Schön, M. P., Bauersachs, J., Buitrago, M., Frost, R. J. A., Schmitteckert, E. M., Lohse, M. J. & Engelhardt, S. A role for caspase-1 in heart failure. *Circ. Res.* **100**, 645–653 (2007).
76. Communal, C., Sumandea, M., de Tombe, P., Narula, J., Solaro, R. J. & Hajjar, R. J. Functional consequences of caspase activation in cardiac myocytes. *Proc. Natl. Acad. Sci. U. S. A.* **99**, 6252–6256 (2002).
77. Eyk, J. E. V., Powers, F., Law, W., Larue, C., Hodges, R. S. & Solaro, R. J. Breakdown and Release of Myofilament Proteins During Ischemia and Ischemia/Reperfusion in Rat Hearts Identification of Degradation Products and Effects on the pCa-Force Relation. *Circ. Res.* **82**, 261–271 (1998).
78. McDonough, J. L., Arrell, D. K. & Eyk, J. E. V. Troponin I Degradation and Covalent Complex Formation Accompanies Myocardial Ischemia/Reperfusion Injury. *Circ. Res.* **84**, 9–20 (1999).
79. Maekawa, A., Lee, J.-K., Nagaya, T., Kamiya, K., Yasui, K., Horiba, M., Miwa, K., Uzzaman, M., Maki, M., Ueda, Y. & Kodama, I. Overexpression of calpastatin by gene transfer prevents troponin I degradation and ameliorates contractile dysfunction in rat hearts subjected to ischemia/reperfusion. *J. Mol. Cell. Cardiol.* **35**, 1277–1284 (2003).
80. Schwartz, S. M., Duffy, J. Y., Pearl, J. M., Goins, S., Wagner, C. J. & Nelson, D. P. Glucocorticoids preserve calpastatin and troponin I during cardiopulmonary bypass in immature pigs. *Pediatr. Res.* **54**, 91–97 (2003).
81. Canty, J. M. & Lee, T.-C. Troponin I Proteolysis and Myocardial Stunning: Now You See It —Now You Don»t. *J. Mol. Cell. Cardiol.* **34**, 375–377 (2002).
82. Thomas, S. A., Fallavollita, J. A., Lee, T. C., Feng, J. & Canty, J. M. Absence of troponin I degradation or altered sarcoplasmic reticulum uptake protein expression after reversible ischemia in swine. *Circ. Res.* **85**, 446–456 (1999).
83. Kim, S.-J., Kudej, R. K., Yatani, A., Kim, Y.-K., Takagi, G., Honda, R., Colantonio, D. A., Van Eyk, J. E., Vatner, D. E., Rasmusson, R. L. & Vatner, S. F. A Novel Mechanism for Myocardial Stunning Involving Impaired Ca2+ Handling. *Circ. Res.* **89**, 831–837 (2001).
84. Prasan, A. M., McCarron, H. C. K., Hambly, B. D., Fermanis, G. G., Sullivan, D. R. & Jeremy, R. W. Effect of treatment on ventricular function and troponin I proteolysis in reperfused myocardium. *J. Mol. Cell. Cardiol.* **34**, 401–411 (2002).

85. Colantonio, D. A., Van Eyk, J. E. & Przyklenk, K. Stunned peri-infarct canine myocardium is characterized by degradation of troponin T, not troponin I. *Cardiovasc. Res.* **63**, 217–225 (2004).
86. Feng, J., Schaus, B. J., Fallavollita, J. A., Lee, T. C. & Canty, J. M. Preload induces troponin I degradation independently of myocardial ischemia. *Circulation* **103**, 2035–2037 (2001).
87. McDonough, J. L., Labugger, R., Pickett, W., Tse, M. Y., MacKenzie, S., Pang, S. C., Atar, D., Ropchan, G. & Van Eyk, J. E. Cardiac troponin I is modified in the myocardium of bypass patients. *Circulation* **103**, 58–64 (2001).
88. Martin, A. F. Turnover of cardiac troponin subunits. Kinetic evidence for a precursor pool of troponin-I. *J. Biol. Chem.* **256**, 964–968 (1981).
89. Jeong, E.-M., Wang, X., Xu, K., Hossain, M. M. & Jin, J.-P. Nonmyofilament-associated troponin T fragments induce apoptosis. *Am. J. Physiol. Heart Circ. Physiol.* **297**, H283-292 (2009).
90. Feng, H.-Z., Hossain, M. M., Huang, X.-P. & Jin, J.-P. Myofilament incorporation determines the stoichiometry of troponin I in transgenic expression and the rescue of a null mutation. *Arch. Biochem. Biophys.* **487**, 36–41 (2009).
91. Zhang, Z., Biesiadecki, B. J. & Jin, J.-P. Selective deletion of the NH2-terminal variable region of cardiac troponin T in ischemia reperfusion by myofibril-associated mu-calpain cleavage. *Biochemistry* **45**, 11681–11694 (2006).
92. Biesiadecki, B. J., Elder, B. D., Yu, Z.-B. & Jin, J.-P. Cardiac troponin T variants produced by aberrant splicing of multiple exons in animals with high instances of dilated cardiomyopathy. *J. Biol. Chem.* **277**, 50275–50285 (2002).
93. Sumandea, M. P., Vahebi, S., Sumandea, C. A., Garcia-Cazarin, M. L., Staidle, J. & Homsher, E. Impact of cardiac troponin T N-terminal deletion and phosphorylation on myofilament function. *Biochemistry* **48**, 7722–7731 (2009).
94. Convertino, V. & Hoffler, G. W. Cardiovascular physiology. Effects of microgravity. *J. Fla. Med. Assoc.* **79**, 517–524 (1992).
95. Demontis, G. C., Germani, M. M., Caiani, E. G., Barravecchia, I., Passino, C. & Angeloni, D. Human Pathophysiological Adaptations to the Space Environment. *Front. Physiol.* **8**, (2017).
96. Herault, S., Fomina, G., Alferova, I., Kotovskaya, A., Poliakov, V. & Arbeille, P. Cardiac, arterial and venous adaptation to weightlessness during 6-month MIR spaceflights with and without thigh cuffs (bracelets). *Eur. J. Appl. Physiol.* **81**, 384–390 (2000).
97. Yu, Z.-B., Zhang, L.-F. & Jin, J.-P. A Proteolytic NH2-terminal Truncation of Cardiac Troponin I That Is Up-regulated in Simulated Microgravity. *J. Biol. Chem.* **276**, 15753–15760 (2001).

98. Zhang, L., Song, Z., Chang, H., Wang, Y.-Y. & Yu, Z.-B. Enhanced N-terminal degradation of troponin I blunts cardiac function responsiveness to isoproterenol in 4-week tail-suspended rats. *Mol. Med. Rep.* **7**, 271–279 (2013).
99. Zhang, L., Wang, Y.-Y. & Yu, Z.-B. [Depressed responsiveness of cardiomyocytes to isoproterenol in simulated weightlessness rats]. *Sheng Li Xue Bao* **59**, 845–850 (2007).
100. Chang, H., Sheng, J.-J., Zhang, L., Yue, Z.-J., Jiao, B., Li, J.-S. & Yu, Z.-B. ROS-Induced Nuclear Translocation of Calpain-2 Facilitates Cardiomyocyte Apoptosis in Tail-Suspended Rats. *J. Cell. Biochem.* **116**, 2258–2269 (2015).
101. Chang, H., Zhang, L., Xu, P.-T., Li, Q., Sheng, J.-J., Wang, Y.-Y., Chen, Y., Zhang, L.-N. & Yu, Z.-B. Nuclear translocation of calpain-2 regulates propensity toward apoptosis in cardiomyocytes of tail-suspended rats. *J. Cell. Biochem.* **112**, 571–580 (2011).
102. Xu, P.-T., Song, Z., Li, Q., Zhang, L., Wang, Y.-Y. & Yu, Z.-B. [Calpain mediates cardiac troponin I degradation in tail-suspended rats]. *Sheng Li Xue Bao* **62**, 415–420 (2010).
103. Ali, M. A. M., Stepanko, A., Fan, X., Holt, A. & Schulz, R. Calpain inhibitors exhibit matrix metalloproteinase-2 inhibitory activity. *Biochem. Biophys. Res. Commun.* **423**, 1–5 (2012).
104. Adams, S. E., Robinson, E. J., Miller, D. J., Rizkallah, P. J., Hallett, M. B. & Allemann, R. K. Conformationally restricted calpain inhibitors †Electronic supplementary information (ESI) available. See DOI: 10.1039/c5sc01158b Click here for additional data file. *Chem. Sci.* **6**, 6865–6871 (2015).
105. Ali, Mohammad M. A. Novel intracellular role of matrix metalloproteinase-2 in cardiac cell injury. (University of Alberta, 2012).
106. Katrukha, A. G., Bereznikova, A. V., Filatov, V. L., Esakova, T. V., Kolosova, O. V., Pettersson, K., Lövgren, T., Bulargina, T. V., Trifonov, I. R., Gratsiansky, N. A., Pulkki, K., Voipio-Pulkki, L.-M. & Gusev, N. B. Degradation of cardiac troponin I: implication for reliable immunodetection. *Clin. Chem.* **44**, 2433–2440 (1998).
107. Madsen, L. H., Lund, T., Grieg, Z., Nygaard, S., Holmvang, L., Jurlander, B., Grande, P., Christensen, G. & Atar, D. Cardiac troponin I degradation in serum of patients with hypertrophic obstructive cardiomyopathy undergoing percutaneous septal ablation. *Cardiology* **114**, 167–173 (2009).
108. Madsen, L. H., Christensen, G., Lund, T., Serebruany, V. L., Granger, C. B., Hoen, I., Grieg, Z., Alexander, J. H., Jaffe, A. S., Eyk, J. E. V. & Atar, D. Time Course of Degradation of Cardiac Troponin I in Patients With Acute ST-Elevation Myocardial Infarction The ASSENT-2 Troponin Substudy. *Circ. Res.* **99**, 1141–1147 (2006).
109. Zhang, P., Kirk, J. A., Ji, W., dos Remedios, C. G., Kass, D. A., Van Eyk, J. E. & Murphy, A. M. Multiple reaction monitoring to identify site-specific troponin I phosphorylated residues in the failing human heart. *Circulation* **126**, 1828–1837 (2012).

110. Li, Y., Zhu, G., Paolocci, N., Zhang, P., Takahashi, C., Okumus, N., Heravi, A., Keceli, G., Ramirez-Correa, G., Kass, D. A. & Murphy, A. M. Heart Failure-Related Hyperphosphorylation in the Cardiac Troponin I C Terminus Has Divergent Effects on Cardiac Function In Vivo. *Circ. Heart Fail.* **10**, (2017).
111. Brundel, B. J. J. M., Henning, R. H., van Gilst, W. H., van Gelder, I. C. & Crijns, H. J. G. M. Molecular adaptations in human atrial fibrillation: mechanisms of protein remodelling. *Neth. Heart J.* **9**, 235–239 (2001).
112. Ke, L., Qi, X. Y., Dijkhuis, A.-J., Chartier, D., Nattel, S., Henning, R. H., Kampinga, H. H. & Brundel, B. J. J. M. Calpain mediates cardiac troponin degradation and contractile dysfunction in atrial fibrillation. *J. Mol. Cell. Cardiol.* **45**, 685–693 (2008).
113. Cummins, B., Auckland, M. L. & Cummins, P. Cardiac-specific troponin-I radioimmunoassay in the diagnosis of acute myocardial infarction. *Am. Heart J.* **113**, 1333–1344 (1987).
114. Katus, H. A., Remppis, A., Looser, S., Hallermeier, K., Scheffold, T. & Kübler, W. Enzyme linked immuno assay of cardiac troponin T for the detection of acute myocardial infarction in patients. *J. Mol. Cell. Cardiol.* **21**, 1349–1353 (1989).
115. Muehlschlegel, J. D., Perry, T. E., Liu, K.-Y., Nascimben, L., Fox, A. A., Collard, C. D., Avery, E. G., Aranki, S. F., D'Ambra, M. N., Shernan, S. K. & Body, S. C. Troponin is superior to electrocardiogram and creatinine kinase MB for predicting clinically significant myocardial injury after coronary artery bypass grafting. *Eur. Heart J.* **30**, 1574–1583 (2009).
116. Harris, B. M., Nageh, T., Marsden, J. T., Thomas, M. R. & Sherwood, R. A. Comparison of cardiac troponin T and I and CK-MB for the detection of minor myocardial damage during interventional cardiac procedures. *Ann. Clin. Biochem.* **37 (Pt 6)**, 764–769 (2000).
117. Saenger, A. K. & Jaffe, A. S. Requiem for a heavyweight: the demise of creatine kinase-MB. *Circulation* **118**, 2200–2206 (2008).
118. Thygesen, K., Alpert, J. S., Jaffe, A. S., Chaitman, B. R., Bax, J. J., Morrow, D. A., White, H. D. & ESC Scientific Document Group. Fourth universal definition of myocardial infarction (2018). *Eur. Heart J.* (2018). doi:10.1093/eurheartj/ehy462
119. Apple, F. S. A New Season for Cardiac Troponin Assays: It's Time to Keep a Scorecard. *Clin. Chem.* **55**, 1303–1306 (2009).
120. Thygesen, K., Alpert, J. S., Jaffe, A. S., Simoons, M. L., Chaitman, B. R. & White, H. D. Third Universal Definition of Myocardial Infarction. *Circulation* **126**, 2020–2035 (2012).
121. Nagarajan, V., Hernandez, A. V. & Tang, W. H. W. Prognostic value of cardiac troponin in chronic stable heart failure: a systematic review. *Heart Br. Card. Soc.* **98**, 1778–1786 (2012).

122. Fortescue, E. B., Shin, A. Y., Greenes, D. S., Mannix, R. C., Agarwal, S., Feldman, B. J., Shah, M. I., Rifai, N., Landzberg, M. J., Newburger, J. W. & Almond, C. S. D. Cardiac troponin increases among runners in the Boston Marathon. *Ann. Emerg. Med.* **49**, 137–143, 143.e1 (2007).
123. Turer, A. T., Addo, T. A., Martin, J. L., Sabatine, M. S., Lewis, G. D., Gerszten, R. E., Keeley, E. C., Cigarroa, J. E., Lange, R. A., Hillis, L. D. & de Lemos, J. A. Myocardial Ischemia Induced by Rapid Atrial Pacing Causes Troponin T Release Detectable by a High-Sensitivity Assay: Insights from a Coronary Sinus Sampling Study. *J. Am. Coll. Cardiol.* **57**, 2398–2405 (2011).
124. Smith, S. C., Ladenson, J. H., Mason, J. W. & Jaffe, A. S. Elevations of cardiac troponin I associated with myocarditis. Experimental and clinical correlates. *Circulation* **95**, 163–168 (1997).
125. Imazio, M., Demichelis, B., Cecchi, E., Belli, R., Ghisio, A., Bobbio, M. & Trinchero, R. Cardiac troponin I in acute pericarditis. *J. Am. Coll. Cardiol.* **42**, 2144–2148 (2003).
126. Bonnefoy, E., Godon, P., Kirkorian, G., Fatemi, M., Chevalier, P. & Touboul, P. Serum cardiac troponin I and ST-segment elevation in patients with acute pericarditis. *Eur. Heart J.* **21**, 832–836 (2000).
127. Giannoni, A., Giovannini, S. & Clerico, A. Measurement of circulating concentrations of cardiac troponin I and T in healthy subjects: a tool for monitoring myocardial tissue renewal? *Clin. Chem. Lab. Med.* **47**, 1167–1177 (2009).
128. Mair, J., Lindahl, B., Hammarsten, O., Müller, C., Giannitsis, E., Huber, K., Möckel, M., Plebani, M., Thygesen, K. & Jaffe, A. S. How is cardiac troponin released from injured myocardium? *Eur. Heart J. Acute Cardiovasc. Care* **7**, 553–560 (2018).
129. Ben Yedder, N., Roux, J. F. & Paredes, F. A. Troponin elevation in supraventricular tachycardia: primary dependence on heart rate. *Can. J. Cardiol.* **27**, 105–109 (2011).
130. Latini, R., Masson, S., Pirelli, S., Barlera, S., Pulitano, G., Carbonieri, E., Gulizia, M., Vago, T., Favero, C., Zdunek, D., Struck, J., Staszewsky, L., Maggioni, A. P., Franzosi, M. G., Disertori, M. & GISSI-AF Investigators. Circulating cardiovascular biomarkers in recurrent atrial fibrillation: data from the GISSI-atrial fibrillation trial. *J. Intern. Med.* **269**, 160–171 (2011).
131. Jensen, J. K., Hallén, J., Lund, T., Madsen, L. H., Grieg, Z., Januzzi, J. L. & Atar, D. Troponin I degradation in serum of patients with acute ischemic stroke. *Scand. J. Clin. Lab. Invest.* **71**, 74–80 (2011).
132. Cui, Y.-X., Ren, H., Lee, C.-Y., Li, S.-F., Song, J.-X., Gao, X.-G. & Chen, H. Characteristics of elevated cardiac troponin I in patients with acute ischemic stroke. *J. Geriatr. Cardiol. JGC* **14**, 401–406 (2017).

133. Beaulieu-Boire, I., Leblanc, N., Berger, L. & Boulanger, J.-M. Troponin elevation predicts atrial fibrillation in patients with stroke or transient ischemic attack. *J. Stroke Cerebrovasc. Dis. Off. J. Natl. Stroke Assoc.* **22**, 978–983 (2013).
134. Labugger, R., Organ, L., Collier, C., Atar, D. & Eyk, J. E. V. Extensive Troponin I and T Modification Detected in Serum From Patients With Acute Myocardial Infarction. *Circulation* **102**, 1221–1226 (2000).
135. Wu, A. H., Feng, Y. J., Moore, R., Apple, F. S., McPherson, P. H., Buechler, K. F. & Bodor, G. Characterization of cardiac troponin subunit release into serum after acute myocardial infarction and comparison of assays for troponin T and I. American Association for Clinical Chemistry Subcommittee on cTnI Standardization. *Clin. Chem.* **44**, 1198–1208 (1998).
136. Katrukha, I. A., Kogan, A. E., Vylegzhanina, A. V., Serebryakova, M. V., Koshkina, E. V., Bereznikova, A. V. & Katrukha, A. G. Thrombin-Mediated Degradation of Human Cardiac Troponin T. *Clin. Chem.* **63**, 1094–1100 (2017).
137. Bates, K. J., Hall, E. M., Fahie-Wilson, M. N., Kindler, H., Bailey, C., Lythall, D. & Lamb, E. J. Circulating immunoreactive cardiac troponin forms determined by gel filtration chromatography after acute myocardial infarction. *Clin. Chem.* **56**, 952–958 (2010).
138. Michielsen, E. C. H. J., Diris, J. H. C., Kleijnen, V. W. V. C., Wodzig, W. K. W. H. & Van Dieijen-Visser, M. P. Investigation of release and degradation of cardiac troponin T in patients with acute myocardial infarction. *Clin. Biochem.* **40**, 851–855 (2007).
139. Cardinaels, E. P. M., Mingels, A. M. A., van Rooij, T., Collinson, P. O., Prinzen, F. W. & van Dieijen-Visser, M. P. Time-dependent degradation pattern of cardiac troponin T following myocardial infarction. *Clin. Chem.* **59**, 1083–1090 (2013).
140. Streng, A. S., de Boer, D., van Doorn, W. P. T. M., Bouwman, F. G., Mariman, E. C. M., Bekers, O., van Dieijen-Visser, M. P. & Wodzig, W. K. W. H. Identification and Characterization of Cardiac Troponin T Fragments in Serum of Patients Suffering from Acute Myocardial Infarction. *Clin. Chem.* **63**, 563–572 (2017).
141. Jacobs, L. H., van de Kerkhof, J., Mingels, A. M., Kleijnen, V. W., van der Sande, F. M., Wodzig, W. K., Kooman, J. P. & van Dieijen-Visser, M. P. Haemodialysis patients longitudinally assessed by highly sensitive cardiac troponin T and commercial cardiac troponin T and cardiac troponin I assays. *Ann. Clin. Biochem.* **46**, 283–290 (2009).
142. Diris, J. H. C., Hackeng, C. M., Kooman, J. P., Pinto, Y. M., Hermens, W. T. & van Dieijen-Visser, M. P. Impaired renal clearance explains elevated troponin T fragments in hemodialysis patients. *Circulation* **109**, 23–25 (2004).
143. deFilippi, C., Seliger, S. L., Kelley, W., Duh, S.-H., Hise, M., Christenson, R. H., Wolf, M., Gaggin, H. & Januzzi, J. Interpreting cardiac troponin results from high-sensitivity assays

in chronic kidney disease without acute coronary syndrome. *Clin. Chem.* **58**, 1342–1351 (2012).

144. Apple, F. S. Counterpoint: Standardization of cardiac troponin I assays will not occur in my lifetime. *Clin. Chem.* **58**, 169–171 (2012).
145. Katrukha, I., Vylegzhanina, A. V., Kogan, A. E., Kharitonov, A. V., Tamm, N. N., Filatov, V. L., Bereznikova, A. V., Koshkina, E. V. & Katrukha, A. G. Human cardiac TnI degradation and antibody selection for the assay development. AACC meeting (2018). Chicago, IL
146. Zahran, S., Figueiredo, V. P., Graham, M. M., Schulz, R. & Hwang, P. M. Proteolytic Digestion of Serum Cardiac Troponin I as Marker of Ischemic Severity. *J. Appl. Lab. Med.* jalm.2017.025254 (2018). doi:10.1373/jalm.2017.025254
147. DeLeon-Pennell, K. Y., Meschiari, C. A., Jung, M. & Lindsey, M. L. Matrix Metalloproteinases in Myocardial Infarction and Heart Failure. *Prog. Mol. Biol. Transl. Sci.* **147**, 75–100 (2017).
148. Spaulding, K., Takaba, K., Collins, A., Faraji, F., Wang, G., Aguayo, E., Ge, L., Saloner, D., Wallace, A. W., Baker, A. J., Lovett, D. H. & Ratcliffe, M. B. Short term doxycycline treatment induces sustained improvement in myocardial infarction border zone contractility. *PLoS ONE* **13**, (2018).
149. Cerisano, G., Buonamici, P., Valenti, R., Sciagrà, R., Raspanti, S., Santini, A., Carrabba, N., Dovellini, E. V., Romito, R., Pupi, A., Colonna, P. & Antoniucci, D. Early short-term doxycycline therapy in patients with acute myocardial infarction and left ventricular dysfunction to prevent the ominous progression to adverse remodelling: the TIPTOP trial. *Eur. Heart J.* **35**, 184–191 (2014).
150. Dunker, A. K., Lawson, J. D., Brown, C. J., Williams, R. M., Romero, P., Oh, J. S., Oldfield, C. J., Campen, A. M., Ratliff, C. M., Hipps, K. W., Ausio, J., Nissen, M. S., Reeves, R., Kang, C., Kissinger, C. R., Bailey, R. W., Griswold, M. D., Chiu, W., Garner, E. C. & Obradovic, Z. Intrinsically disordered protein. *J. Mol. Graph. Model.* **19**, 26–59 (2001).
151. Tompa, P. & Csermely, P. The role of structural disorder in the function of RNA and protein chaperones. *FASEB J. Off. Publ. Fed. Am. Soc. Exp. Biol.* **18**, 1169–1175 (2004).
152. Uversky, V. N. A decade and a half of protein intrinsic disorder: Biology still waits for physics. *Protein Sci.* **22**, 693–724 (2013).
153. Iakoucheva, L. M., Radivojac, P., Brown, C. J., O'Connor, T. R., Sikes, J. G., Obradovic, Z. & Dunker, A. K. The importance of intrinsic disorder for protein phosphorylation. *Nucleic Acids Res.* **32**, 1037–1049 (2004).
154. Chance, R. E. & Frank, B. H. Research, development, production, and safety of biosynthetic human insulin. *Diabetes Care* **16 Suppl 3**, 133–142 (1993).

155. Lilie, H., Schwarz, E. & Rudolph, R. Advances in refolding of proteins produced in E. coli. *Curr. Opin. Biotechnol.* **9**, 497–501 (1998).
156. Yamaguchi, H. & Miyazaki, M. Refolding Techniques for Recovering Biologically Active Recombinant Proteins from Inclusion Bodies. *Biomolecules* **4**, 235–251 (2014).
157. Hwang, P. M., Pan, J. S. & Sykes, B. D. Targeted expression, purification, and cleavage of fusion proteins from inclusion bodies in Escherichia coli. *FEBS Lett.* **588**, 247–252 (2014).
158. Hwang, P. M., Pan, J. S. & Sykes, B. D. A PagP fusion protein system for the expression of intrinsically disordered proteins in Escherichia coli. *Protein Expr. Purif.* **85**, 148–151 (2012).
159. Hwang, P. M., Choy, W.-Y., Lo, E. I., Chen, L., Forman-Kay, J. D., Raetz, C. R. H., Privé, G. G., Bishop, R. E. & Kay, L. E. Solution structure and dynamics of the outer membrane enzyme PagP by NMR. *Proc. Natl. Acad. Sci. U. S. A.* **99**, 13560–13565 (2002).
160. Booth, P. J. & Curran, A. R. Membrane protein folding. *Curr. Opin. Struct. Biol.* **9**, 115–121 (1999).
161. Misawa, S. & Kumagai, I. Refolding of therapeutic proteins produced in Escherichia coli as inclusion bodies. *Biopolymers* **51**, 297–307 (1999).
162. Gross, E. & Witkop, B. Nonenzymatic Cleavage of Peptide Bonds: The Methionine Residues in Bovine Pancreatic Ribonuclease. *J. Biol. Chem.* **237**, 1856–1860 (1962).
163. Krezel, A., Kopera, E., Protas, A. M., Poznański, J., Wysłouch-Cieszyńska, A. & Bal, W. Sequence-specific Ni(II)-dependent peptide bond hydrolysis for protein engineering. Combinatorial library determination of optimal sequences. *J. Am. Chem. Soc.* **132**, 3355–3366 (2010).
164. Kopera, E., Belczyk-Ciesielska, A. & Bal, W. Application of Ni(II)-Assisted Peptide Bond Hydrolysis to Non-Enzymatic Affinity Tag Removal. *PLoS ONE* **7**, (2012).
165. Garcia-Mira, M. M. & Sanchez-Ruiz, J. M. pH corrections and protein ionization in water/guanidinium chloride. *Biophys. J.* **81**, 3489–3502 (2001).
166. Michaux, C., Pomroy, N. C. & Privé, G. G. Refolding SDS-Denatured Proteins by the Addition of Amphipathic Cosolvents. *J. Mol. Biol.* **375**, 1477–1488 (2008).
167. Haynes, W. M. *CRC handbook of chemistry and physics : a ready-reference book of chemical and physical data*. (Boca Raton, Florida : CRC Press, [2014], 2014).
168. Vogt, W. Oxidation of methionyl residues in proteins: tools, targets, and reversal. *Free Radic. Biol. Med.* **18**, 93–105 (1995).
169. Fontana, A., Dalzoppo, D., Grandi, C. & Zambonin, M. Chemical cleavage of tryptophanyl and tyrosyl peptide bonds via oxidative halogenation mediated by o-iodosobenzoic acid. *Biochemistry* **20**, 6997–7004 (1981).

170. Griffiths, S. W., King, J. & Cooney, C. L. The Reactivity and Oxidation Pathway of Cysteine 232 in Recombinant Human α1-Antitrypsin. *J. Biol. Chem.* **277**, 25486–25492 (2002).
171. Kaminskaia, N. V., Johnson, T. W. & Kostić, N. M. Regioselective Hydrolysis of Tryptophan-Containing Peptides Promoted by Palladium(II) Complexes. *J. Am. Chem. Soc.* **121**, 8663–8664 (1999).
172. Hong, J., Jiao, Y., He, W., Guo, Z., Yu, Z., Zhang, J. & Zhu, L. His-Oriented Peptide Hydrolysis Promoted by cis-[Pt(en)(H2O)2]2+: a New Specific Peptide Cleavage Site. *Inorg. Chem.* **49**, 8148–8154 (2010).
173. DeWood, M. A., Spores, J., Notske, R., Mouser, L. T., Burroughs, R., Golden, M. S. & Lang, H. T. Prevalence of total coronary occlusion during the early hours of transmural myocardial infarction. *N. Engl. J. Med.* **303**, 897–902 (1980).
174. O'Gara, P. T., Kushner, F. G., Ascheim, D. D., Casey, D. E., Chung, M. K., de Lemos, J. A., Ettinger, S. M., Fang, J. C., Fesmire, F. M., Franklin, B. A., Granger, C. B., Krumholz, H. M., Linderbaum, J. A., Morrow, D. A., Newby, L. K., Ornato, J. P., Ou, N., Radford, M. J., Tamis-Holland, J. E., Tommaso, J. E., Tracy, C. M., Woo, Y. J., Zhao, D. X. & CF/AHA Task Force. 2013 ACCF/AHA guideline for the management of ST-elevation myocardial infarction: executive summary: a report of the American College of Cardiology Foundation/American Heart Association Task Force on Practice Guidelines. *Circulation* **127**, 529–555 (2013).
175. Amsterdam, E. A., Wenger, N. K., Brindis, R. G., Casey, D. E., Ganiats, T. G., Holmes, D. R., Jaffe, A. S., Jneid, H., Kelly, R. F., Kontos, M. C., Levine, G. N., Liebson, P. R., Mukherjee, D., Peterson, E. D., Sabatine, M. S., Smalling, R. W. & Zieman, S. J. 2014 AHA/ACC Guideline for the Management of Patients With Non–ST-Elevation Acute Coronary Syndromes: Executive Summary: A Report of the American College of Cardiology/American Heart Association Task Force on Practice Guidelines. *Circulation* **130**, 2354–2394 (2014).
176. Babuin, L. & Jaffe, A. S. Troponin: the biomarker of choice for the detection of cardiac injury. *CMAJ Can. Med. Assoc. J.* **173**, 1191–1202 (2005).
177. White, H. D. Pathobiology of troponin elevations: do elevations occur with myocardial ischemia as well as necrosis? *J. Am. Coll. Cardiol.* **57**, 2406–2408 (2011).
178. Jaffe, A. S. & Wu, A. H. B. Troponin Release—Reversible or Irreversible Injury? Should We Care? *Clin. Chem.* **58**, 148–150 (2012).
179. Steen, H., Giannitsis, E., Futterer, S., Merten, C., Juenger, C. & Katus, H. A. Cardiac troponin T at 96 hours after acute myocardial infarction correlates with infarct size and cardiac function. *J. Am. Coll. Cardiol.* **48**, 2192–2194 (2006).

180. Shave, R., Ross, P., Low, D., George, K. & Gaze, D. Cardiac troponin I is released following high-intensity short-duration exercise in healthy humans. *Int. J. Cardiol.* **145**, 337–339 (2010).
181. Sandoval, Y., Smith, S. W., Thordsen, S. E. & Apple, F. S. Supply/demand type 2 myocardial infarction: should we be paying more attention? *J. Am. Coll. Cardiol.* **63**, 2079–2087 (2014).
182. Müller, A. L. & Dhalla, N. S. Role of various proteases in cardiac remodeling and progression of heart failure. *Heart Fail. Rev.* **17**, 395–409 (2012).
183. Holly, T. A., Drincic, A., Byun, Y., Nakamura, S., Harris, K., Klocke, F. J. & Cryns, V. L. Caspase Inhibition Reduces Myocyte Cell Death Induced by Myocardial Ischemia and Reperfusion In Vivo. *J. Mol. Cell. Cardiol.* **31**, 1709–1715 (1999).
184. Inserte, J., Hernando, V. & Garcia-Dorado, D. Contribution of calpains to myocardial ischaemia/reperfusion injury. *Cardiovasc. Res.* **96**, 23–31 (2012).
185. Schulz, R. Intracellular targets of matrix metalloproteinase-2 in cardiac disease: rationale and therapeutic approaches. *Annu. Rev. Pharmacol. Toxicol.* **47**, 211–242 (2007).
186. Tate, J. R., Bunk, D. M., Christenson, R. H., Barth, J. H., Katrukha, A., Noble, J. E., Schimmel, H., Wang, L., Panteghini, M. & IFCC Working Group on Standardization of Cardiac Troponin I. Evaluation of standardization capability of current cardiac troponin I assays by a correlation study: results of an IFCC pilot project. *Clin. Chem. Lab. Med.* **53**, 677–690 (2015).
187. Tate, J. R., Bunk, D. M., Christenson, R. H., Katrukha, A., Noble, J. E., Porter, R. A., Schimmel, H., Wang, L., Panteghini, M. & IFCC Working Group on Standardization of Troponin I. Standardisation of cardiac troponin I measurement: past and present. *Pathology (Phila.)* **42**, 402–408 (2010).
188. Zhang, J., Guy, M. J., Norman, H. S., Chen, Y.-C., Xu, Q., Dong, X., Guner, H., Wang, S., Kohmoto, T., Young, K. H., Moss, R. L. & Ge, Y. Top-down quantitative proteomics identified phosphorylation of cardiac troponin I as a candidate biomarker for chronic heart failure. *J. Proteome Res.* **10**, 4054–4065 (2011).
189. Katrukha, A. G., Bereznikova, A. V., Filatov, V. L., Esakova, T. V., Kolosova, O. V., Pettersson, K., Lövgren, T., Bulargina, T. V., Trifonov, I. R., Gratsiansky, N. A., Pulkki, K., Voipio-Pulkki, L. M. & Gusev, N. B. Degradation of cardiac troponin I: implication for reliable immunodetection. *Clin. Chem.* **44**, 2433–2440 (1998).
190. Bunk, D. M. & Welch, M. J. Characterization of a New Certified Reference Material for Human Cardiac Troponin I. *Clin. Chem.* **52**, 212–219 (2006).
191. McManus, B. M., Chow, L. H., Wilson, J. E., Anderson, D. R., Gulizia, J. M., Gauntt, C. J., Klingel, K. E., Beisel, K. W. & Kandolf, R. Direct myocardial injury by enterovirus: a

central role in the evolution of murine myocarditis. *Clin. Immunol. Immunopathol.* **68**, 159–169 (1993).

192. Esfandiarei, M. & McManus, B. M. Molecular Biology and Pathogenesis of Viral Myocarditis. *Annu. Rev. Pathol. Mech. Dis.* **3**, 127–155 (2008).
193. Maekawa, Y., Ouzounian, M., Opavsky, M. A. & Liu, P. P. Connecting the missing link between dilated cardiomyopathy and viral myocarditis: virus, cytoskeleton, and innate immunity. *Circulation* **115**, 5–8 (2007).
194. Gao, C. Q., Sawicki, G., Suarez-Pinzon, W. L., Csont, T., Wozniak, M., Ferdinandy, P. & Schulz, R. Matrix metalloproteinase-2 mediates cytokine-induced myocardial contractile dysfunction. *Cardiovasc. Res.* **57**, 426–433 (2003).
195. Luo, H., Wong, J. & Wong, B. Protein degradation systems in viral myocarditis leading to dilated cardiomyopathy. *Cardiovasc. Res.* **85**, 347–356 (2010).
196. Steen, H., Giannitsis, E., Futterer, S., Merten, C., Juenger, C. & Katus, H. A. Cardiac troponin T at 96 hours after acute myocardial infarction correlates with infarct size and cardiac function. *J. Am. Coll. Cardiol.* **48**, 2192–2194 (2006).
197. Christenson, R. H., Bunk, D. M., Schimmel, H., Tate, J. R. & I, on behalf of the I. W. G. on S. of T. Point: Put Simply, Standardization of Cardiac Troponin I Is Complicated. *Clin. Chem.* **58**, 165–168 (2012).
198. Ebashi, S., Ebashi, F. & Maruyama, K. A New Protein Factor promoting Contraction of Actomyosin. *Nature* **203**, 645–646 (1964).
199. Ebashi, S., Ebashi, F. & Kodama, A. Troponin as the Ca++-receptive Protein in the Contractile System. *J. Biochem. (Tokyo)* **62**, 137–138 (1967).
200. Biesiadecki, B. J., Tachampa, K., Yuan, C., Jin, J.-P., de Tombe, P. P. & Solaro, R. J. Removal of the cardiac troponin I N-terminal extension improves cardiac function in aged mice. *J. Biol. Chem.* **285**, 19688–19698 (2010).
201. Wattanapermpool, J., Guo, X. & Solaro, R. J. The unique amino-terminal peptide of cardiac troponin I regulates myofibrillar activity only when it is phosphorylated. *J. Mol. Cell. Cardiol.* **27**, 1383–1391 (1995).
202. Cai, F., Li, M. X., Pineda-Sanabria, S. E., Gelozia, S., Lindert, S., West, F., Sykes, B. D. & Hwang, P. M. Structures reveal details of small molecule binding to cardiac troponin. *J. Mol. Cell. Cardiol.* **101**, 134–144 (2016).
203. Suskiewicz, M. J., Sussman, J. L., Silman, I. & Shaul, Y. Context-dependent resistance to proteolysis of intrinsically disordered proteins. *Protein Sci. Publ. Protein Soc.* **20**, 1285–1297 (2011).
204. Liu, Z. & Huang, Y. Advantages of proteins being disordered. *Protein Sci. Publ. Protein Soc.* **23**, 539–550 (2014).

205. Katrukha, I. A., Kogan, A. E., Vylegzhanina, A. V., Kharitonov, A. V., Tamm, N. N., Filatov, V. L., Bereznikova, A. V., Koshkina, E. V. & Katrukha, A. G. Full-Size Cardiac Troponin I and Its Proteolytic Fragments in Blood of Patients with Acute Myocardial Infarction: Antibody Selection for Assay Development. *Clin. Chem.* **64**, 1104–1112 (2018).
206. Solaro, R. J. Troponin I, stunning, hypertrophy, and failure of the heart. *Circ. Res.* **84**, 122–124 (1999).
207. Bolli, R. & Marbán, E. Molecular and cellular mechanisms of myocardial stunning. *Physiol. Rev.* **79**, 609–634 (1999).
208. Ferdinandy, P. & Schulz, R. Nitric oxide, superoxide, and peroxynitrite in myocardial ischaemia-reperfusion injury and preconditioning. *Br. J. Pharmacol.* **138**, 532–543 (2003).
209. Miyamae, M., Camacho, S. A., Weiner, M. W. & Figueredo, V. M. Attenuation of postischemic reperfusion injury is related to prevention of [Ca2+]m overload in rat hearts. *Am. J. Physiol.* **271**, H2145-2153 (1996).
210. Marban, E., Kitakaze, M., Kusuoka, H., Porterfield, J. K., Yue, D. T. & Chacko, V. P. Intracellular free calcium concentration measured with 19F NMR spectroscopy in intact ferret hearts. *Proc. Natl. Acad. Sci.* **84**, 6005–6009 (1987).
211. Hughes, B. G. & Schulz, R. Targeting MMP-2 to treat ischemic heart injury. *Basic Res. Cardiol.* **109**, 424 (2014).
212. Viappiani, S., Nicolescu, A. C., Holt, A., Sawicki, G., Crawford, B. D., León, H., van Mulligen, T. & Schulz, R. Activation and modulation of 72kDa matrix metalloproteinase-2 by peroxynitrite and glutathione. *Biochem. Pharmacol.* **77**, 826–834 (2009).
213. Bolli, R., Patel, B. S., Jeroudi, M. O., Lai, E. K. & McCay, P. B. Demonstration of free radical generation in ‘stunned’ myocardium of intact dogs with the use of the spin trap alpha-phenyl N-tert-butyl nitrone. *J. Clin. Invest.* **82**, 476–485 (1988).
214. Vander Heide, R. S. & Steenbergen, C. Cardioprotection and myocardial reperfusion: pitfalls to clinical application. *Circ. Res.* **113**, 464–477 (2013).
215. Yasmin, W., Strynadka, K. D. & Schulz, R. Generation of peroxynitrite contributes to ischemia-reperfusion injury in isolated rat hearts. *Cardiovasc. Res.* **33**, 422–432 (1997).
216. Franco, S. J. & Huttenlocher, A. Regulating cell migration: calpains make the cut. *J. Cell Sci.* **118**, 3829–3838 (2005).
217. Lebart, M.-C. & Benyamin, Y. Calpain involvement in the remodeling of cytoskeletal anchorage complexes. *FEBS J.* **273**, 3415–3426 (2006).
218. Siegmund, B., Ladilov, Y. V. & Piper, H. M. Importance of sodium for recovery of calcium control in reoxygenated cardiomyocytes. *Am. J. Physiol.* **267**, H506-513 (1994).

219. Neri, M., Riezzo, I., Pascale, N., Pomara, C. & Turillazzi, E. Ischemia/Reperfusion Injury following Acute Myocardial Infarction: A Critical Issue for Clinicians and Forensic Pathologists. *Mediators Inflamm.* **2017**, (2017).
220. McCartney, C.-S. E., MacLeod, J. A., Greer, P. A. & Davies, P. L. An easy-to-use FRET protein substrate to detect calpain cleavage in vitro and in vivo. *Biochim. Biophys. Acta Mol. Cell Res.* **1865**, 221–230 (2018).
221. Kelly, J. C., Cuerrier, D., Graham, L. A., Campbell, R. L. & Davies, P. L. Profiling of calpain activity with a series of FRET-based substrates. *Biochim. Biophys. Acta* **1794**, 1505–1509 (2009).
222. Yoshida, K., Inui, M., Harada, K., Saido, T. C., Sorimachi, Y., Ishihara, T., Kawashima, S. & Sobue, K. Reperfusion of rat heart after brief ischemia induces proteolysis of calspectin (nonerythroid spectrin or fodrin) by calpain. *Circ. Res.* **77**, 603–610 (1995).
223. Chen, M., Won, D.-J., Krajewski, S. & Gottlieb, R. A. Calpain and mitochondria in ischemia/reperfusion injury. *J. Biol. Chem.* **277**, 29181–29186 (2002).
224. Zahran, S., Pan, J. S., Liu, P. B. & Hwang, P. M. Combining a PagP fusion protein system with nickel ion-catalyzed cleavage to produce intrinsically disordered proteins in E. coli. *Protein Expr. Purif.* **116**, 133–138 (2015).
225. Delaglio, F., Grzesiek, S., Vuister, G. W., Zhu, G., Pfeifer, J. & Bax, A. NMRPipe: A multidimensional spectral processing system based on UNIX pipes. *J. Biomol. NMR* **6**, 277–293 (1995).
226. Johnson, B. A. Using NMRView to visualize and analyze the NMR spectra of macromolecules. *Methods Mol. Biol. Clifton NJ* **278**, 313–352 (2004).
227. De Simone, A., Cavalli, A., Hsu, S.-T. D., Vranken, W. & Vendruscolo, M. Accurate random coil chemical shifts from an analysis of loop regions in native states of proteins. *J. Am. Chem. Soc.* **131**, 16332–16333 (2009).
228. Camilloni, C., De Simone, A., Vranken, W. F. & Vendruscolo, M. Determination of Secondary Structure Populations in Disordered States of Proteins Using Nuclear Magnetic Resonance Chemical Shifts. *Biochemistry* **51**, 2224–2231 (2012).
229. Kabsch, W., Mannherz, H. G., Suck, D., Pai, E. F. & Holmes, K. C. Atomic structure of the actin: DNase I complex. *Nature* **347**, 37–44 (1990).
230. Baghirova, S., Hughes, B. G., Poirier, M., Kondo, M. Y. & Schulz, R. Nuclear matrix metalloproteinase-2 in the cardiomyocyte and the ischemic-reperfused heart. *J. Mol. Cell. Cardiol.* **94**, 153–161 (2016).
231. Elce, J. S., Hegadorn, C., Gauthier, S., Vince, J. W. & Davies, P. L. Recombinant calpain II: improved expression systems and production of a C105A active-site mutant for crystallography. *Protein Eng.* **8**, 843–848 (1995).
232. Sheterline, P., Clayton, J. & Sparrow, J. Actin. *Protein Profile* **2**, 1–103 (1995).

233. Gasteiger, E., Gattiker, A., Hoogland, C., Ivanyi, I., Appel, R. D. & Bairoch, A. ExPASy: the proteomics server for in-depth protein knowledge and analysis. *Nucleic Acids Res.* **31**, 3784–3788 (2003).
234. Blumenschein, T. M. A., Stone, D. B., Fletterick, R. J., Mendelson, R. A. & Sykes, B. D. Dynamics of the C-terminal region of TnI in the troponin complex in solution. *Biophys. J.* **90**, 2436–2444 (2006).
235. Murakami, K., Yumoto, F., Ohki, S., Yasunaga, T., Tanokura, M. & Wakabayashi, T. Structural basis for Ca2+-regulated muscle relaxation at interaction sites of troponin with actin and tropomyosin. *J. Mol. Biol.* **352**, 178–201 (2005).
236. Kumar, S., Ratnikov, B. I., Kazanov, M. D., Smith, J. W. & Cieplak, P. CleavPredict: A Platform for Reasoning about Matrix Metalloproteinases Proteolytic Events. *PloS One* **10**, e0127877 (2015).
237. Eckhard, U., Huesgen, P. F., Schilling, O., Bellac, C. L., Butler, G. S., Cox, J. H., Dufour, A., Goebeler, V., Kappelhoff, R., auf dem Keller, U., Klein, T., Lange, P. F., Marino, G., Morrison, C. J., Prudova, A., Rodriguez, D., Starr, A. E., Wang, Y. & Overall, C. M. Active site specificity profiling datasets of matrix metalloproteinases (MMPs) 1, 2, 3, 7, 8, 9, 12, 13 and 14. *Data Brief* **7**, 299–310 (2016).
238. Eckhard, U., Huesgen, P. F., Schilling, O., Bellac, C. L., Butler, G. S., Cox, J. H., Dufour, A., Goebeler, V., Kappelhoff, R., Keller, U. A. dem, Klein, T., Lange, P. F., Marino, G., Morrison, C. J., Prudova, A., Rodriguez, D., Starr, A. E., Wang, Y. & Overall, C. M. Active site specificity profiling of the matrix metalloproteinase family: Proteomic identification of 4300 cleavage sites by nine MMPs explored with structural and synthetic peptide cleavage analyses. *Matrix Biol. J. Int. Soc. Matrix Biol.* **49**, 37–60 (2016).
239. Turk, B. E., Huang, L. L., Piro, E. T. & Cantley, L. C. Determination of protease cleavage site motifs using mixture-based oriented peptide libraries. *Nat. Biotechnol.* **19**, 661–667 (2001).
240. Cuerrier, D., Moldoveanu, T. & Davies, P. L. Determination of peptide substrate specificity for mu-calpain by a peptide library-based approach: the importance of primed side interactions. *J. Biol. Chem.* **280**, 40632–40641 (2005).
241. Apple, F. S., Collinson, P. O. & IFCC Task Force on Clinical Applications of Cardiac Biomarkers. Analytical characteristics of high-sensitivity cardiac troponin assays. *Clin. Chem.* **58**, 54–61 (2012).
242. Eberli, F. R. Stunned myocardium--an unfinished puzzle. *Cardiovasc. Res.* **63**, 189–191 (2004).
243. Heyndrickx, G. R., Millard, R. W., McRitchie, R. J., Maroko, P. R. & Vatner, S. F. Regional myocardial functional and electrophysiological alterations after brief coronary artery occlusion in conscious dogs. *J. Clin. Invest.* **56**, 978–985 (1975).

244. Bolli, R., Zhu, W. X., Thornby, J. I., O'Neill, P. G. & Roberts, R. Time course and determinants of recovery of function after reversible ischemia in conscious dogs. *Am. J. Physiol.* **254**, H102-114 (1988).
245. Heusch, G. & Schulz, R. Characterization of hibernating and stunned myocardium. *Eur. Heart J.* **18 Suppl D**, D102-110 (1997).
246. Ehring, T., Schulz, R. & Heusch, G. Characterization of 'hibernating' and 'stunned' myocardium with focus on the use of calcium antagonists in 'stunned' myocardium. *J. Cardiovasc. Pharmacol.* **20 Suppl 5**, S25-33 (1992).
247. Gao, W. D., Atar, D., Backx, P. H. & Marban, E. Relationship between intracellular calcium and contractile force in stunned myocardium. Direct evidence for decreased myofilament Ca2+ responsiveness and altered diastolic function in intact ventricular muscle. *Circ. Res.* **76**, 1036–1048 (1995).
248. Gao, W. D., Liu, Y., Mellgren, R. & Marban, E. Intrinsic myofilament alterations underlying the decreased contractility of stunned myocardium. A consequence of Ca2+-dependent proteolysis? *Circ. Res.* **78**, 455–465 (1996).
249. McDonald, K. S., Moss, R. L. & Miller, W. P. Incorporation of the troponin regulatory complex of post-ischemic stunned porcine myocardium reduces myofilament calcium sensitivity in rabbit psoas skeletal muscle fibers. *J. Mol. Cell. Cardiol.* **30**, 285–296 (1998).
250. Davis, J. P., Norman, C., Kobayashi, T., Solaro, R. J., Swartz, D. R. & Tikunova, S. B. Effects of Thin and Thick Filament Proteins on Calcium Binding and Exchange with Cardiac Troponin C. *Biophys. J.* **92**, 3195–3206 (2007).
251. Anfinsen, C. B. Principles that govern the folding of protein chains. *Science* **181**, 223–230 (1973).
252. Oates, M. E., Romero, P., Ishida, T., Ghalwash, M., Mizianty, M. J., Xue, B., Dosztányi, Z., Uversky, V. N., Obradovic, Z., Kurgan, L., Dunker, A. K. & Gough, J. D^2P^2: database of disordered protein predictions. *Nucleic Acids Res.* **41**, D508-516 (2013).
253. Gatsogiannis, C., Merino, F., Roderer, D., Balchin, D., Schubert, E., Kuhlee, A., Hayer-Hartl, M. & Raunser, S. Tc toxin activation requires unfolding and refolding of a β-propeller. *Nature* (2018). doi:10.1038/s41586-018-0556-6
254. Watzinger, N., Maier, R., Reiter, U., Reiter, G., Fuernau, G., Wonisch, M., Fruhwald, F. M., Schumacher, M., Zweiker, R., Rienmueller, R. & Klein, W. Clinical applications of cardiovascular magnetic resonance. *Curr. Pharm. Des.* **11**, 457–475 (2005).
255. McKay, R. G. "Ischemia-guided" versus "early invasive" strategies in the management of acute coronary syndrome/non–ST-segment elevation myocardial infarction: The interventionalist's perspective. *J. Am. Coll. Cardiol.* **41**, S96–S102 (2003).

256. Roffi, M., Patrono, C., Collet, J.-P., Mueller, C., Valgimigli, M., Andreotti, F., Bax, J. J., Borger, M. A., Brotons, C., Chew, D. P., Gencer, B., Hasenfuss, G., Kjeldsen, K., Lancellotti, P., Landmesser, U., Mehilli, J., Mukherjee, D., Storey, R. F., Windecker, S., Baumgartner, H., Gaemperli, O., Achenbach, S., Agewall, S., Badimon, L., Baigent, C., Bueno, H., Bugiardini, R., Carerj, S., Casselman, F., Cuisset, T., Erol, Ç., Fitzsimons, D., Halle, M., Hamm, C., Hildick-Smith, D., Huber, K., Iliodromitis, E., James, S., Lewis, B. S., Lip, G. Y. H., Piepoli, M. F., Richter, D., Rosemann, T., Sechtem, U., Steg, P. G., Vrints, C., Luis Zamorano, J. & Management of Acute Coronary Syndromes in Patients Presenting without Persistent ST-Segment Elevation of the European Society of Cardiology. 2015 ESC Guidelines for the management of acute coronary syndromes in patients presenting without persistent ST-segment elevation: Task Force for the Management of Acute Coronary Syndromes in Patients Presenting without Persistent ST-Segment Elevation of the European Society of Cardiology (ESC). *Eur. Heart J.* **37**, 267–315 (2016).
257. Mills, N. L., Churchhouse, A. M. D., Lee, K. K., Anand, A., Gamble, D., Shah, A. S. V., Paterson, E., MacLeod, M., Graham, C., Walker, S., Denvir, M. A., Fox, K. A. A. & Newby, D. E. Implementation of a Sensitive Troponin I Assay and Risk of Recurrent Myocardial Infarction and Death in Patients With Suspected Acute Coronary Syndrome. *JAMA* **305**, 1210–1216 (2011).

Appendix A

Proteolysis of cTnI [1-77] by MMP-2

Mass spectrometry data cTnI [1-77]

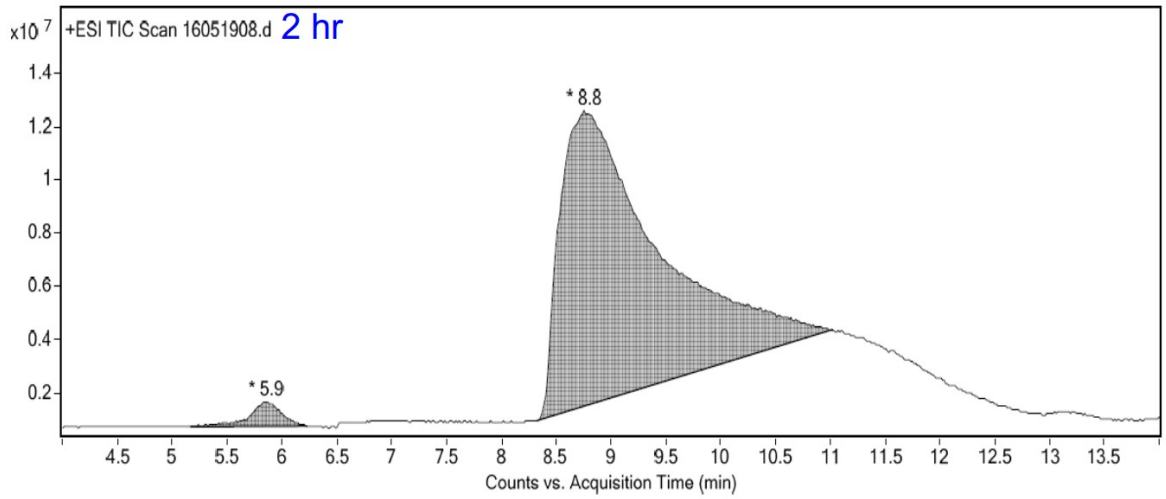

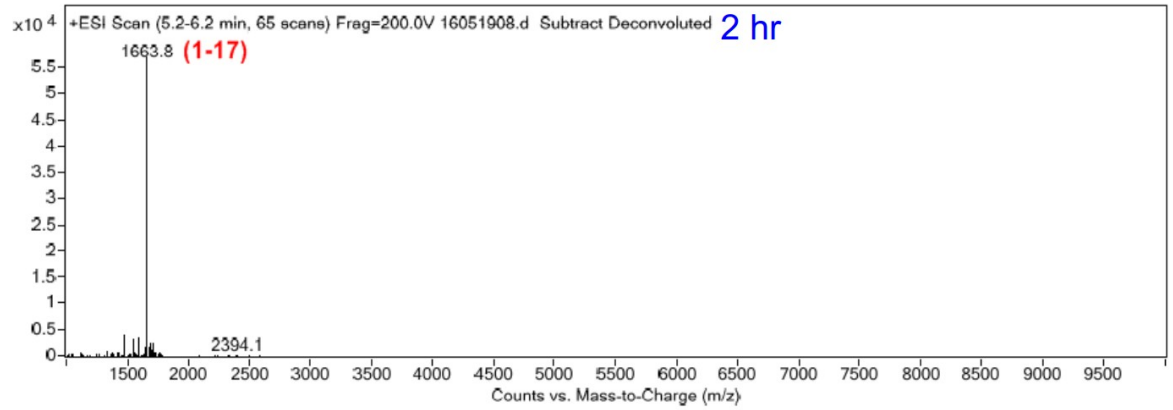

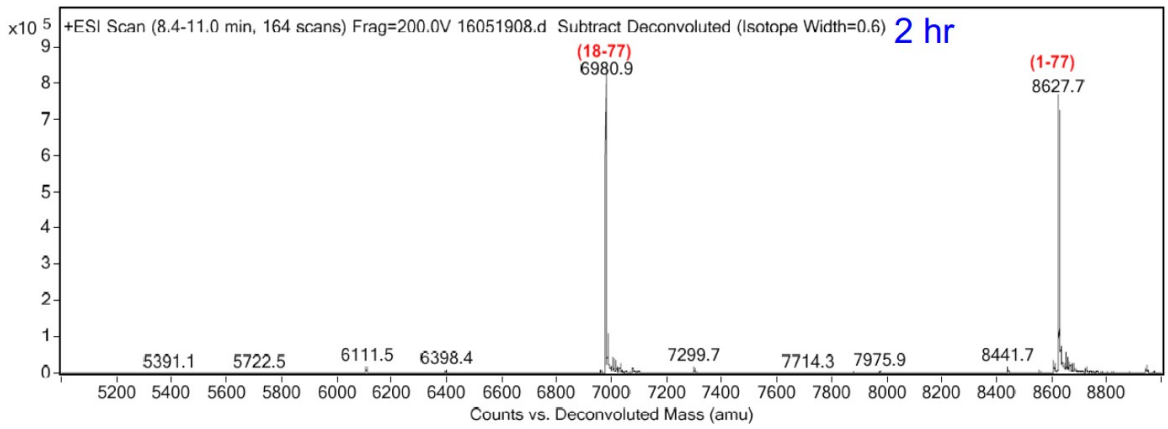
x10 5
+ESI Scan (8.4-11.0 min, 164 scans) Frag=200.0V 16051908.d Subtract Deconvoluted (Isotope Width=0.6)
2 hr
(18-77)
6980.9
(1-77)
8627.7
5391.1
5722.5
6111.5
6398.4
7299.7
7714.3
7975.9
8441.7
Counts vs. Deconvoluted Mass (amu)

Proteolysis of cTnI [135-209] by MMP-2

Mass spectrometry data cTnI [135-209]

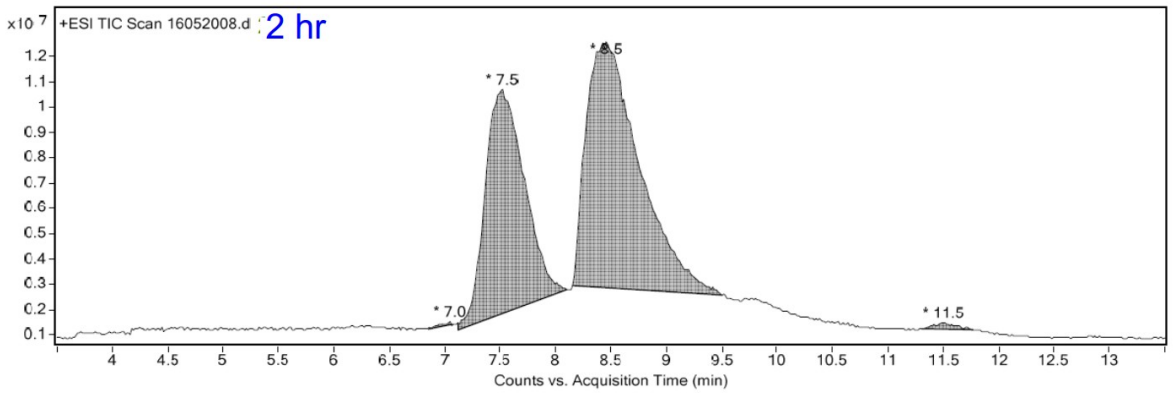

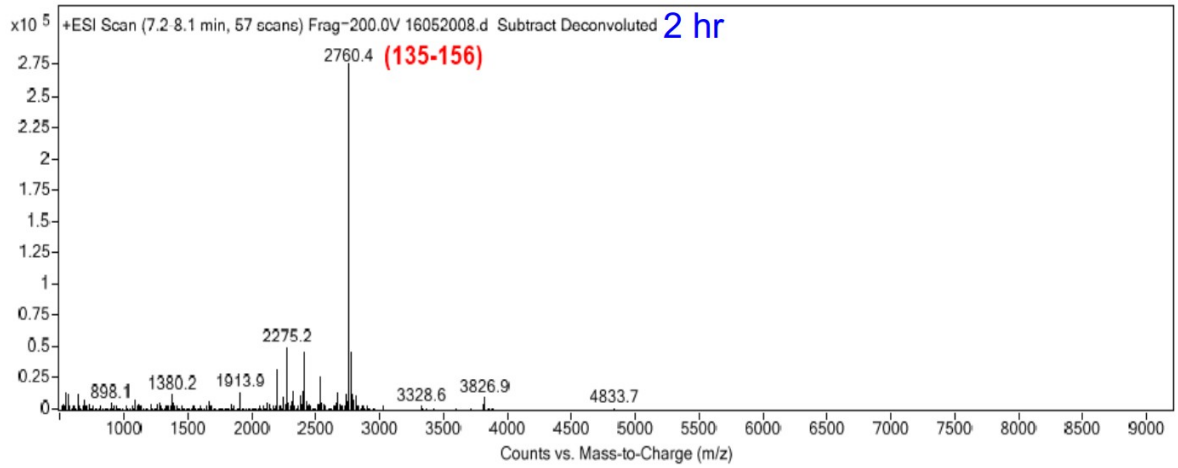

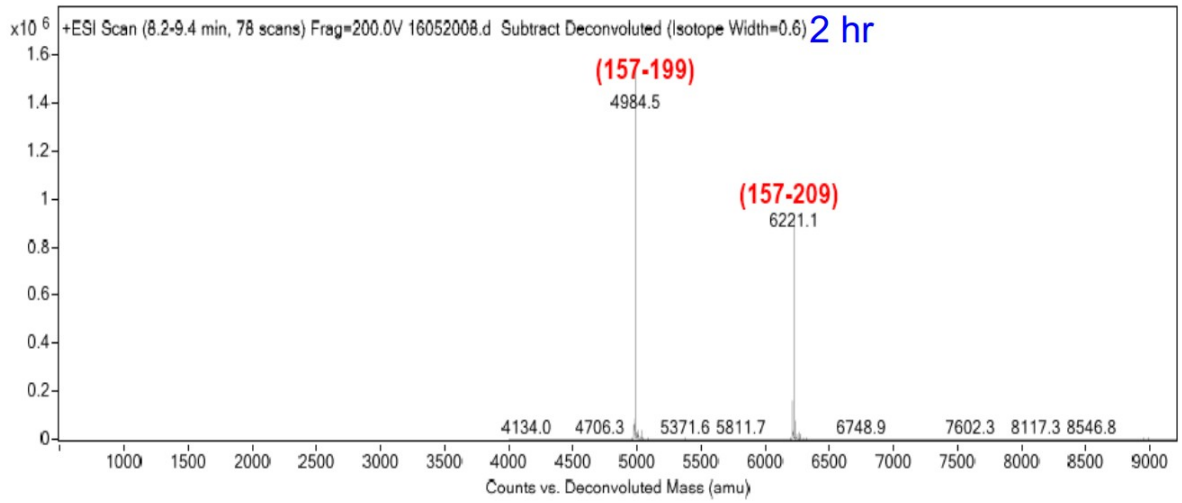
x10 6
+ESI Scan (8.2-9.4 min, 78 scans) Frag=200.0V 16052008.d Subtract Deconvoluted (Isotope Width=0.6)
2 hr
(157-199)
4984.5
(157-209)
6221.1
4134.0
4706.3
5371.6
5811.7
6748.9
7602.3
8117.3
8546.8
Counts vs. Deconvoluted Mass (amu)

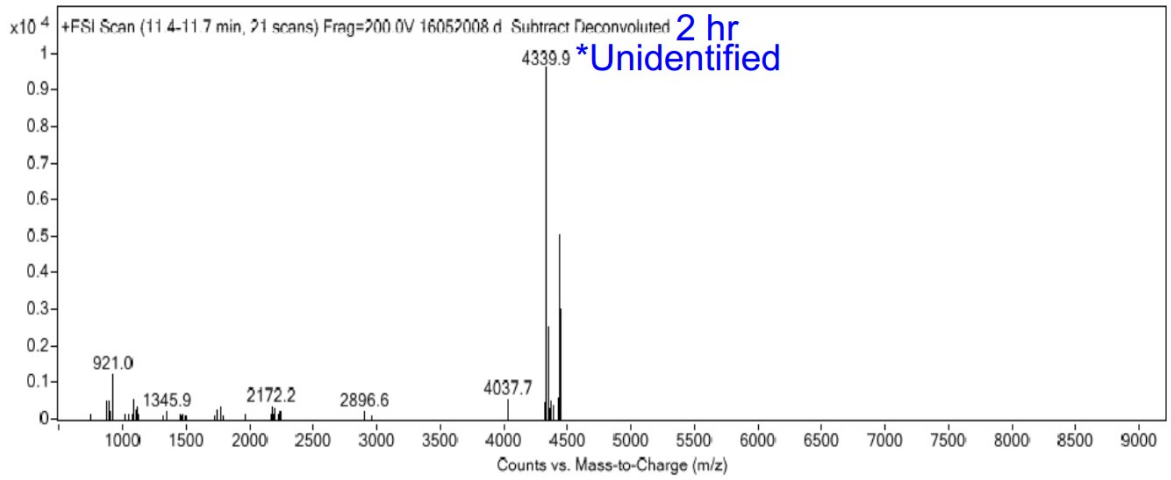
x10 4
+ESI Scan (11.4-11.7 min, 21 scans) Frag=200.0V 16052008.d Subtract Deconvoluted
2 hr
4339.9
*Unidentified
921.0
1345.9
2172.2
2896.6
4037.7
Counts vs. Mass-to-Charge (m/z)

Appendix B

Proteolysis of cTnI [1-77] by μ-calpain

Mass spectrometry data cTnI [1-77]

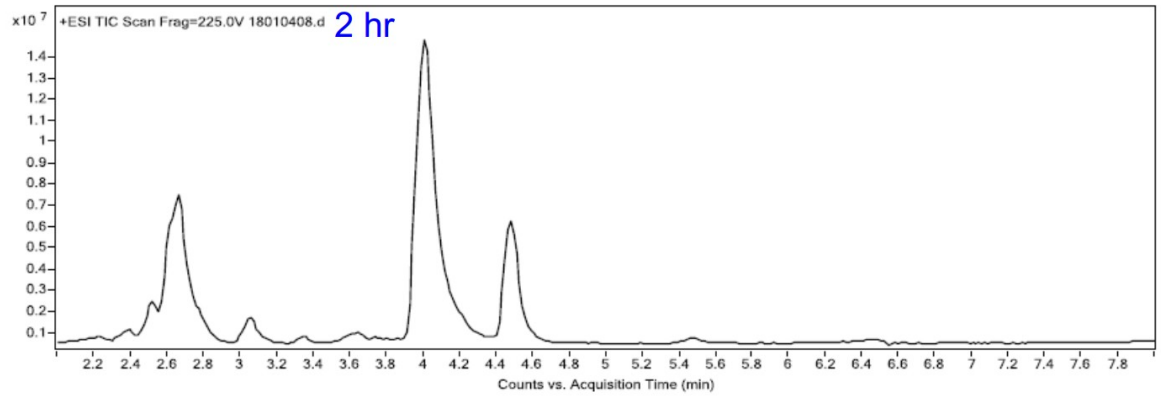

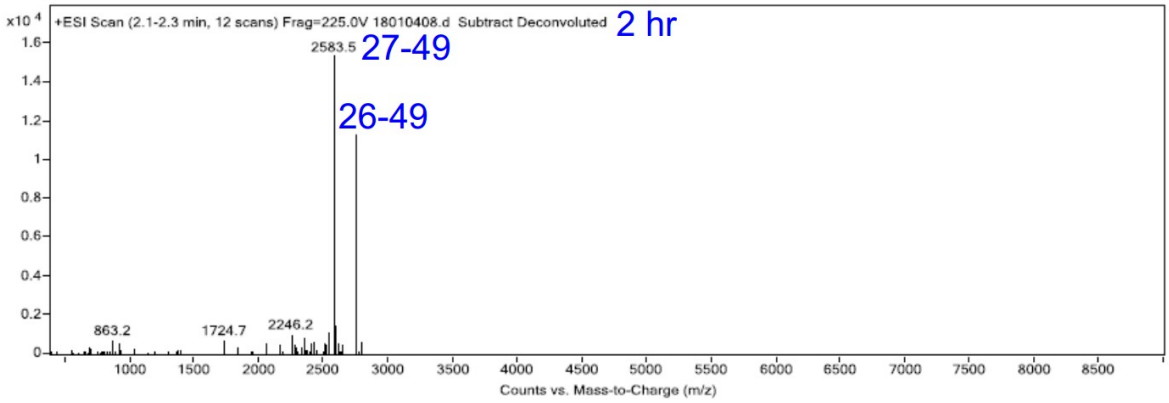

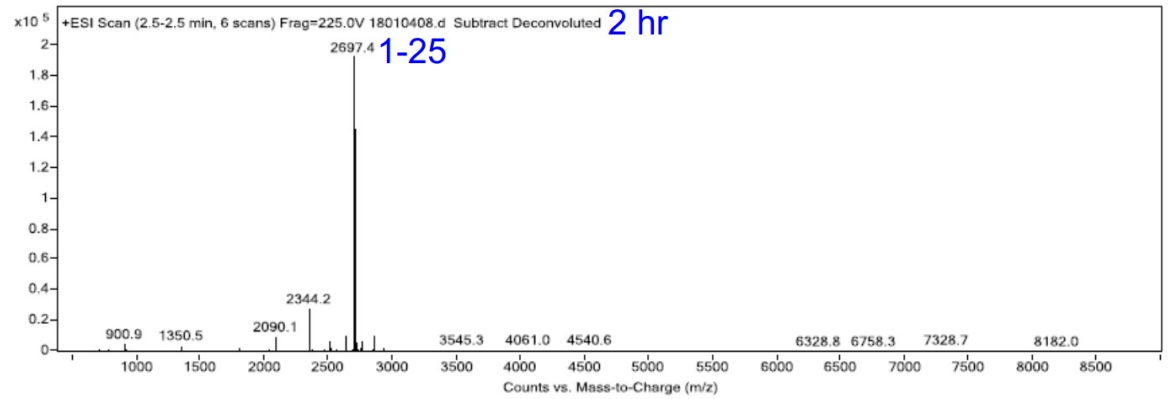
x10 5
+ESI Scan (2.5-2.5 min, 6 scans) Frag=225.0V 18010408.d Subtract Deconvoluted
2 hr
2697.4
1-25
2344.2
2090.1
900.9
1350.5
3545.3
4061.0
4540.6
6328.8
6758.3
7328.7
8182.0
Counts vs. Mass-to-Charge (m/z)

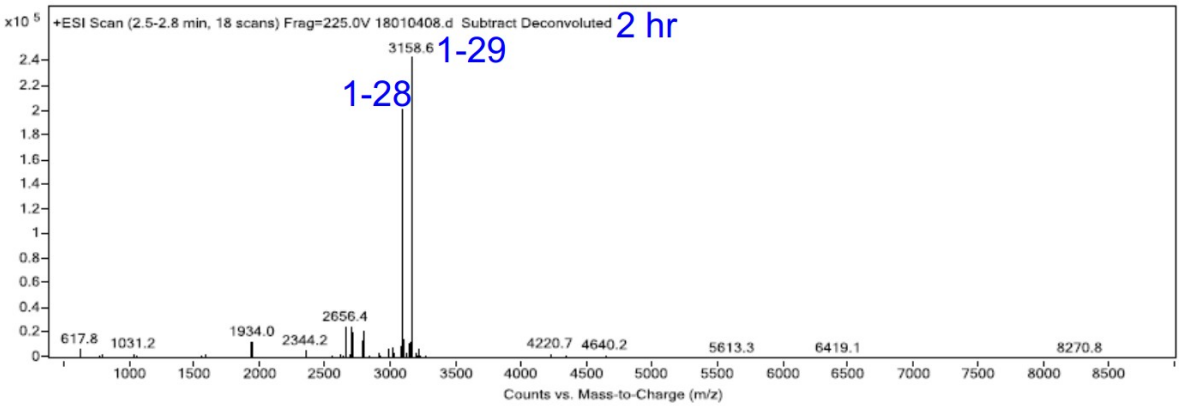
x10 5
+ESI Scan (2.5-2.8 min, 18 scans) Frag=225.0V 18010408.d Subtract Deconvoluted
2 hr
3158.6
1-29
1-28
2656.4
617.8
1031.2
1934.0
2344.2
4220.7
4640.2
5613.3
6419.1
8270.8
Counts vs. Mass-to-Charge (m/z)

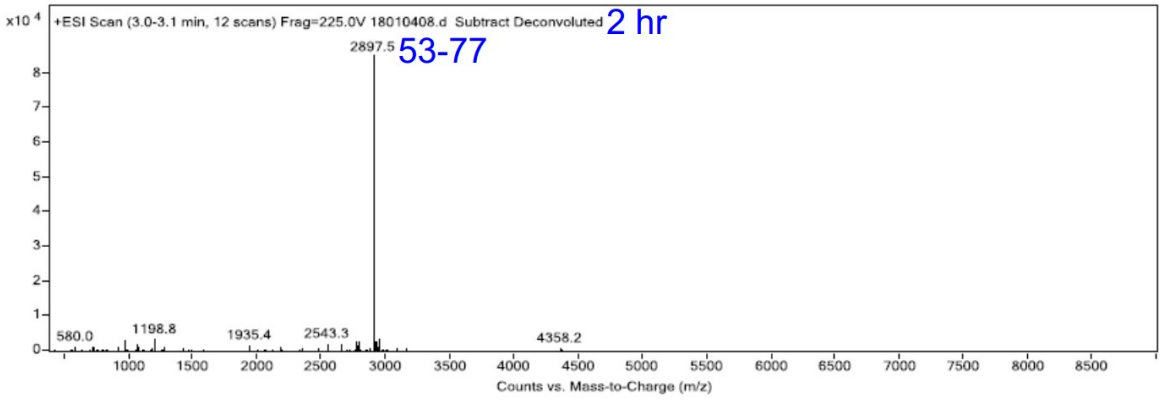
x10 4
+ESI Scan (3.0-3.1 min, 12 scans) Frag=225.0V 18010408.d Subtract Deconvoluted
2 hr
2897.5
53-77
580.0
1198.8
1935.4
2543.3
4358.2
Counts vs. Mass-to-Charge (m/z)

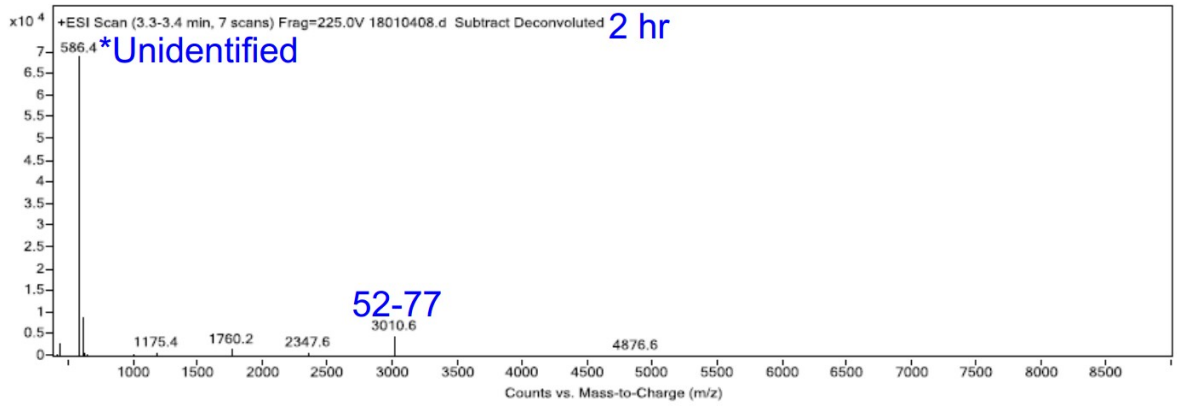
+ESI Scan (3.3-3.4 min, 7 scans) Frag=225.0V 18010408.d Subtract Deconvoluted
2 hr
586.4 *Unidentified
52-77
3010.6
1175.4
1760.2
2347.6
4876.6
Counts vs. Mass-to-Charge (m/z)

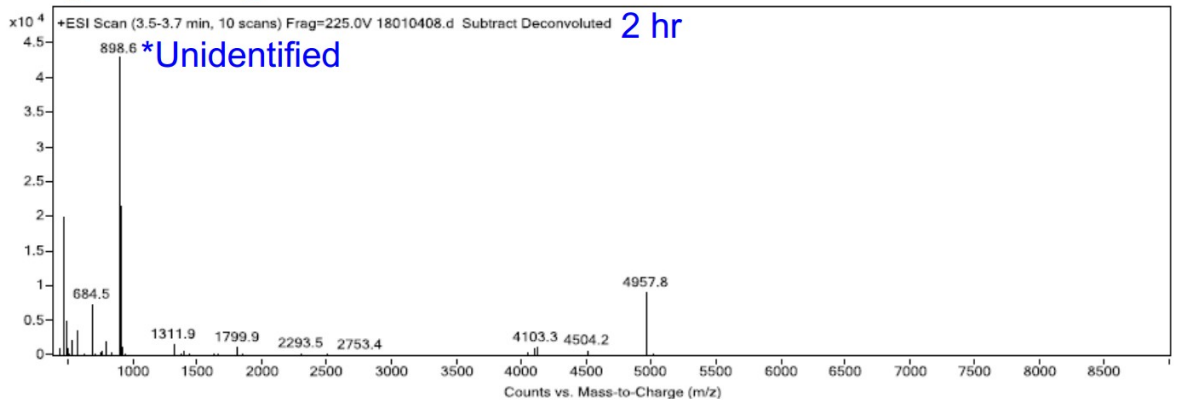
+ESI Scan (3.5-3.7 min, 10 scans) Frag=225.0V 18010408.d Subtract Deconvoluted
2 hr
898.6 *Unidentified
684.5
4957.8
1311.9
1799.9
2293.5
2753.4
4103.3
4504.2
Counts vs. Mass-to-Charge (m/z)

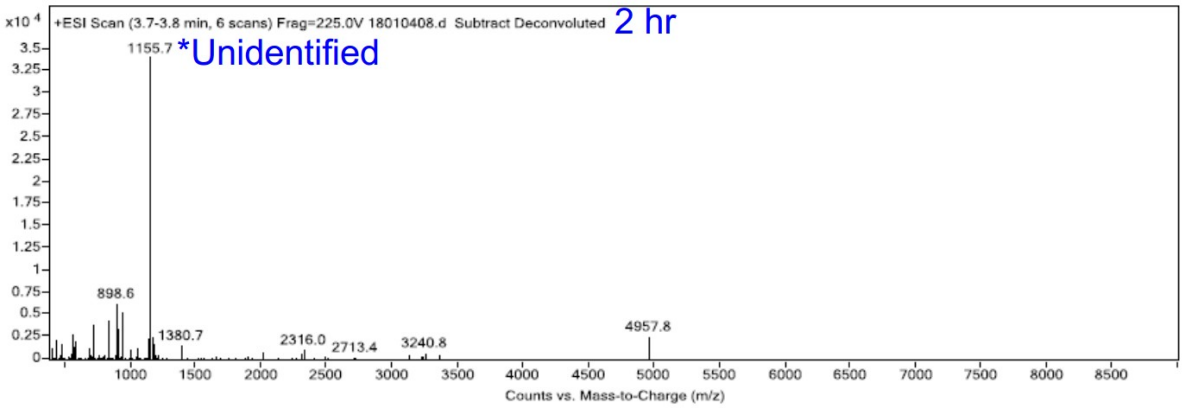
+ESI Scan (3.7-3.8 min, 6 scans) Frag=225.0V 18010408.d Subtract Deconvoluted
2 hr
1155.7 *Unidentified
898.6
1380.7
2316.0
2713.4
3240.8
4957.8
Counts vs. Mass-to-Charge (m/z)

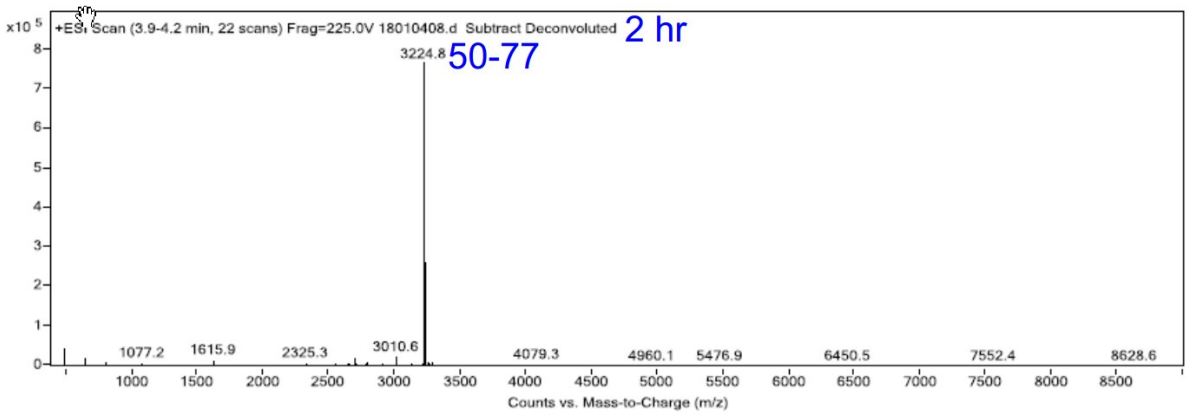
x10 5
+ESI Scan (3.9-4.2 min, 22 scans) Frag=225.0V 18010408.d Subtract Deconvoluted
2 hr
3224.8
50-77
1077.2
1615.9
2325.3
3010.6
4079.3
4960.1
5476.9
6450.5
7552.4
8628.6
Counts vs. Mass-to-Charge (m/z)

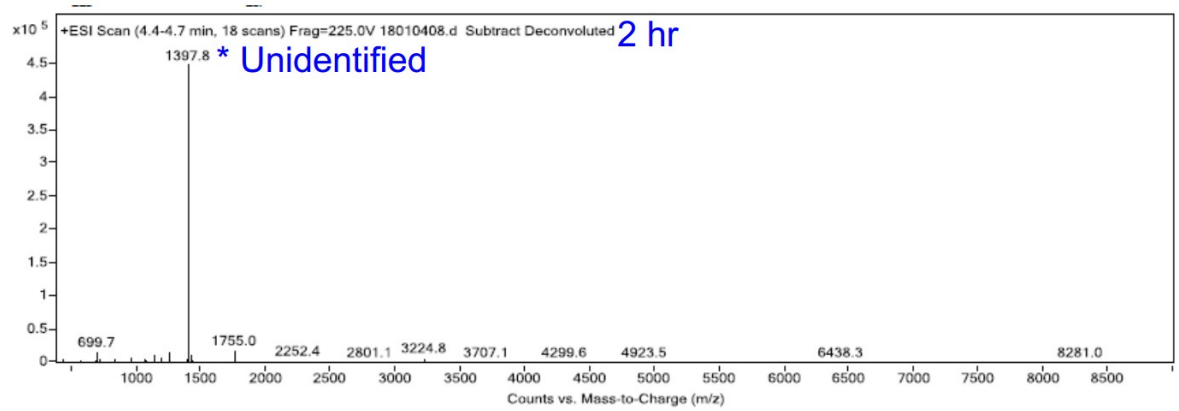
x10 5
+ESI Scan (4.4-4.7 min, 18 scans) Frag=225.0V 18010408.d Subtract Deconvoluted
2 hr
1397.8
* Unidentified
699.7
1755.0
2252.4
2801.1
3224.8
3707.1
4299.6
4923.5
6438.3
8281.0
Counts vs. Mass-to-Charge (m/z)

Appendix C

Proteolysis of cTnI [135-209] by μ-calpain

Mass spectrometry data cTnI [135-209]

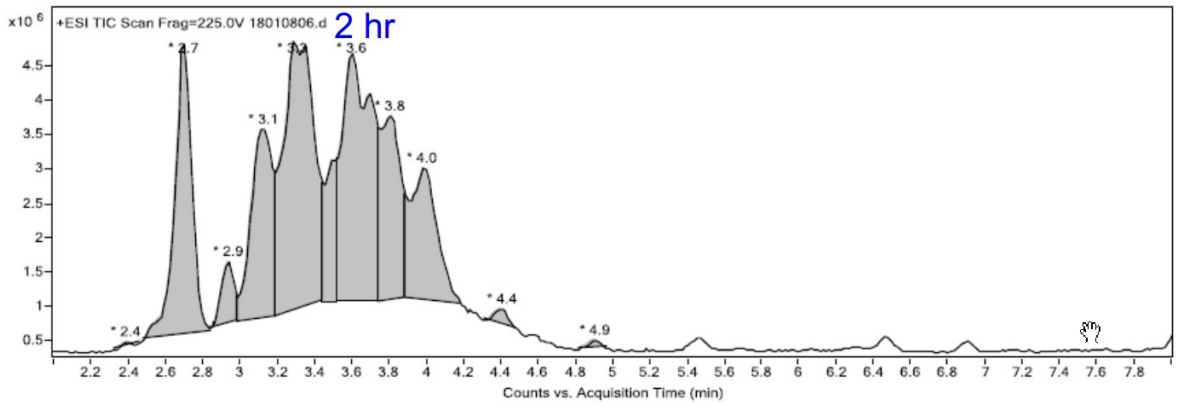

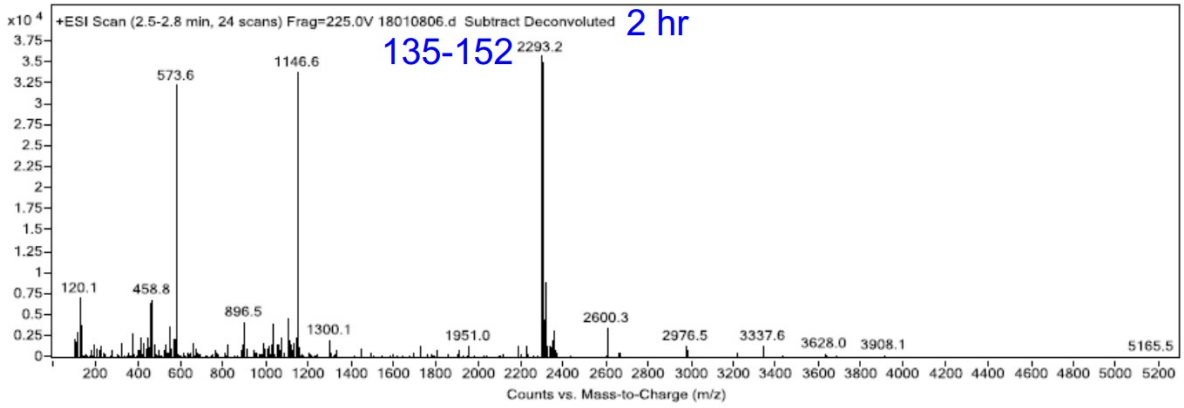

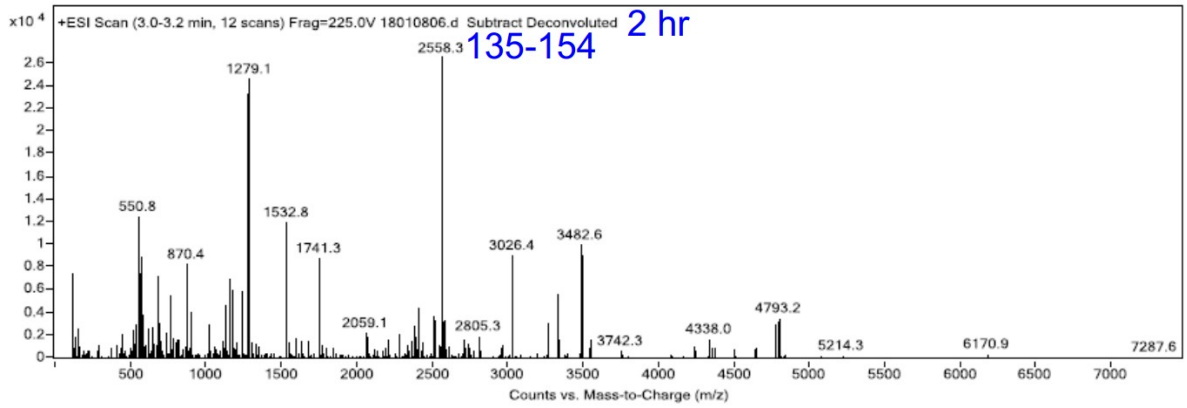
x10 4
+ESI Scan (3.0-3.2 min, 12 scans) Frag=225.0V 18010806.d Subtract Deconvoluted
2 hr
135-154
2558.3
1279.1
550.8
1532.8
870.4
1741.3
3026.4
3482.6
2059.1
2805.3
4793.2
4338.0
3742.3
5214.3
6170.9
7287.6
Counts vs. Mass-to-Charge (m/z)

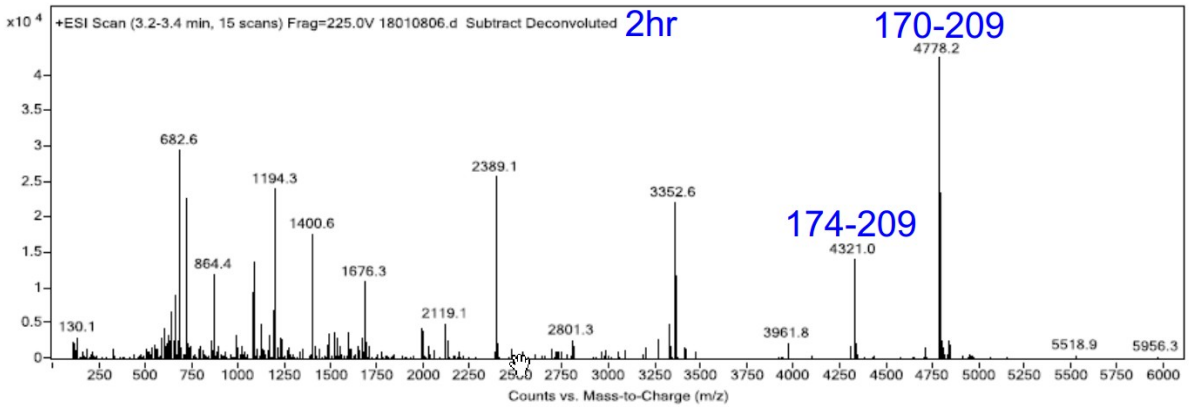
x10 4
+ESI Scan (3.2-3.4 min, 15 scans) Frag=225.0V 18010806.d Subtract Deconvoluted
2hr
170-209
4778.2
682.6
2389.1
1194.3
3352.6
1400.6
174-209
4321.0
864.4
1676.3
2119.1
130.1
2801.3
3961.8
5518.9
5956.3
Counts vs. Mass-to-Charge (m/z)

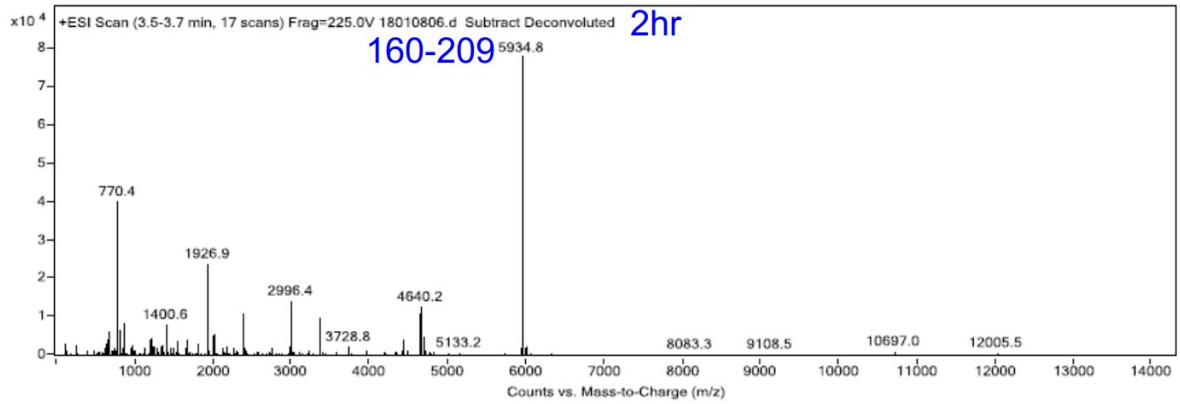
x10 4
+ESI Scan (3.5-3.7 min, 17 scans) Frag=225.0V 18010806.d Subtract Deconvoluted
2hr
160-209
5934.8
770.4
1926.9
2996.4
4640.2
1400.6
3728.8
5133.2
8083.3
9108.5
10697.0
12005.5
Counts vs. Mass-to-Charge (m/z)

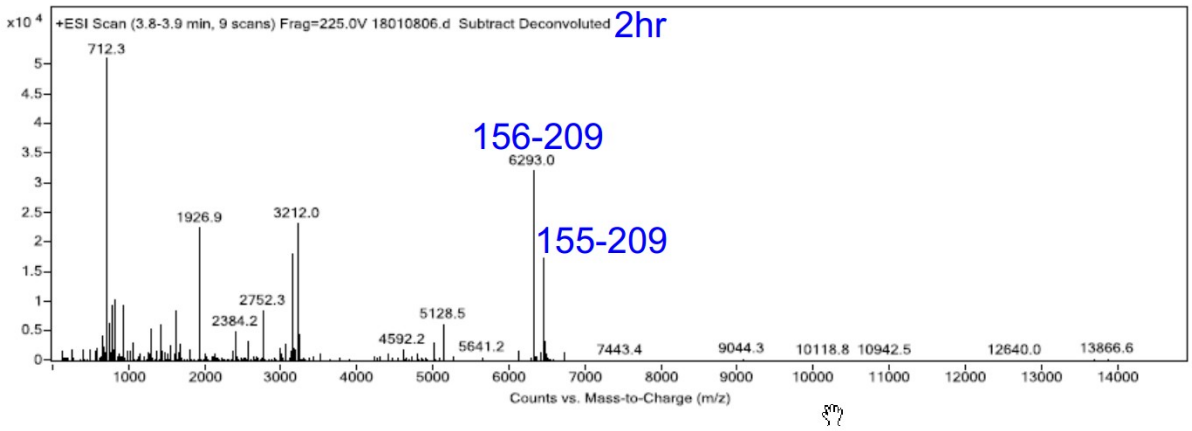
x10 4
+ESI Scan (3.8-3.9 min, 9 scans) Frag=225.0V 18010806.d Subtract Deconvoluted
2hr
712.3
156-209
6293.0
1926.9
3212.0
155-209
2752.3
2384.2
5128.5
4592.2
5641.2
7443.4
9044.3
10118.8
10942.5
12640.0
13866.6
Counts vs. Mass-to-Charge (m/z)

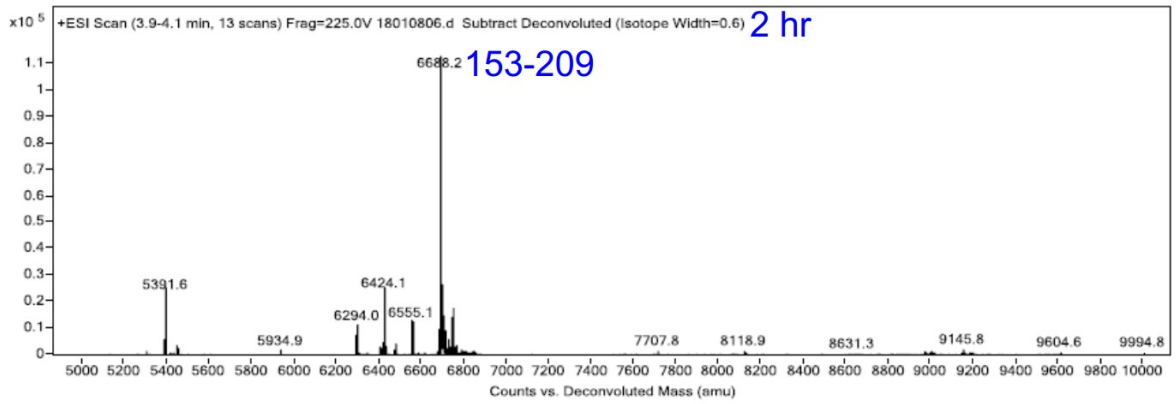
x10 5
+ESI Scan (3.9-4.1 min, 13 scans) Frag=225.0V 18010806.d Subtract Deconvoluted (Isotope Width=0.6)
2 hr
6688.2
153-209
5391.6
6424.1
6294.0
6555.1
5934.9
7707.8
8118.9
8631.3
9145.8
9604.6
9994.8
Counts vs. Deconvoluted Mass (amu)